INVESTIGATION OF THE POTENTIAL OF POST-TRANSLATIONAL MODIFICATIONS AS BIOMARKERS AND THERAPEUTIC TARGETS FOR AMYOTROPHIC LATERAL SCLEROSIS DISEASE

by
Melis Kalkan

Submitted to Graduate School of Natural and Applied Sciences
in Partial Fulfillment of the Requirements
for the Degree of Doctor Philosophy in
Biotechnology

Yeditepe University
2023

INVESTIGATION OF THE POTENTIAL OF POST-TRANSLATIONAL MODIFICATIONS AS BIOMARKERS AND THERAPEUTIC TARGETS FOR AMYOTROPHIC LATERAL SCLEROSIS DISEASE

APPROVED BY:

Prof. Dr. Fikrettin Şahin ……
(Thesis Supervisor)
(Yeditepe University)

Assoc. Prof. Dr. Ayşegül Doğan ……
(Yeditepe University)

Assist. Prof. Dr. Hüseyin Çimen ……
(Yeditepe University)

Assoc. Prof. Dr. Hüseyin Abdik ……
(İstanbul Sabahattin Zaim University)

Assist. Prof. Dr. Mehmet Ozansoy ……
(Bahçeşehir University)

DATE OF APPROVAL: ..../..../2023

I hereby declare that this thesis is my own work and that all information in this thesis has been obtained and presented in accordance with academic rules and ethical conduct. I have fully cited and referenced all material and results as required by these rules and conduct, and this thesis study does not contain any plagiarism. If any material used in the thesis requires copyright, the necessary permissions have been obtained. No material from this thesis has been used for the award of another degree.

I accept all kinds of legal liability that may arise in case contrary to these situations.

Name, Last name Melis Kalkan.....

Signature .....

Dedicated to Suna Kıraç and my family

who were the inspiration and support of this thesis…

ACKNOWLEDGEMENTS

First and foremost, I would like to express my profound and immense gratitude to my thesis advisor, Prof. Dr. Fikrettin Şahin, for his unlimited support and encouragement. It always has been a privilege to work with him. He was beyond a thesis advisor to me at all times, he was like a father. I feel very lucky that my academic life has enlightened me with his vision.

Thanks should also go to Dr. Burcu Kasapoğlu Usta, without her guidance, support, and generous help, I could not have undertaken this project.

I would like to thank my thesis committee members including Assist. Prof. Dr. Hüseyin Çimen, Assoc. Prof. Dr. Ayşegül Doğan, Assist. Prof. Dr. Mehmet Ozansoy, and Assoc. Prof. Dr. Hüseyin Abdik for their estimable and formative comments and suggestions during this project.

I would like to express my heartfelt gratitude to Suna and İnan Kıraç Foundation, and TÜBİTAK-BİDEB for their financial support during this project.

Special thanks to Başak Şentürk, Ezgi Taşkan, Bilge Kabataş, Selinay Şenkal, and all members of the Molecular Diagnostic Laboratory whom I had the pleasure of working and collaborating with.

I would like to acknowledge my dearest friends Merve Yıldırım and Polen Koçak for their love, and support, for being there for me at all times, and for making the past years much more fun throughout the whole process. And I am also thankful for Naz Ünsal, whom I always see as my little sister, for her support and motivation with a heart of pure love.

Finally, I would like to express my deepest appreciation to beloved my family. Words cannot express my gratitude to my marvelous parents Güler Kalkan and Hacı Kalkan, for their unlimited support and endless love; to my precious brother Mert Kalkan, who is the blessing of my life, for making me laugh even in the hardest times and to my sister Serpil Kalkan who always stood by me and provided strength. It would not have been possible to complete my Ph.D. study and accomplish any of my goals without their unlimited contribution and support.

ABSTRACT

INVESTIGATION OF THE POTENTIAL OF POST-TRANSLATIONAL MODIFICATIONS AS BIOMARKERS AND THERAPEUTIC TARGETS FOR AMYOTROPHIC LATERAL SCLEROSIS DISEASE

Amyotrophic lateral sclerosis (ALS) is a neurodegenerative and fatal disease that affects upper and lower motor neurons with damage to the motor neurons in the cortex, brainstem, and spinal cord regions. ALS results in death due to painless and progressive muscle weakness and respiratory failure after progression to paralysis from atrophy. Although there is an increased knowledge about ALS generated in a series of genetic and molecular pathological researches, the aetiology of many ALS cases is still unknown. The diagnosis of ALS is established through a comprehensive evaluation of the patient's medical history and clinical symptoms. These diagnostic methods can take a long time and be quite costly. Thus, the discovery of new biomarkers for the diagnosis of ALS is needed. Some recent studies have shown that post-translational modifications in several proteins may be indicative as biomarkers in the course of neurodegenerative diseases. This study aimed to investigate the post-translational modifications, such as ubiquitination and sumoylation II/III, of the proteins in the central nervous system (CNS) of B6SJL-Tg (SOD1G93A)1Gur /J) transgenic mouse model of ALS, as candidate biomarkers for the diagnosis of ALS. To compare the *in vivo* findings with the *in vitro* model, NSC-34 cells were mutated into $SOD1^{G93A}$ after neural differentiation. Proteome profiling via the 2D-PAGE method showed that there was a significant difference between proteins from 105-day-old transgenic mouse brains and wild-type mouse brains. As a result of LC-MS/MS analysis, this protein was determined to be a Rho-related GTP protein (Rhob). Post-translational modifications of proteins obtained from the *in vivo* and *in vitro* models were analyzed by the Simple Wes method and were found to have no ubiquitination and sumoylation II/III modifications within the range determined according to the target protein.

ÖZET

AMYOTROFİK LATERAL SKLEROZ HASTALIĞI İÇİN OLARAK TRANSLASYON SONRASI MODİFİKASYONLARIN BİYOBELİRTEÇ POTANSİYELİ VE TERAPÖTİK HEDEFLERİNİN İNCELENMESİ

Amyotrofik lateral skleroz (ALS), beyin sapı, korteks ve omurilik bölgelerindeki motor nöronlara zarar vererek üst ve alt motor nöronları etkileyen ölümcül nörodejeneratif bir hastalıktır. ALS, felce yol açan atrofi sonrası ağrısız ve ilerleyici kas güçsüzlüğü ve solunum yetmezliği nedeniyle ölümle sonuçlanır. Bir dizi genetik ve moleküler patolojik çalışmada ALS hakkında artan bir bilgi birikimine rağmen, çok sayıda ALS vakasının sebebi hala bilinmemektedir. Çeşitli sistemleri etkileyen bir hastalık olarak tanımlanan ALS'nin çeşitli faktörlerden kaynaklandığına inanılmaktadır. ALS tanısı hastanın öyküsü ve klinik bulguları ile konur. Bu tanı yöntemleri uzun zaman alabilir ve oldukça maliyetli olabilir. Bu nedenle, ALS için yeni biyobelirteçlerin tanımlanması teşhis için esastır. Son zamanlarda yapılan bazı çalışmalar, biyobelirteç olarak adlandırılan bir dizi proteinin post-translasyonel modifikasyonların, nörodejeneratif hastalıkların seyrinde etkili olabileceğini göstermiştir. Bu çalışmada, B6SJL-Tg (SOD1G93A)1Gur /J) ALS transgenic fare modeli merkezi sinir sistemindeki (MSS) proteinlerin, translasyon sonrası modifikasyonlarının, ubikuitinasyon ve Sumolasyon II/III, biyobelirteç potansiyelinin araştırılması amaçlanmıştır. *In vivo* bulguları *in vitro* modelle karşılaştırmak için NSC-34 hücreleri, nöral farklılaşmadan sonra $SOD1^{G93A}$ mutasyonunaa uğratıldı. 2D-PAGE ile protein profilleme sonucunda, 105 günlük transgenik fare beyinlerinden ve vahşi tip fare beyinlerinden alınan proteinler arasında belirli bir fark oluşturan protein lekeleri tespit edildi ve LC-MS/MS analizlerinin sonunda, bu proteinin Rho ilişkili GTP proteini (Rhob) olduğu saptanmıştır. *In vivo* ve *in vitro* modelden elde edilen proteinlerin translasyon sonrası modifikasyonları, Simple Wes yöntemiyle analiz edilmiş ve hedef protein göre belirlenen aralıkta ubiquitination ve sumoylation II/III modifikasyonlarına sahip olmadığı bulunmuştur.

TABLE OF CONTENTS

LIST OF FIGURES

LIST OF TABLES

LIST OF SYMBOLS/ABBREVIATIONS

ALS	Amyotrophic lateral sclerosis
2-D08	Sumoylation inhibitor
2D-PAGE	Two-dimensional polyacrylamide gel electrophoresis
AMPA	α-amino-3-hydroxy-5-methyl-4-isoxazole propionic acid
atRA	all-trans retinoic acid
BSA	Bovine serum albumin
C21orf2	Chromosome 21 open reading frame 2
C9ORF72	Chromosome 9 open reading frame 72
Cas9	Caspase 9
CCT6A	Chaperonin Containing TCP1 Subunit 6A
cDNA	Complementary DNA
CHMP2B	Charged multivesicular body protein 2B
CK	Creatine kinase
CNS	Central nervous system
CPTAC	Clinical proteomic tumor analysis consortium
DCTN1	Dynactin subunit 1 gene
DH2O	Distilled water
DMEM	Dulbecco's modified eagle medium
DMSO	Dimethyl sulfoxide
DNA	Deoxyribonucleic acid
DNase	Deoxyribonuclease
DUB	Deubiquitinases/deubiquitylases inhibitor
EGFR	Epidermal growth factor receptor
EMG	Electromyography
ER	Endoplasmic
FACS	Fluorescent-activated cell sorting
fALS	Familial amyotrophic lateral sclerosis
FBS	Fetal bovine serum
FDA	U.S. food and drug administration
FTD	Frontotemporal dementia

GAP43	Growth-associated protein 43
GFP	Green fluorescence protein
HbA1c	Glycosylated hemoglobin
HIV	Human immunodeficiency virus
HTLV	Human T cell leukemia virus
IEF	Isoelectric focusing
kDa	Kilodalton
LMN	Lower motor neuron
MAP2	Microtubule-associated protein 2
MAPT	Microtubule-associated protein tau
MND	Motor neuron disease
MRI	Magnetic resonance imaging
NCS	Nerve conduction study
NEAA	Nonessential amino acids
NEFH	Neurofilament heavy chain
NEK1	NIMA-related kinase 1
NS	Neuroscore
OPTN	Optineurin
PBS	Phosphate-buffered saline
PCR	Polymerase chain reaction
PD	Parkinson's disease
PND	Postnatal day
PSA	Penicillin/streptomycin/amphotericin
PTM	Post-translational modification
qPCR	Quantitative polymerase chain reaction
RHOB	Ras homolog family member B
RIPA	Radioimmunoprecipitation assay
RNA	Ribonucleic acid
ROS	Reactive oxygen species
sALS	Sporadic amyotrophic lateral sclerosis
SOD1	Copper/zinc superoxide dismutase
SQSTM1	p62/sequestosome 1
TAE	Tris acetate-EDTA

TBK1	TANK-binding kinase 1
TDP43/TARDBP	Transactive response DNA binding protein 43
TUBA4A	Tubulin 4A
UBQLN2	Ubiquilin 2
UMN	Upper motor neuron
VAPB	VAMP-associated proteins B
VASP	Vasodilator-induced phosphoprotein
VCP	Valosin-containing protein
WES	Simple western system
WT	Wild-type
ZBTB44	Zinc Finger And BTB Domain Containing 44
ZNF	Zinc finger nuclease

1. INTRODUCTION

1.1. DEFINITION OF ALS DISEASE

Amyotrophic lateral sclerosis (ALS), is one of the most lethal neurodegenerative diseases which affect the motor neurons (MNs) [1]. ALS is characterized by progressive MNs degeneration in the brain stem, motor cortex, and spinal cord, causing paralysis of muscles and eventually death [2,3]. The death of MNs in the spinal cord severely impairs basic vital movements, including breathing. Respiratory failure is usually the main reason for the death of ALS patients [1].

The National ALS Registry reports that more than 12,000 people are diagnosed with ALS, with a prevalence of 3.9 cases per 100,000 people in the U.S. The ALS Association also reported that almost 6,000 people have diagnosed with ALS each year [4].

Roughly estimated, it can be said that approximately 1,500 to 4,500 patients are diagnosed with ALS each year in Turkey, and a total of 8000-10000 patients are living with ALS. Today, unfortunately, there is no epidemiological study carried out on ALS disease in Turkey. The majority of individuals diagnosed with ALS, approximately ninety percent, die within a period of 5 to 7 years following the onset of the disease. The remaining ten percent consists of those who live up to 15-20 years and the world's longest-living ALS patient, Stephen Hawking, is the first one with 50 years [5]. Patients who lose their breathing ability require breathing aid equipment, which is crucial for the survival of patients [1].

ALS is described as a fatal neuromuscular disease that is associated with both upper motor neuron (UMN) and lower motor neuron (LMN) degeneration. Since there are glutamatergic connections between upper MNs and lower MNs localizing in the central nervous system (CNS), commands are transferred toward the lower MNs from upper MNs [6]. Upper motor neurons constitute about 150,000 of two billion cells in the brain, which means, mathematically, they could be considered insignificant, however, their function is quite important [7]. Lower MN cell bodies are presented both in the ventral horn of the spinal cord and specific nuclei in the brainstem and thus, similar to upper MNs, are settling within the CNS. Their axonal projections and connection exceeding CNS (Figure 1.1.) is one of the

important properties of LMNs. MNs have cholinergic properties and transfer signals from upper MNs, interneurons (INs), and from sensory neurons (SNs) [6].

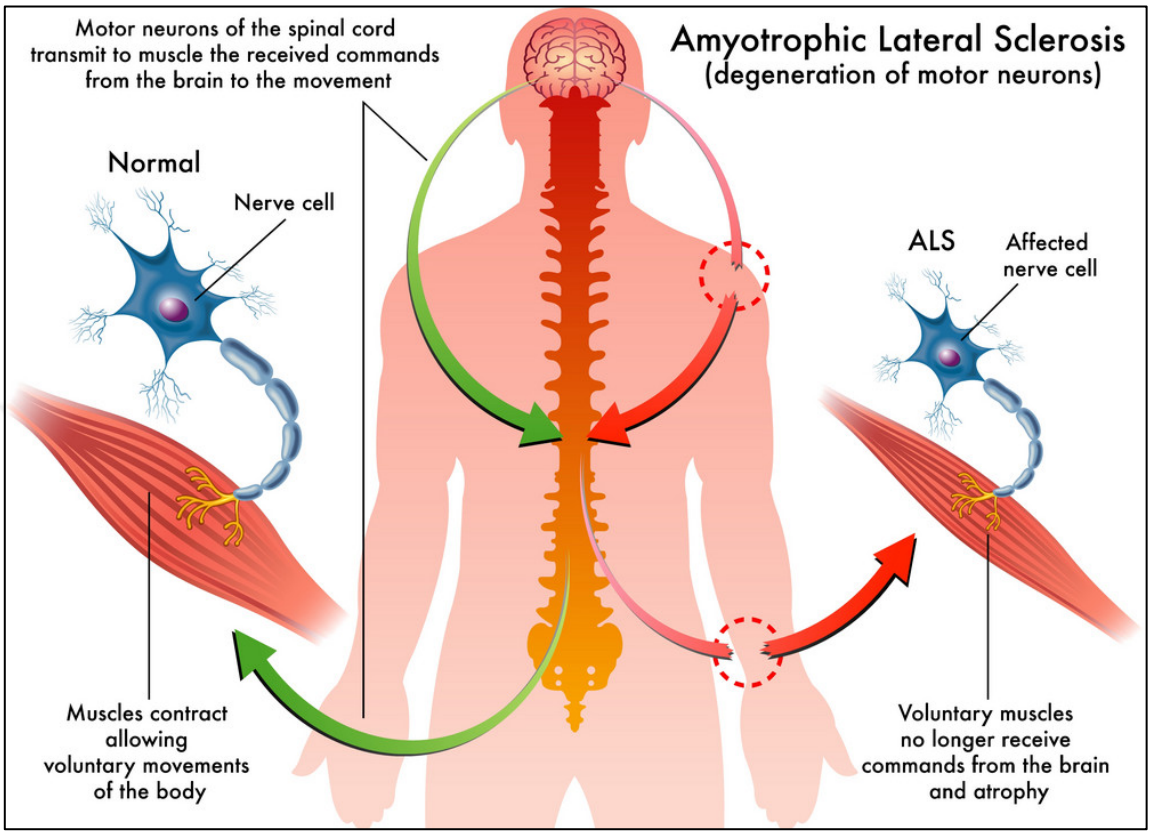

Figure 1.1. Schematic representation of ALS disease [8]

1.2. ALS EPIDEMIOLOGY

As a result of the statistical studies, the incidence, and prevalence of ALS, which vary according to the region, are 1.5 - 2.4 and 4.45 per 100,000 people, respectively. The risk of developing amyotrophic lateral sclerosis increases with age, and this risk is associated with both genetic inheritance and gender [9]. The peak incidence occurs between the ages of 60 and 75. However, this disease is known to affect people of all ages [10].

The heritability is higher in mother-daughter pairs, even though it occurs 20% more frequently in men [11]. The onset age of patients with familial ALS (fALS) is approximately 10 years younger than those with sporadic ALS. Sporadic ALS (sALS) constitutes the major part of cases with 90-95% [12,13]. The residual 5-10% is found as hereditary and familial ALS [14,15]. The average life expectancy is 3-5 years from the onset of symptoms [15,16].

1.3. AETIOLOGY

1.3.1. Non-genetic Factors

Similar to other neurodegenerative disorders, it is widely postulated that ALS arises from a complex interplay of genetic predisposition, triggers from the environment, and age-related malfunction [17]. Historically, epidemiological investigations have primarily centered on examining lifestyle choices and exposure to toxicants as potential risk factors for ALS [18]. The research conducted have identified several risk variables that were studied, such as smoking, physical activity, education level, occupational exposure, dietary habits, and physical fitness. These risk factors have been found to have a causal association, as indicated by the findings of the studies [19].

According to a recent study, the presence of heavy metals in cigarettes has been found to contribute to ALS development by inducing neurotoxicity, oxidative stress, and inflammation [20]. The presence of formaldehyde in the smoke from cigarettes has been linked with higher death risk among individuals. The act of smoking has been widely acknowledged as the foremost non-genetic trigger for ALS [21].

Examining the effect of occupation-related factors on ALS, ALS was found to be associated with occupations involving diesel exhaust, lead, agriculture, and construction. Exposure to pesticides, fertilizers, herbicides, pesticides, and agricultural chemicals such as formaldehyde has been linked to ALS. Long-term formaldehyde exposure was associated with a mortality rate for ALS that was more than 2 times that of those who had not been exposed [21,22].

A relationship between physical activity and ALS risk has not been established, although athletes have a higher risk of ALS. Several genes associated with exercising (ciliary neurotrophic factor, leukemia inhibitory factor, and vascular endothelial growth factor 2) are considered potential risk factors for ALS, and this risk is expected to be higher in athletes [23,24].

High intracellular calcium levels result from glutamate receptor overstimulation, resulting in neuron death. Omega 3 fatty acids, vitamin E, and fiber, which are believed to have anti-inflammatory properties, might have a protective effect, according to studies showing that

consuming high levels of glutamate and fat may have a negative impact on patients with ALS [25,26].

A substantial amount of information about environmental factors is derived from surveys, which rely on the memories of the subjects, resulting in recall bias [19]. Consequently, there may be an absence of data regarding the incidence and quantity of exposure to environmental factors. Further research is required to comprehend these factors and the underlying mechanisms that link ALS.

1.3.2. Genes Involved

Several genes are now known to be associated with ALS, and this number doubles every 4 years [27]. Among these, three major genes have been studied. Mutations have been discovered in each exon of the Copper/Zinc superoxide dismutase gene (SOD1) [28]. Some well-characterized SOD1 variants do not cause a reduction in dismutase activity, but instead, support gain of toxic function [29,30]. The other major gene is TARDBP encoding the TDP-43 protein. TDP-43, a ribonucleoprotein family member, is a DNA and RNA-binding protein. It participates in numerous cellular mechanisms, like gene transcription, microRNA processing, RNA splicing, mRNA transfer, and maintenance. In ALS, ubiquitinated TDP-43 is one of the most common cytoplasmic inclusion components [31]. Studies on the TARDP gene have shown that RNA processing deficiencies are critical for ALS pathogenesis. And these studies also revealed that the TDP-43 inclusions has a prominant function in the pathway of disease along with being a marker of passive neuronal death [32,33]. The third major discovery in ALS was the locus on chromosome 9, which resulted in the discovery of a large expansion of a hexanucleotide repeat in intron 1 of the C9ORF72 gene. The mutation in this gene has been discovered to be the most prevalent cause of ALS; approximately 30% of familial ALS and 10% of sporadic cases [34].

1.3.2.1. *SOD1*

In 1993, Copper/Zinc superoxide dismutase 1 (SOD1) was found as the first gene which is associated with ALS [30]. The SOD1 gene has five short exons that are separated by four introns. One of the three superoxide dismutase enzymes, SOD1, which constitutes

approximately 0.5% of the overall protein content within the human brain, is responsible for converting oxygen and hydrogen peroxide from naturally occurring free superoxide radicals produced by cell metabolism. Wildtype (WT) SOD1 is found in about 0.1% of the cell proteins in the cytoplasm, organelles, and nuclei, therefore, it may be presumed as a relatively abundant amount [35,36].

Each subunit of the ubiquitously expressed 153-amino acid polypeptide SOD1 contains a zinc ion for stabilization and a copper ion for catalysis. These two subunits are packaged and combined with hydrophobic interactions between β-sheet wires to produce an immensely stable dimer. In the disintegration reaction, the superoxide radical undergoes reduction resulting in the formation of hydrogen peroxide. Then, the reduction of the aforementioned compound occurs by the enzymatic action of glutathione peroxidase, resulting in the formation of water. Previously, SOD1 was regarded as a protein localized inside the cytosol, but recent studies uncovered its presence in mitochondria and the intermembrane region of the nucleus. The amino acid sequence of SOD1 has been discovered to be substantially conserved throughout evolution, indicating that SOD1 serves a crucial function [37-39].

SOD1 gene mutations are responsible for 10 to 20% of fALS and 5% of sALS worldwide [35]. Since the discovery of the relationship with the disease, more than a hundred mutations have been announced. In general, mutations are linked to a 50-80% decrease in enzyme activity compared to wild-type activity [30,40].

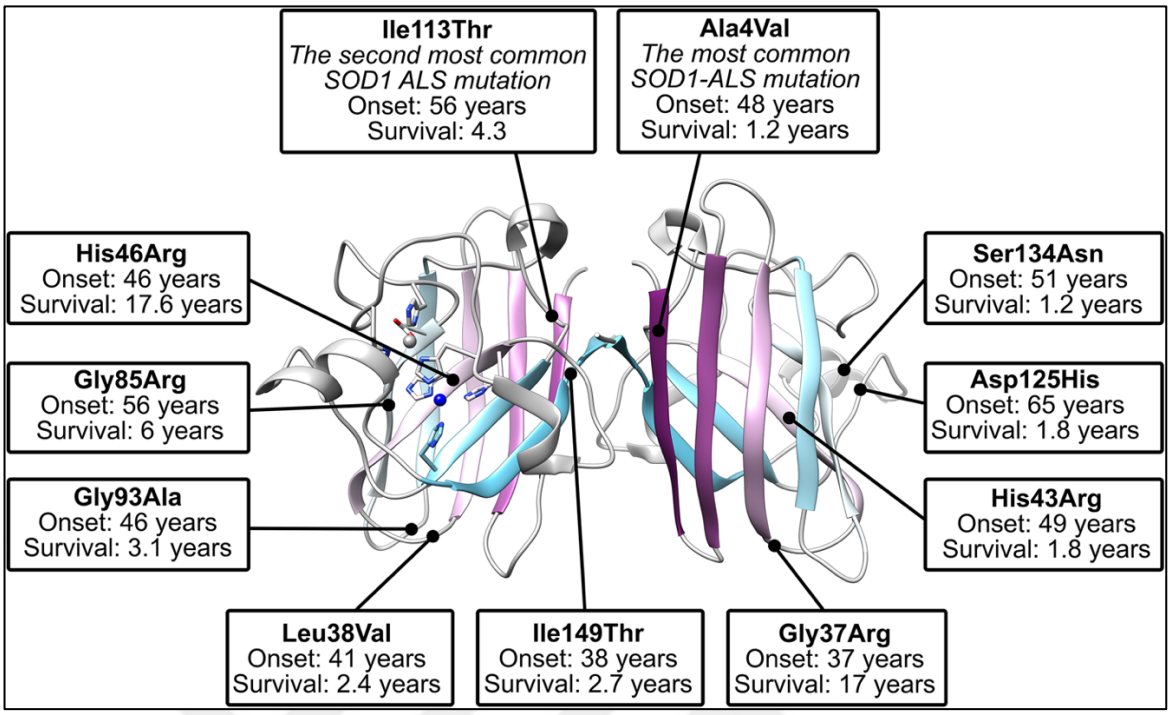

Figure 1.2. Commonly studied ALS mutants within the SOD1 dimer structure [41].

SOD1-related ALS forms have yet to be definitively clarified as to whether they were caused by a loss of enzyme activity, or acquisition of neurotoxic properties. Although it was once believed that decreases in enzymatic dismutase activity promoted oxidative stress and excitotoxicity in MNs, degeneration may be triggered by aggregation of harmful mutant SOD1 protein, which results in inappropriate interaction with mitochondria. SOD1 aggregates are attracted to mitochondria in the spinal cord and crosslinked to membrane components [42-44].

Mutations in SOD1 result in the misfolding of SOD1 polypeptide, which can contribute to the development of aggregates, particularly under conditions of oxidative stress. Mutant SOD1 expression in motor neurons alters illness onset, albeit it is not always sufficient to initiate disease [45-48].

There are more than 170 known missense mutations in SOD1 that result in a toxic gain of function. The A4V mutation is known to be the most prevalent mutation in the United States that causes ALS. After the disease onset, patients with AV4 mutations have a mean survival of only 1,4 years. This mutation type typically damages lower motor neurons and shows fast onset of symptoms and rapid disease development resulting in aggressive phenotype as an outcome of predominantly limb or bulbar muscle weakness [49].

D90A has found to be the most common mutation in Europe. Inheritance pattern of this mutation may be both dominant and recessive, however, it is inherited recessively in the majority of cases. In general, this mutation is associated with a milder disease profile than the A4V SOD1 variation. The late-phase spread of disease to non-motor neurons was discovered in patients with the D90A mutation, resulting in a life expectancy of up to 10 years after the onset of symptoms [50,51].

1.3.2.2. *C9ORF72*

In 2011, DeJesus-Hernandez et al. found that most of the fALS cases were related to a mutation on human chromosome 9. The mutation is caused by the excessive repeated expansion of hexanucleotides in the first intron of the C9ORF72 gene. [52]. Approximately 40% of all diagnosed FALS are related to C9ORF72 mutations as well as frontotemporal dementia (FTD). While the healthy population had the expansion of fewer than 23 repetitions, it was discovered that the affected patients varied in repeat size in different regions of their brains up to 5000. In studies conducted, there was no consistent relationship between repetition size and severity [53].

There are three main hypotheses regarding the role of C9ORF72 in the ALS disease mechanism. The first of these indicates a C9ORF72 loss of function, wherein re-expansions causes reduced regulation of a C9ORF72 contributing to disease. Another theory involves RNA dysregulation, as C9ORF72 patients exhibit nuclear RNA foci. These RNA foci may interfere with healthy RNA homeostasis by directing crucial binding proteins and splicing factors, or they may be hampered by RNA-containing repeats, potentially generating aberrant secondary structures that cause RNA-mediated toxicity. The last theory relates to the accumulation of toxic sensory and antisense repeat proteins as dipeptide repeats which occur in the spinal cord and brain [54].

1.3.2.3. *TARDBP*

TDP43 is known as a major component of the intracellular and cytoplasmic inclusions in neurons and glia of patients diagnosed with sporadic ALS and familial ALS. More than thirty alterations in the TARDBP gene that encodes the TDP43 protein were detected in 3-4% of

FALS patients. Alterations in TARDBP lead to TDP43 hyperphosphorylation and ubiquitin aggregation. Entity of the TDP43 inclusions may cause various proteinopathies [55].

Protein mutations that cause to accumulation of oxidative stress are prevalent in neurodegenerative diseases. TDP43 inclusion formation is induced by glutathione depletion and indicates that TDP43 disorder is linked with reactive oxygen species. In some studies, it was concluded that induced by oxidative stress TDP43 aggregates. These then multiply mRNA molecules, first leading to degradation of the mitochondria and then to neurodegeneration. These findings indicate a potential function of TDP43 inclusions in proteinopathies [33,56].

1.3.2.4. *Other genes*

Mutations in numerous different genes, most of which are inherited autosomally dominantly, have been found in ALS in recent years. Despite their rarity, several of these mutations point to critical disease processes associated with MN susceptibility and degeneration. Several of the genes are involved in protein breakdown, suggesting a key role in defective proteostasis in amyotrophic lateral sclerosis. Optineurin (OPTN), valosin-containing protein (VCP), ubiquitin 2 (UBQLN2), VAMP-associated proteins B and C, Tubulin 4A (TUBA4A), profilin 1 (PFH1), Dynactin subunit 1 gene (DCTN1), chromosome 21 open reading frame 2 (C21orf2) and NIMA-related kinase 1 (NEK1) are all found to be associated with amyotrophic lateral sclerosis [57].

1.4. MODELS OF ALS

1.4.1. SOD1-G93A Mutated Mouse Model

In 1993, Rosen et al. defined the gene encoding Cu/Zn superoxide dismutase 1 (SOD1) as the first gene known to cause amyotrophic lateral sclerosis [30]. Mutations of SOD1 occur in twenty percent of the patient populations diagnosed with fALS. SOD1 is known to be an antioxidant enzyme, but it is still unknown how mutations cause pathology and disease. Through the discovery of the gene related to ALS, technologies of genetic engineering have

been used to generate mouse models to get more information about the pathogenesis of the disease. After the identification of mutations in the SOD1 gene, a transgenic mouse line overexpressing the human SOD1 gene with the G93A mutation, was created and became the first in vivo model of ALS [58]. It remains the most widely used animal model in ALS studies.

These transgenic mice show progressive hindlimb weakness resulting in paralysis and death. The overexpression level of mutant SOD1 is related to the disease onset and shortened life span of the mouse while overexpression of nonmutated SOD1 cause no phenotypic change [59].

SOD1-G93A mice have greatly contributed to the knowledge of astroglia involvement, axonal transformation deficiencies, glutamate toxicity, protein misfolding, and mitochondrial abnormalities [60]. Transgenic mouse develops motor neuron degeneration, depending on their genetic background and leading to paralysis and death after a period of 4 to 5 months. [61].

These transgenic mice are sensitive to changes in the genetic background and have been found to erase the copy number on the germline and therefore have to be rigorously monitored in each generation [59]. To investigate the genetic regions that were sensitive to both initial and progression, a large number of studies were conducted on traditional mapping experiments. SOD1-G93A mice were utilized in preclinical efficacy research and the discovery stages of U.S. Food and Drug Administration (FDA) approved therapies [62].

1.4.2. *In Vitro* Model of ALS: NSC-34 Cells

Various cell line cultures and primary cultures of MNs have been used for the investigation of molecular mechanisms underlying ALS. The NSC-34 cell line is the most widely utilized cell in ALS studies. The NSC-34 cell line is generated by fusing mouse neuroblastoma cell N18TG2 with spinal cord MNs of embryonic mice. There are two types of cells present in an NSC-34 cell culture: smaller, undifferentiated cells with the ability to divide, and larger, multinucleate cells. Choline acetyltransferase and acetylcholine production are two motor neuron characteristics that are expressed by these cells. After being exposed to the differentiation and maturation process, this cell line demonstrates several physiological and

morphological characteristics of MNs [63,64].

In the case of exposure to ALS-CSF, these cells exhibited several abnormal changes, like phosphorylated neurofilament aggregation and increased ER stress [65]. In recent years, the NSC-34 cell line has been identified as an appropriate model for MN-related diseases, particularly ALS, and has been used in many studies [66].

1.5. CLINICAL FEATURES

ALS occurs in many different ways and it has been accepted that different clinical presentations have caused differences in survival for years. Although individuals may have different symptoms, changes occur in their ability to perform daily tasks such as muscle weakness, disturbance in speech, or dressing up shoes or tying shoes. However, over time, frequent falls, slow speechlessness, poor performance in the workplace, and difficulty in catching breath while performing various tasks, are the first symptoms of most ALS cases and are characterized by progressive weakness, atrophy, dysarthria, dysphagia, and hyperreflexia. It is important to acknowledge that clinical characteristics of sporadic and hereditary ALS are similar and can not be distinguished [67,68].

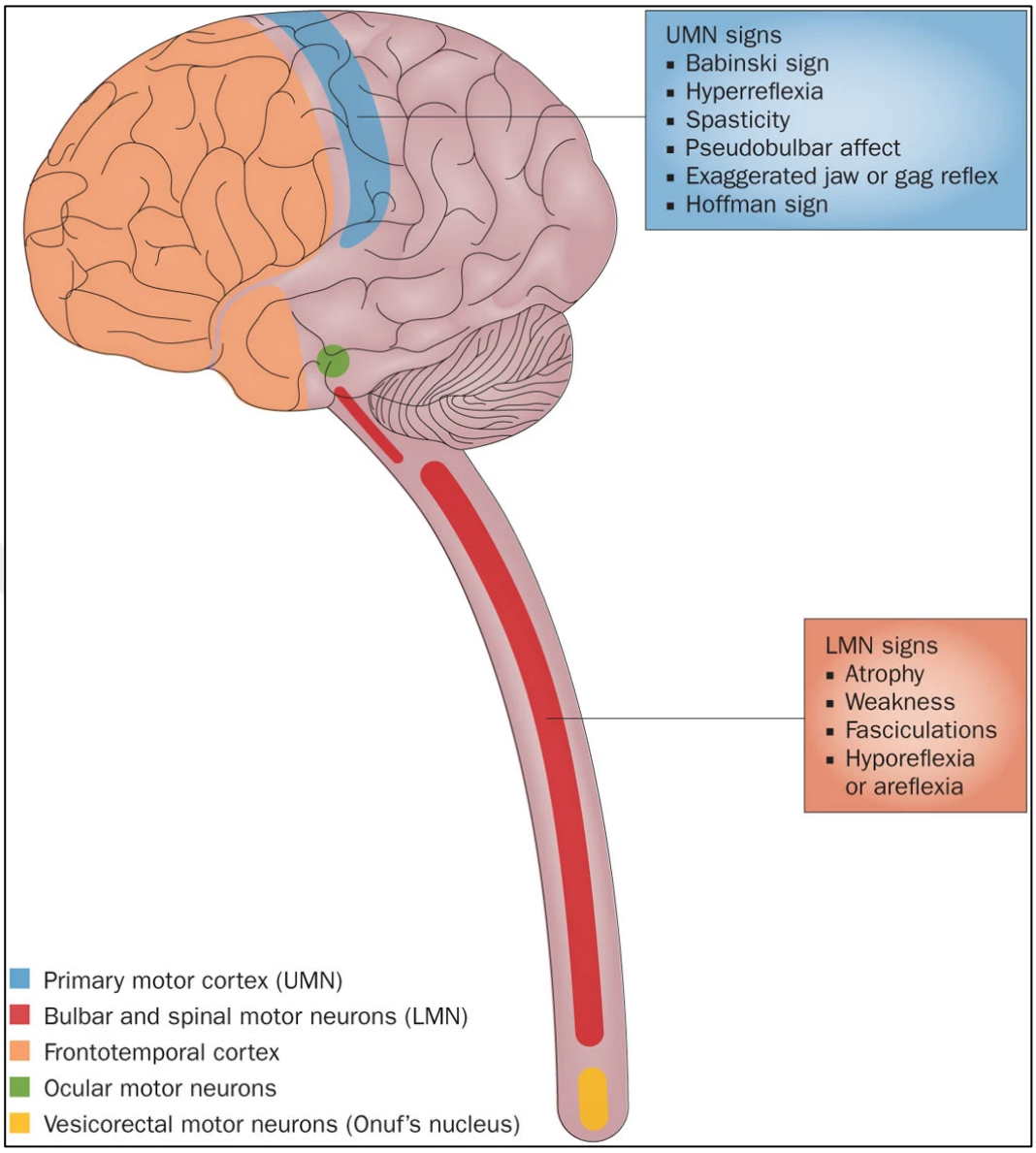

Figure 1.3. Phenotypic variability of UMN and LMN symptoms [69].

The heterogeneity of ALS has been demonstrated in other clinical features such as incidence rate and baseline age. The onset sites can be categorized into three groups bulbar, upper, and lower limb. With the progression of ALS, motor neuron degeneration-related symptoms do not remain confined to the site of onset instead they spread to other sites. [70,71].

However, the only source of variability in clinical features is not the onset site. In addition, patients are classified according to the weakness of motor neurons. The disease is divided into the following subtypes with varying incidence and prognosis: classical, bulbar, pyramidal, respiratory, flail arm, flail limb, lower motor neuron, and upper motor neuron [73].

The rate of progression of amyotrophic lateral sclerosis ALS exhibits variability among individual patients. In older patients with a classical type of disease, age, and bulbar onset were linked to worse prognosis, whereas, younger patients who have the disease with upper motor neuron predominancy had a slower progression [74]. The lower motor neuron type of disease is known to with its poor prognosis as a result of the high risk of thromboembolic disease as a consequence of the complications such as respiratory infection and disability. In general, life expectancy decreases to 2-3 years after the disease begins to involve the respiratory system. [71].

Amyotrophic lateral sclerosis is no longer considered a disease that only causes motor neuron degeneration. While the spatial function and memory are retained, patients exhibit cognitive impairment symptoms and neuropsychiatry such as apathy, anger and empathy loss, increased anxiety, depression, sleep difficulties, and dietary changes. Over time, executive dysfunction, which is seen as an adverse prognostic indication, tends to deteriorate. Patients may develop cognitive impairment with time, which may be related to poor motor function [75-77].

1.6. DIAGNOSIS

There is no singular test that can definitively diagnose ALS. Initial diagnosis is based on a patient's detailed medical history, symptoms observed during a physical examination, and various tests to rule out other mimetic diseases. On the other hand, symptoms affecting both the LMNs and/or the UMNs are strong indicators that the disease is present [78].

The diagnostic procedure consists of three steps. A consultation with a neurologist is always the initial step in any investigation. Following an in-depth review of the medical history of patients, the neurologist will perform a comprehensive physical examination that will emphasize the patient's muscle strength, reflexes, coordination, and sensation. The neurologist also continues to make neurological examinations at regular intervals to monitor the development and progression of symptoms such as muscle weakness, muscle atrophy, and spasticity [79].

Some of the common ALS features to be assessed during the neurologist's examination include loss of control of some emotional responses, loss of judgment abilities, muscle

weakness, LMN features such as muscle shrinkage, and UMN features such as hyperactive reflexes. In addition, the neurologist also documents changes in the individual's speech pattern. This examination evaluates the tongue and the muscles involved in biting and swallowing [78,79].

In the initial phases of the ALs, distinguishing the symptoms of ALS from those of other treatable disorders can be difficult because these symptoms can resemble. In most cases, a neurologist will conduct various tests to exclude any other potential causes of the symptoms [80].

The time required for confirming a diagnosis will depend on the symptom type, progression rate, and alternative diagnoses that must be excluded. After conducting these tests, ALS may still be difficult to diagnose. Consequently, patients are typically referred to a neuromuscular specialist. When presenting a second opinion to confirm a diagnosis, the neuromuscular specialist may also require repeating some previous tests to determine if there has been a change over time [81].

The subsequent stage in the diagnostic procedure typically involves a series of tests including magnetic resonance imaging (MRI) of the head, neck as well as lower vertebrae; electromyography (EMG) for testing nerve conductions; and numerous blood, urine, and genetic tests [79,82].

1.6.1. Electromyography (EMG)

Electromyography (EMG) is an important step in the diagnosis process since it uses a unique recording technology to measure the electrical activity of muscle fibers. The initial stage in electromyography (EMG) is to give the nerves a series of mild electric shocks to determine whether or not there is any nerve damage and to assess the speed that signals are sent to the muscle. This test determines whether the patient has nerve blocks, which is a feature of multifocal motor neuropathy illness. Additionally, this test establishes whether the sensory conducting nerves are impaired, which might represent neurological diseases other than ALS [83].

In the following step of the procedure, the electrical activity of the various muscles under investigation is evaluated. To accomplish this, a quite fine needle is inserted into the targeted

muscles for analyzing the pattern of electrical activity inside those muscles. This step of the EMG does not involve an electric stimulus [83].

Nerve conduction study (NCS) is one other regular test, that uses electrical activity measurements from the nerves and muscles to determine how effectively the nerves can send signals to the muscles. Some particular anomalies in NCS and EMG could point to a peripheral neuropathy or myopathy muscle disease rather than amyotrophic lateral sclerosis. Although magnetic resonance imaging scans are used as non-invasive techniques in addition to electromyography and nerve conduction studies, they often show normal results in patients with ALS [84].

1.6.2. Additional tests

To avoid misdiagnosis, a physician may request additional blood or urine tests according to the patient's symptoms, and previous results of tests and examinations. In some cases, some viruses such as human immunodeficiency virus (HIV), human T cell leukemia virus or poliovirus may exhibit symptoms that closely resemble ALS. Many neurological diseases, like multiple sclerosis (MS), post-polio syndrome, and frontotemporal dementia (FTD), are known to share similarities with specific characteristics of the disease [85,86].

For some cases, a lumbar puncture may be necessary in case of the patient shows atypical ALS characteristics, like spinal nerve abnormalities or spasticity symptoms. In addition, a muscle biopsy might be required to diagnose muscular diseases in some patients with uncommon paralysis, pain, or extremely increased creatine kinase (CK) levels. It is not recommended to conduct genetic testing for ALS unless the patient’s family has a disease history [87].

The third and last step in diagnosing ALS is accomplished once the results of these tests are collected and the neurologist has determined whether or not the patient suffers from ALS. In certain cases, due to the absence of the symptoms needed to accomplish the diagnosis, which is especially common at the earlier stages of the ALS. In this scenario, neurologists would need to do these tests and examinations regularly to monitor any changes that may occur over time [79].

1.7. ALS BIOMARKERS

In population-based ALS studies, in many patients, a definite diagnosis is made approximately one year after the onset of symptoms, which prevents/does not allow early treatment with a disease-modifying drug. Additionally, some of the anterior horn neurons are considered to be degenerated when distal muscle wasting is observable. Accordingly, if degeneration is unrecoverable at that stage, it may not be enough to rely on symptoms and clinical examination to trigger intervention. Therefore, biomarkers for early diagnosis may be beneficial if the risk of ALS progression can be diagnosed before the disease onset [88]. In addition to being critical for proper patient registration in clinical studies, an early and precise diagnosis is necessary for providing specialized treatment for ALS patients [89].

ALS biomarker sources include a range of human bio-liquids, CSF, blood, saliva, and urine. CSF is known as the perfect bio-fluid in terms of biomarker potential due to its approach to cells that show cell death during ALS and to the central nervous system regions. While blood is prominent with the advantage of being more accessible, in comparison to CSF, the proteins associated with the neuronal activity have higher degree of protein complexity, accompanied by decreased concentrations [90].

Over the past decades, the biomarker studies of ALS using CSF and blood have increased in number. These studies compared changes in proteins in the CSF of patients, compared to healthy control or neurological disease subjects other than ALS, with the help of gel-based systems and ELISA [91].

In CSF, increased interleukin 6, interleukin 8, complement 3, prostaglandin E2, major cationic protein1, peroxynitrite, and neopterin levels have been demonstrated [92]. Activated microglial cells/macrophages have also increased the release of cyclooxygenase 2, cannabinoid receptor type 2, and purinergic receptor P2X7 in the inflammatory cascade. Identification of antineuronal antigens against GM1 gangliosides and sulfides in CSF has been demonstrated in a study and may suggest that an autoimmune mechanism may cause motor neuron degeneration [93,94].

Many studies are showing increased oxidative damage metabolites in postmortem neuronal tissues of sALS and fALS cases. Increased protein carbonyl levels were seen in the central nervous system materials [95]. Increased levels of 4-hydroxy-2,3-trans-nonenal levels due

to oxidative stress in lipids within the CSF are consistent with the intensity of the disease, yet not compatible with its progression. At the same time, the protein nitration marker 3-nitrotyrosine, which is formed by tyrosine and peroxynitrite reaction, has increased in the CSF of ALS patients and is compatible with clinical findings [96,97].

Excessive and long-term stimulation by glutamate results in the persistence of calcium passage throughout the α-amino-3-hydroxy-5-methyl-4-isoxazole propionic acid (AMPA) receptors, which are permeable to calcium in motor neurons and cause death. When calcium flow exceeds the buffering capacity of mitochondria, it stimulates the production of reactive oxygen species (ROS) by disrupting protein balance and activating apoptosis mechanisms [98,99].

It can also be mentioned that the muscles also provide information about the disease. In addition, transcriptomic studies have also been of great benefit in early and late-stage patients. Nevertheless, these examinations are not performed in the earlier stages since the removal of muscle tissue is a painful and invasive method [100].

However, the number of samples used in most analyzes is limited to the selection of control subjects and lack of validation in a different patient cohort. Early alterations in patient metabolism as well as protein levels and post-translational modifications can be an important tool to identify biomarkers to detect ALS at the earlier phases of disease and to monitor during disease progression [89].

1.8. POST-TRANSLATIONAL MODIFICATIONS

The proteome of a cell contains a greater number of proteins than predicted based on the number of genes encoding proteins. Various processes account for this discrepancy. Post-translational modification, often known as PTM, is a later stage in the process of protein synthesis. It refers to the chemical modifications, either reversible or irreversible, that can occur in proteins following the translation step. These alterations encompass the enzymatic hydrolysis of peptide linkages, as well as the incorporation of distinct chemical groups, lipids, carbohydrates, and entire proteins onto the side chains of amino acids. The alterations of polypeptide chains broaden the variety of structures and properties of amino acids, thus diversifying the structure and function of proteins. [101].

The generation of functional protein is distinct from the process of protein synthesis. For polypeptides to function, they must be transformed into specific three-dimensional structures. Furthermore, many proteins must undergo PTM processes to acquire their functional properties. Examples of such alterations include the addition of small molecules like phosphate and methyl, as well as the covalent bonding of complex molecules like carbohydrates and lipids. Enzymes catalyze the reaction wherein the modifying molecules attach to specific amino acids on the protein [102].

These modifications are usually reversible. Particular enzymes perform the modification process. This enables the cell to quickly regulate the protein activity in response to a stimulant. Cleavage of the peptide bond is another kind of PTM. This process is carried out predominantly by proteases and infrequently by autocatalysis. Different organelles of the cell are capable of undergoing PTM processes. In general, PTM is rapid, reversible, time- and location-dependent but these properties vary with the nature of the modification [103,104].

PTM is utilized for various reasons in multiple processes in cells. Enzyme regulation, intracellular protein localization, protein-protein interaction, intracellular signal transfection, and cell division can be counted among these processes. Hundreds of PTMs are estimated to exist within the cell [101]. The addition of chemical groups like phosphate, methyl, and hydroxyl, the addition of more complex compounds like lipid and sugar, and the addition of tiny peptides like ubiquitin are some of the most commonly reported and reasonably well-characterized PTMs [105]. Some proteins can contain multiple and distinct PTM modifications simultaneously. Analyses using mass spectrophotometry, for instance, uncovered the fact that various kinds of modifications to the p53 tumor suppressor were carried out in each of the 50 different amino acids. If it is assumed that the variety and number of PTMs on a protein at any given time dictate its function, it is easy to comprehend that the effect of PTM on a protein like p53 can be quite complex [106].

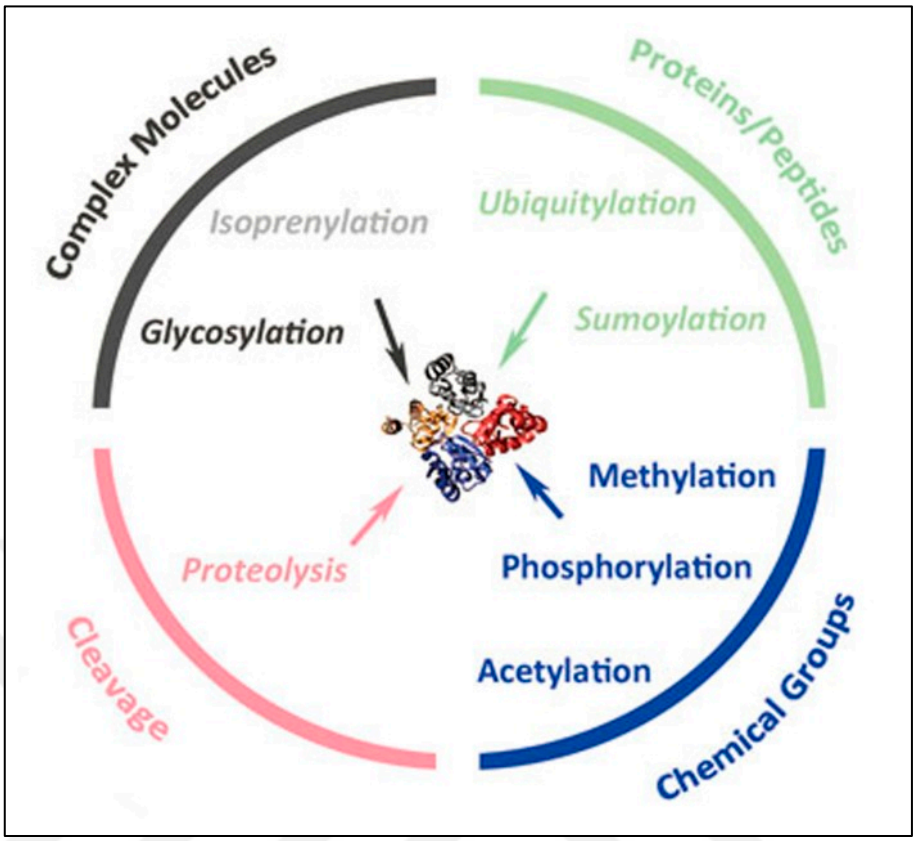

Figure 1.4. Types of post-translational modifications [107]

1.8.1. Ubiquitylation

Ubiquitylation has important functions in the regulation of numerous cellular activities. Examples of these activities include protein degradation, signal transmission, intracellular localization, and DNA repair [108].

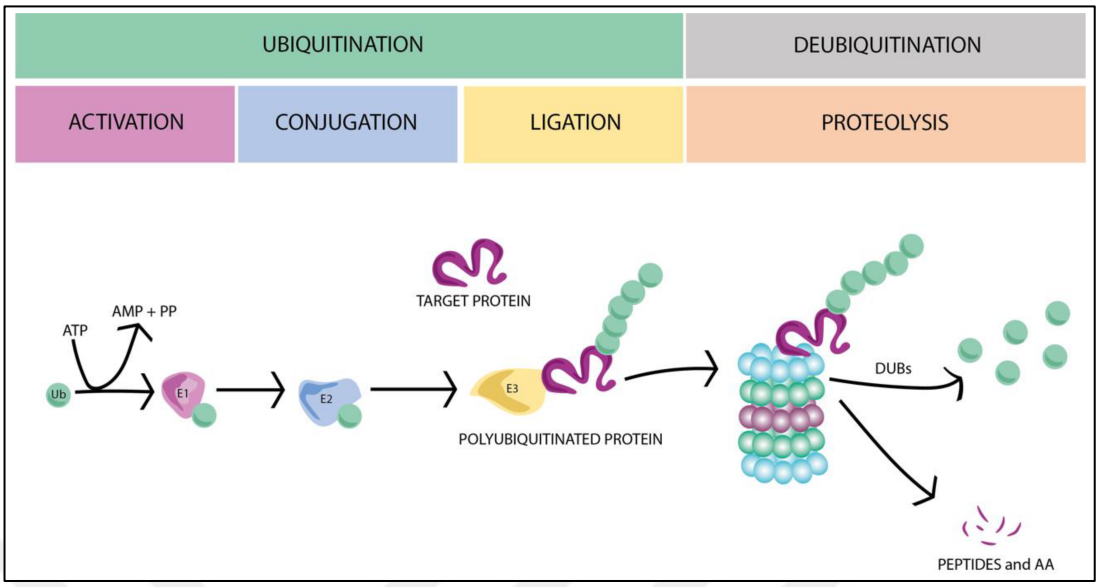

Figure 1.5. Ubiquitin-proteasome system [109]

Ubiquitylation occurs by covalently binding the 76-amino acid-sized ubiquitin protein to the target protein. Three different enzymes, E1-ubiquitin activating enzyme, E2-ubiquitin conjugating enzyme, and E3-ubiquitin ligase, are responsible for this lysine process. The E3 enzyme, which is found in hundreds of different eukaryotic organisms, is responsible for determining the specificity of the target protein [108].

The most prevalent function of ubiquitylation of proteins is that the corresponding proteins function as a signal for 26S proteasomes to cleave them. To enable a protein to be cleaved in this manner by the proteasome, it is frequently necessary to covalently bind multiple ubiquitins to its terminal, a process known as polyubiquitylation. A particular lysine amino acid on ubiquitin proteins is responsible for polyubiquitylation. In addition, pathogens commonly use ubiquitylation to reorganize certain elements in the host organism. Although some pathogen proteins possess E3 enzyme activity, some pathogens modify the activity of E3 enzymes in the host organism and direct them to novel protein targets [110].

1.8.2. Sumoylation

The SUMO proteins and the post-translational modification cycle both take on crucial tasks for the cell once they have been notified of their presence. Abnormalities in the sumoylation cycle, which can affect either the central or the peripheral nervous system, have recently become interesting and have been the subject of research. The discovery of link between SUMO proteins and neurodegenerative diseases that affect the CNS has been discovered in several investigations [111].

SUMO proteins are inactive when they are not functioning, and their expression from SUMO genes produces precursor molecules that are also inactive. In the presence of a cellular stimulus, the E1 enzyme (activating enzyme) is required for the activation of SUMO proteins. The E1 (conjugating enzyme, Ubc9) enzyme is activated, and the E3 (Ligase) enzyme binds to the SUMO target protein, allowing SUMOs activated by the E1 enzyme to bind to their targets. When the sumoylation effect of the SUMO protein has ceased, SENP enzymes separate SUMO and the target protein [112].

Reversible covalent bonds between SUMO proteins and lysine groups in target proteins are one type of post-translational modification. SUMOs can also form non-covalent bonds between a large number of proteins. It was identified that mediators known as SIMs, which stand for the Sumo interaction motif, were involved in these non-covalent connections. SIM-formed bonds are present in the proteins of nerve cells and synaptic proteins. Sumoylation is essential for the survival of cells. Sumoylation allows SUMO proteins to accomplish their biochemical functions [113].

1.9. POST-TRANSLATIONAL MODIFICATIONS AS BIOMARKERS

Modifications to the metabolome and proteome are necessary to maintain cellular homeostasis. Post-translational modifications (PTMs) can modify protein abundance, protein activity, protein function, protein-protein interactions, and protein localization at the proteome level. Since all of the proteins have the potential to be modified after translation, the role of PTMs as the keys to cellular homeostasis is essential to the pathogenesis as both markers and drivers, ensuring that abnormal PTM patterns are linked with a variety of

diseases [114].

Investigation of disease mechanisms has long been aided by cell culture and animal models. Nevertheless, omic-based investigations require the analysis of clinical specimens. In disease models and clinical samples, PTMs for the sensitive drug can be identified. A wide variety of PTM analyses have been developed, and certain alterations in PTMs have been identified as possible biomarkers to this day. To conduct PTM-specific research, it is necessary to verify potential biomarkers and corresponding analyses [115].

One instance of a post-translational modification (PTM) that has promise as a biomarker for chronic heart failure (CHF) is the phosphorylation of cardiac troponin I (cTnI). In a study, top-down quantitative proteomics approach was utilized to identify the phosphorylation of cTnI as a potential biomarker for chronic heart failure (CHF). The methods used by the researchers aimed to conduct a complete assessment of post-translational modifications (PTMs) in proteins isolated from both normal and diseased tissues. This study discovered a correlation between the phosphorylation of cTnI and congestive heart failure (CHF), indicating its potential utility as a biomarker for this particular medical disease [116].

During antiplatelet treatment, the levels of phosphorylation of vasodilator-induced phosphoprotein (VASP) are examined. These levels serve as an indicator of P2Y12 receptor inhibition. Blood types are determined by the unique glycan structures that are found on the surface of red blood cells. In addition, there is a comprehensive list of putative biomarkers that have been described in the scientific literature, and the diagnostic or predictive value of these biomarkers is still being validated in several different instances [117].

When the complexities of human health and disease are considered, it is generally agreed that a single molecule cannot adequately serve as a precise biomarker to predict diagnosis. Recent studies have shown that protein expression and the study of PTMs are useful in merging many levels of omics [118].

One other example of a post-translational modification (PTM) that has been subject to investigation as a potential biomarker is to glycosylation in the context of hepatocellular carcinoma (HCC) associated with hepatitis B virus. The utilization of glycosylation as a means of post-translational modification has been examined as a novel approach for identifying biomarkers associated with liver illnesses, such as hepatocellular carcinoma (HCC). The authors proposed that, apart from tumor markers, several other factors such as

HBV genotype, HBV genomic alterations, host genome mutations in HBV-infected hepatocytes, and gene expression patterns of HCC cells could potentially function as candidate biomarkers for HBV-related hepatocellular carcinoma (HCC). According to this study, these post-translational modifications (PTMs), in conjunction with other biomarkers, has the capability to forecast the prognosis of hepatocellular carcinoma (HCC) patients. [119].

The investigation of phosphorylation of β-amyloid aggregates has also been conducted as a potential biomarker for neurodegenerative diseases, with a specific emphasis on Alzheimer's disease (AD). The recent study revealed that phosphorylation has the ability to alter the molecular stability of β-amyloid plaques. The present study examines the potential impact of the PTM on the aggregation and toxicity of β-amyloid, a hallmark feature associated with Alzheimer's disease. The comprehension of the significance of phosphorylation in the pathogenesis of neurodegenerative conditions has the potential to offer valuable insights into the evolution of these diseases and facilitate the development of precise therapeutic interventions. [120].

2. AIM OF STUDY

The diagnosis of ALS is determined by the patient's medical history and clinical manifestations. These diagnostic procedures are time-consuming in addition to being expensive. Several methods for optimizing and shortening these diagnostic methods have been proposed, and it has been seen that a robust biomarker will have an important value for ALS diagnosis. Due to the lack of objective molecular markers for ALS, a definitive diagnosis cannot be made until the disease has progressed. There is an intense need for disease-sensitive biomarkers in the diagnosis of ALS. In some of the recent research, post-translational modifications are effective in the course of neurodegenerative diseases in several proteins designated as biomarker candidates.

In this study, we have aimed to detect potential ALS biomarker candidates by profiling proteins and also comparing post-translational modification differences of proteins derived from the ALS-like NSC-34 cell line and also CNS tissues of both healthy mice and the B6SJL-Tg (SOD1G93A) transgenic mouse model. In addition to potential biomarker research, the search for the target proteins identified as a result of this study may also be important in future studies for understanding the molecular mechanisms that cause motor neuron degeneration and finding new targets in drug development.

3. MATERIALS AND METHODS

3.1. ETHICAL APPROVAL

Approval from the Institutional Animal Care and Welfare Committee of Yeditepe University (Turkey) was been received for animal procedures before initiating the study.

3.2. ANIMAL SELECTION

Transgenic mouse line B6SJL-Tg(SOD1G93A)1Gur/J) expressing G93A mutated SOD1 gene was purchased from the Jackson Laboratory (Bar Harbor, ME, USA). Six weeks-old male transgenic and female wild-type C57BL6/J mice were bred. Mice were fed ad libitum and had unfettered water access under a 12:12-hour light/dark cycle at 20-23°C [121].

3.3. GENOTYPING

Material for genotyping was derived from DNA isolated from mouse ear clippings, and genotyping was performed by conventional polymerase chain reaction (PCR) via CFX96 Touch Real-Time PCR detection system (Bio-Rad, Hercules, CA) by using particular primers as specified by The Jackson Laboratory and Q5 Hot Start High-Fidelity 2X Master Mix (# M0270L, New England Biolabs, MA, USA) with 10 ng template DNA. The primers and reagents utilized throughout the PCR technique are listed in Tables 2.1 and 2.2. The PCR conditions are listed in Table 2.3.

Table 3.1. Information about the primers used in transgenic mice genotyping

Primer Name	**Forward primer Sequence**	**Reverse primer Sequence**	**Product Length**
Internal Positive Control Primers for *SOD1* gene	5'CTA GGC CAC AGA ATT GAA AGA TCT'3	5'GTA GGT GGA AAT TCT AGC ATC ATC C '3	324 base pair
Transgene Primers for *SOD1* gene	5' CAT CAG CCC TAA TCC ATC TGA'3	5' CGC GAC TAA CAA TCA AAG TGA'3	236 base pair

Table 3.2. PCR mixture content

Component	**Volume**	**Final Concentration**
Q5 Hot Start High-Fidelity 2X Master Mix	10 µl	1X
Forward Primer	1 µl	0.5 µM
Reverse Primer	1 µl	0.5 µM
Internal Positive Control Forward Primer	1 µl	0.5 µM
Template DNA (10 ng)	5 µl	
dH_2O	1 µl	
Total volume	20 µl	

Table 3.3. Experimental protocol for standard PCR

Pre-denaturation	95°C	5 minutes
Denaturation	95°C	30 seconds
Annealing	60°C x 30	30 seconds
Extension	72°C	30 seconds
Last extension	72°C	2 minutes

TAE buffer was used to generate a 2.5% agarose gel for loading the PCR products. Samples were run at 110 volts for 35 minutes, and the gel was analyzed under UV with Bio-Rad ChemiDoc (Bio-Rad, Hercules, CA) and Image Lab Software.

3.4. NEUROSCORING OF TRANSGENIC MOUSE MODEL

The motor activity of SOD1 transgenic animals was examined to determine the staging of the disease when early and late symptoms began to develop following animal birth, as was formerly done with SOD1-G93A mutation (+) transgenic mice. According to the onset of early and late symptoms of the disease, two-time points for sample collection were identified, and protein samples were collected at these two-time points. Using the NeuroScore (NS) scoring model [121] the disease progression was evaluated, as described in the literature.

NeuroScore system primarily focuses on the daily progression of hindlimb dysfunction induced by hindlimb deficits, which are considered the initial symptom of disease in SOD1-G93A mice. The system allows for accurate observation of the beginning of paresis, disease progression, and intensity [121]. The brain scores of each mouse were determined through daily observation of their performance on tests described below.

1. The mouse was suspended by its tail from the top of the cage for one to two seconds. Meanwhile, the tremor and retraction of the hindlimbs were evaluated. To maintain accuracy, the test was conducted three times, and the associated observations were recorded.

2. The stride of the mouse was observed while traveling across a smooth, clean surface, with a minimum walking distance of 25 centimeters.

3. The mouse was turned on its right and left sides, and the time it took to right itself without assistance was measured in the "righting reflex" test.

Following the results of these tests, the intensity of the symptoms exhibited by the animals was graded between 0 and 4 using the scale described below.

• NS0 (Presymptomatic): When a mouse is suspended by its tail, its hindlimbs can often extend from the lateral midline to the side and can keep its posture straight for a minimum of two seconds. The mouse is capable of walking normally when permitted.

• NS1 (Initial symptoms): When a mouse is suspended and held by the tail, its hindlimbs are unable to expand entirely from the lateral midline, are partially closed backward, or tremble. Its gait is either unaffected or a little slowed.

• NS2 (Paresis): When a mouse is suspended by its tail, its hindlimbs are closed or unable to open considerably. Once the mouse is tilted to the right or left, it requires about 10 seconds to self-correct its position. During walking, the toes are observed to be bent backward at least twice.

• NS3 (Paralysis): The mouse's hindlimbs are paralyzed or barely move at all while it is hanging on its tail. When permitted to walk, the mouse can move forward but is unable to use its hindlimbs. It has been observed that a mouse can show a righting reflex within 10 seconds when it leans to the right or left.

• NS4 (Human endpoint): The hindlimbs of a mouse completely paralyze when it is held by its tail. The righting reflex vanishes when the mouse is allowed to walk once it has been tilted to the right or left.

Mice were slaughtered at the outset of the NS1 phase (early-onset) on postnatal day 105 (PND 105) and also at the outset of the NS0 phase on postnatal day 60 (PND60) which was considered a pre-symptomatic period. As indicated in Table 2.4, the experimental process was carried out in six groups. Groups were adjusted according to tissue sample, genotype, and disease onsets. Two tissues were collected from each of six wild-type, 60-day-old and 105-day-old $SOD1^{G93A}$ mutated transgenic mice. A total of 16 mice were used and 32 tissues

were obtained.

Table 3.4. Information about the animal groups used in the experiments

Genotype	Tissue	Age	Number of Mice	Number of Tissue
Wild Type	Brain	105	6	6
Wild Type	Spinal Cord	105		6
$SOD1^{G93A}$	Brain	60	4	6
$SOD1^{G93A}$	Spinal Cord	60		6
$SOD1^{G93A}$	Brain	105	6	6
$SOD1^{G93A}$	Spinal Cord	105		6
TOTAL			16	32

3.5. CULTURE OF NSC-34 CELLS

The NSC-34 cell line (#CLU140, Cedarlane, CELLutions Biosystems, Burlington, CA) was chosen as an MN-like cell model. NSC-34 cells were cultured in a proliferation medium comprised of Dulbecco's Modified Eagle's Medium/high-glucose (DMEM/high-glucose, #11965092, Thermo-Fisher Scientific, Gibco, Waltham, MA, USA) supplemented with 10% of Fetal Bovine Serum (FBS) (#10500-056, Thermo Fisher Scientific, Gibco, Waltham, MA, USA), 1% of Penicillin/Streptomycin/Amphotericin (PSA) (#15140-122, Thermo Fisher Scientific, Gibco, Waltham, MA, USA). All *in-vitro* cell culture experiments were performed in a Laminar Flow Cabin (Heal Force Class II Biosafety Cabinet A2, China). And cells were incubated in the humidified incubator at 37°C, with 5% (v/v) CO_2 and 95% (v/v) air conditions.

NSC-34 cells were subcultured at 80% confluency. Phosphate Buffered Saline (PBS, 1X) was used to wash the cells (#BE17-517Q, Lonza, Switzerland) and cells were detached from the cell culture flask by incubating with 0.05% (w/v) Trypsin-EDTA (0.25%, (#25200056, Thermo-Fisher Scientific, Gibco, Waltham, MA, USA) for 5 minutes at 37°C. DMEM/high medium with 10% FBS was added with a 1:2 ratio at the end of incubation time. Then cell

suspension was centrifuged at 1300 rpm for 5 minutes. The appropriate amount of complete medium was added to the pellet and cells were diluted in fresh media right before being seeded in a suitable cell culture flask.

NSC-34 cells were seeded as 5000 cell/m2 with differentiation medium consisting of DMEM/Ham's F12 Plus medium, (#10565018, Thermo Fisher Scientific, Gibco, Waltham, MA, USA) 1% of FBS, 1% of modified Eagle's medium nonessential amino acids (NEAA) (#11140050, Thermo Fisher Scientific, Gibco, Waltham, MA, USA), 0.5% of PSA and 1 lM all-trans retinoic acid (atRA) (#R2625, Merck, Sigma Aldrich, NJ, USA). Cells were incubated for 8 days. Fresh differentiation medium was exchanged every 2 days until the differentiation process was completed.

Cell number was counted 24 hours after plating and after 2, 4, 6, and 8 days of differentiation using a 1:1 ratio of cell suspension:Trypan Blue Solution (#T10282, Thermo Fisher Scientific, Invitrogen, Waltham, MA, USA) in total volume of 10 µl with help of Countess cell counting chamber slides (#C10228, Thermo-Fisher Scientific, Invitrogen, Waltham, MA, USA) and Countess II FL system (Thermo-Fisher Scientific, Invitrogen, Waltham, MA, USA).

3.6. RNA EXTRACTION AND RT- PCR

Total RNA was extracted from both differentiated and undifferentiated NSC-34 cells. Trizol reagent (#15596026, Thermo-Fisher Scientific, Ambion, Waltham, MA, USA) was used for RNA phase separation, and the RNA isolation procedure was continued with RNAqueous - Micro Total RNA Isolation Kit (#AM1931, Thermo-Fisher Scientific, Invitrogen, Waltham, MA, USA) according to the manufacturer's instructions. Concentrations of isolated RNA were measured by using Nanodrop 2000 UV-Vis Spectrophotometer (#ND-2000, Thermo-Fisher Scientific, Waltham, MA, USA). Subsequently, 5 ng of RNA was reverse transcribed into cDNA using a QuantiTect Reverse Transcription kit (#205311, Qiagen, Hilden, Germany).

3.7. Q-PCR

Expression levels of neırural marker genes were measured with quantitative polymerase chain reaction (qPCR) by using, iTaq Universal SYBR Green supermix (#1725124, Biorad, Germany) via CFX96 Real-Time System (#1845096, Biorad, Germany). Protocol was performed according to the instructor's manual with the primers listed below in Table 2.5. where "F" and "R" refer to forward and reverse primers respectively.

Table 3.5. Primer list of qPCR analysis

Primer Name	F/R	Sequence
ChAt_F	F	ccaaccaagccaagcaatct
ChAt_R	R	aaggataggggagcagcaacaa
18S rRNA_F	F	cggctaccacatccaaggaa
rRNA_R	R	gctggaattaccgcggct
MAPT_F	F	aaggggtattgggcagaagg
MAPT_R	R	cttttcctgtgggagcgaag
MAP2_F	F	tgccacctgtttctctccac
MAP2_R	R	tcttttgcttgctcgggatt
GAP-43_F	F	taaggaaagtgcccgacagg
GAP-43_R	R	tgagcaggacaggagaggaaa
AChE_F	F	accttccctggcttttccac
AChE_R	R	gcatccaacactcctgacca

3.8. TISSUE AND PROTEIN ISOLATION

The study was performed within 3 groups wild-type control, SOD1-G93A mutated pre-symptomatic, and SOD1-G93A symptomatic. The age of the experimental animals was determined as 60 days, before the beginning of the disease symptoms, and 105 days as the symptoms were observed for the SOD1 transgenic model.

Mice were anesthetized with Sevarone (#4456, Getz Pharma, Pakistan) and decapitated. Brains and spinal cords were microdissected and collected. Immediately after dissection, brains and spinal cords were exposed to liquid nitrogen and stored at -80^{o}C for the long term.

Proteins in brain and spinal cord tissues were isolated by using homogenizer-assisted extraction. Tissues were cut into small pieces and lysis buffer, containing radioimmunoprecipitation assay (RIPA) buffer (#89900, ThermoFisher Scientific, Waltham, MA, USA) deubiquitinases/deubiquitylases inhibitor (DUB) (#SI9619, Life Sensors, PA, USA), 2-D08 Sumoylation Inhibitor (#HY-11416, MedChemExpress, NJ, USA), Protease Inhibitor Coctail, (PI) (#P8340, Sigma Aldrich, USA), Sodium orthovanadate (#S6508, Sigma Aldrich, USA). Proteins were purified via acetone precipitation. Samples were incubated with ice cold acetone and after centrifugation supernatant discarded and pellet was dissolved in PBS. Protein depletion was performed via Pierce™ Top 12 Abundant Protein Depletion Spin Columns (#85165, Thermo Fisher, MA, USA) according to the instructor's manual. Each sample was added on different depletion spin column and incubated with the mixture in column for 60 minutes at room temperature via end-over-end shaker. Bottom closure of columns were twisted off and columns were placed into Eppendorf tubes. Then each column was centrifuged at 1000 x g for 2 minutes. Columns were discarded and depleted protein samples in Eppendorf tubes were stored at -20^{o}C for further experiments.

3.9. IMMUNOCYTOCHEMISTRY (ICC)

The NSC-34 cells were plated at a density of 5000 cells per square centimeter to perform an immunocytochemistry assay. These cells were subsequently subjected to a differentiation process. At the end of the 8 days, NSC-34 cells were fixed with 4% (w/v) paraformaldehyde and permeabilized in PBS + 0.01% (v/v) Triton X-100 (#T8787, Sigma Aldrich, Merck, NJ, USA). Non-specific binding sites were blocked by 5% bovine serum albumin (BSA; #0332,

VWR Life Science, PA, USA), cells were incubated with the primary antibody, β-III-tubulin (TUBB3, polyclonal, 1:1000; #ab18207, Abcam, USA), at 4°C over-night. Then cells were incubated with goat polyclonal Secondary Antibody to Rabbit IgG - H&L (#ab150077, Abcam, USA). Nuclear staining was performed with Hoechst 33342 stain (1:2000; #H3570, Invitrogen, USA). Cells were monitored via Confocal Laser Scanning Microscope (Zeiss LSM 700, Germany)

3.10. PLASMID ISOLATION

Two lentiviruses, plv-AcGFP-SOD1 (G93A) (#27142, Addgene, MA, USA) and plv-AcGFP-SOD1(wt) (#27138, Addgene, MA, USA), which were carrying the gene with the human SOD1-G93A mutated gene and wild-type human SOD1 gene respectively, were selected as transfection vectors. Detailed information about both of the plasmids is shown in Table 2.6. below.

Table 3.6. Properties of the plasmids

Bacterial Resistance	Ampicillin
Growth Temperature	37^{o}C
Growth Strain	Stbl3
Gene/Insert name	SOD1
Species	*H. sapiens* (human)
Insert Size (bp)	470
Tag/Fusion Protein	AcGFP

Plasmids were supplied in bacteria as agar stab. For bacterial growth, Stbl3 cells were inoculated overnight at 37^{o}C in Luria-Bertani (LB) broth (#L3522, Sigma Aldrich, Merck,

NJ, USA) supplemented with 100 ug/ml ampicillin (#A939, Sigma Aldrich, Merck, NJ, USA). Then, an inoculant was used to enable the production of plasmids on a larger scale culture with the same medium and growth conditions for midi-prep isolation. Isolation of plasmids was done via ZymoPURETM II Plasmid Midiprep Kit (#D4200, ZYMO Research, CA, USA) as described in the manufacturer's protocol. DNA concentrations were measured via Nanodrop 2000 UV-Vis Spectrophotometer (#ND-2000, Thermo-Fisher Scientific, Waltham, MA, USA)

3.11. TRANSFECTION

40000 NSC-34 were seeded in each well of 6-well culture flask and incubated for 24 hours. Transfection was accomplished by using FuGENE® HD Transfection Reagent (E2311, Promega, Madison, WI, USA). All process was performed according to the manufacturer's manual. The ratio of FuGENE®HD transfection reagent:plasmid DNA was 4:1. FuGENE® HD Transfection Reagent/DNA complex was allowed to incubate for 15 minutes at room temperature before being added to each well of NSC-34 cells to be transfected. Transfection was performed in three groups: SOD1-G93A, SOD-1 WT, and the negative control, which were transfected with plv-AcGFP-SOD1 (G93A) plasmid DNA, plv-AcGFP-SOD1 (wt) plasmid DNA, and FuGENE only, respectively. Cells were grown in complete media for 96 hours.

3.12. WESTERN BLOT ANALYSIS

For capillary electrophoresis analysis of the proteins, The Simple Western™ system (Wes™, ProteinSimple, California, USA) was used. 40 µl of deionized water was added to both Biontinylated Ladder and DTT which were all supplied as powder in 12-230 kDa Separation Module (#SM-W001, Protein Simple, CA, USA). After mixing gently, 20 µl of DTT solution and 20 µl of deionized water was added to Fluorescence Master Mix which was also supplied as a powder in the separation module. Protein content was adjusted to 0.5 mg/ml with PBS-diluted 0.1X Sample Buffer (#PS-FL01-8, ProteinSimple, CA USA). Then, 1 volume of the 5X Fluorescence Master Mix was mixed with four volumes of the protein sample. The samples were incubated at 95°C for 5 minutes via heat-block (#BSH5002-2B, Benchmark

Scientific, NJ, USA), subsequently were precipitated, and kept on ice. Ready-to-use Luminol-S and Peroxide, provided in Anti-Rabbit Detection Module (DM001, Protein Simple, CA, USA) and Anti-Mouse Detection Module (DM002, Protein Simple, CA, USA), were mixed in a ratio of 1:1, and stored on ice.

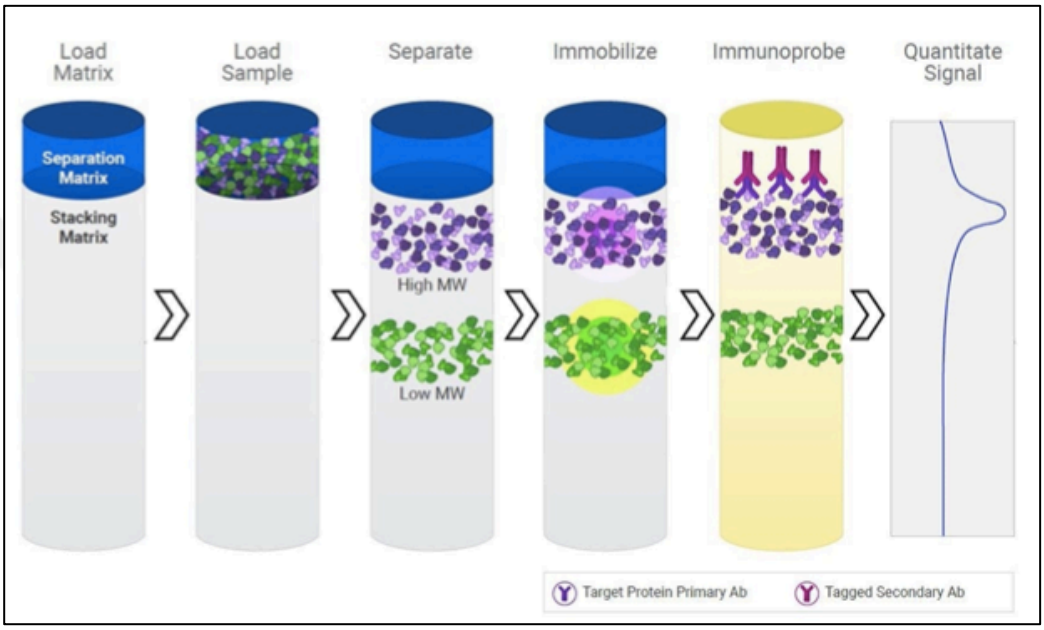

Figure 3.1. WES automated procedure schema [122]

The following primary and secondary antibodies were optimized, and diluted in Antibody Diluent supplied within detection modules, and used for Wes analysis: Anti-Ubiquitin antibody [Ubi-1] (dilution 1:100, #ab7254, Abcam, Cambridge, UK), Sumo-II/III (18H8) rabbit monoclonal antibody (dilution 1:100, #4971, Cell Signalling Technology, Leiden, The Netherlands), β-actin monoclonal antibody (#66009, Proteintech, IL, USA), Anti-rabbit IgG, HRP-linked Antibody (dilutions: 1:500, #7074, Cell Signalling Technology Leiden, The Netherlands), Goat anti-mouse IgG, HRP-linked Antibody (dilutions: 1:500, #7076, Cell Signalling Technology Leiden, The Netherlands).

Primary antibody, secondary antibody, 5% BSA in PBS solution as blocking buffer, and Streptavidin-HRP were added to the assay plates suitable for specified 13-Capillary Cartridge (#SM W001, ProteinSimple, California, USA) and 25-Capillary Cartridge (#SM W003, ProteinSimple, California, USA), according to the manufacturer's protocol. The

amount and dilution of each chemical are shown in Table 2.7. below. After loading all required materials, the plate was centrifuged for 5 minutes at 2500 rpm at room temperature then subsequently placed on and run in the WES system.

Table 3.8. Solutions and amounts used in the WES system

Material	Amount (µl)
Prepared Samples	3 µl
Biotinylated Ladder	5 µl
Antibody Diluent	10 µl
Primary Antibody	10 µl
Secondary Antibody	10 µl
Luminol-Peroxide Mix	15 µl

3.13. 2-DIMENSIONAL POLYACRYLAMIDE GEL ELECTROPHORESIS (2D-PAGE)

Depleted protein samples were diluted to 1 µg/µl with the appropriate amount of ReadyPrep/Sample-Rehydration Buffer (#1632083, Biorad, CA, USA). 200 µl of diluted samples were loaded in the wells of the IEF focusing tray, then the gel site of IPG strips (11 cm, 4-7 pH gradient; #1632015, Biorad, CA, USA), were placed in the wells, as the gel side penetrating the sample. Then, 1 ml of mineral oil was poured onto each strip.

IPG strips were exposed to passive rehydration at 50V for 12 h. Isoelectric focusing (IEF) was performed in a Bio-Rad Protean i12IEF Cell system (#1646000J3, Biorad, CA, USA) as follows: 250V for 20 min, increase up to 8000V over 1 h and 8000V steady until total of 26,000V–h had elapsed. After the IEF, IPG strips were incubated with ReadyPrep Equilibrium Buffer I and ReadyPrep Equilibrium Buffer II for 20 minutes each.

The second dimension was performed with PowerPac Universal System (#1645070, Biorad, CA, USA) system; and 4–20% polyacrylamide gradient midi format gels (Criterion TGX gels; #3450104, Biorad, CA, USA) were used. Precision Plus Dual Color Protein Marker (#1610374, Biorad, CA, USA) was used as a protein ladder and 3 µl of it was added in the

well reserved for ladder. IPG strips were placed gently on Criterion TGX Gels. Liquidified overlay agarose (#1632111, Biorad, CA, USA) was poured on IPG strips embedded in gel. The system was run at 200V by using 1X Tris/Glycine/SDS running buffer (TGS; #1610732, Biorad, CA, USA). All gels were incubated with a fixation solution, consisting of 40% (v/v) ethanol and 10% (v/v) acetic acid, overnight at room temperature. After fixation, each gel was stained with 1X Flamingo Stain (#1610492, Biorad, CA, USA) for 3 hours at room temperature with agitation and monitored via Chemi-Doc XR imaging system (Bio-Rad).

3.14. FLUORESCENCE ASSOCIATED CELL SORTING (FACS)

To eliminate the transfected cells from non-transfected cells, Fluorescent-Activated Cell Sorting (FACS) strategy was used via S3e Cell Sorter (#1451005, Biorad, Germany). NSC-34 cells were removed from the surfaces with trypsin and centrifuged at 200xg for 5 min. The supernatant was discarded and cells were washed with 1X PBS. Subsequently, the cells were passed through 0.70 µm strainers and incubated in 1 ml PBS solution on ice until the sorting process.

Untransfected control NSC-34 cells were utilized for the determination of the presence of cell population and to adjust the voltages of the FSC, SSC, and FL-1 channels. 5000 events were read and the population gate was determined. GFP-positive NSC-34 cells were read via the FL-1 (488nm) channel. GFP-positive cells were directed to a serum-free medium containing flow tubes. The FACS process was continued until all cells were distributed. Sorted cells were centrifuged at 200xg for 5 minutes and serum-free medium was discarded. Cells were either cultured or stored for follow-up experiments.

3.15. MASS SPECTROMETRY

3.15.1 In-Gel Cut of The Proteins

Proteins were identified via ABSCIEX MALDI-TOF/TOF 5800 system (Applied Biosystems, Framingham, MA, USA) at Kocaeli University Medical Biology Proteomics

Laboratory. Gels were cut at the sites of target protein spots and protein spots were exposed to in-gel tryptic digestion via an in-gel digestion kit as described in the manufacturer's protocol (#89871, Pierce, Thermo Fisher Scientific, USA). Gel pieces were shrinked with 100% acetonitrile and incubated for 15 minutes at temperature. Then gel pieces were allowed to air dry for 10 minutes. Gel pieces were swelled by incubating with activated trypsin. Samples were digested with digestion buffer at 30oC overnight with agitation. Desaltation of the samples was done with 10 µl of ZipTipC18 (Millipore, USA) and peptide elution was performed with %1 FA solution.

3.15.2. Nano-Liquid Chromatography Mass Spectrometry (nLC-MS/MS) Analysis

The analysis of peptides was conducted using the nLC-MS/MS system, specifically the Ultimate 3000 RSLC nano system (Dionex, Thermo Scientific, CA, USA). This system is coupled with a Q-Exactive mass spectrometer, (Thermo Scientific, USA). The Xcalibur 4.0 software (Thermo Fisher Scientific, USA), was employed to manage and regulate the entire system. The separation using high-performance liquid chromatography (HPLC) was conducted utilizing mobile phases A (containing 0.1% formic acid) and B (comprising 80% acetonitrile and 0.1% formic acid). A trap column was employed for the purpose of concentrating and desalting the truncated peptides. Subsequently, the peptides were placed onto an Acclaim PepMap RSLC C18 analytical column (dimensions: 75 µm × 15 cm x 2 µm, with a diameter of 100 Å) (Thermo Scientific, CA, USA), in order to achieve chromatographic separation. The acquisition of MS1 spectra involved conducting a comprehensive scan using the following parameters: a resolution of 70,000, a scan range spanning from 400 to 2000 m/z, an automated gain control (AGC) target of 3×E6, a maximum injection period of 60 ms, and a sputtering voltage of 2.3 kV. The study of MS/MS was conducted using a data-dependent acquisition method, wherein the top 10 precursor ions were selected. The MS2 study involved the utilization of collision-induced dissociation, specifically higher-energy collisional dissociation (HCD). The analysis was conducted using the following parameters: a resolution of 17,500, an automatic gain control (AGC) setting of 1E6, a maximum injection duration of 100 ms, a normalized isolation window of 2.0 m/z, and a collision energy (NCE) of 27. The instrument was calibrated using the LTQ Velos ESI Positive Ion Calibration Solution (#88323, Pierce, USA), which is a standard positive calibrator, immediately before to each analysis.

3.15.3. nLC-MS/MS Data Analysis

The raw data was analyzed and the target protein was identified using Proteome Discoverer 2.2 software (Thermo Scientific, USA). The following parameters were used during the analyses: a peptide mass tolerance of 10 ppm, an MS/MS mass tolerance of 0.2 Da, a mass accuracy of 2 ppm, a tolerance low value of 1, a minimum peptide length of 6 amino acids, and specific modifications including cysteine carbamidomethylation, methionine oxidation, and asparagine deamination. A minimum value of 1 was assigned to represent the amount of distinct peptides detected for each protein. Subsequently, the Uniprot database was utilized to conduct a search on the acquired data.

3.16. STATISTICAL ANALYSIS

All statistical analysis was performed by using GraphPad Prism statistical software 8.0 (GraphPad Software, La Jolla, CA, USA), unpaired t-test and Welch's test analysis were carried out. Results with P-values ≤ 0.05 were considered statistically significant.

4. RESULTS

4.1. GENOTYPING

Since its initial publication in 1994, the transgenic SOD1-G93A transgenic mouse model still is the most extensively utilized transgenic animal for mimicking ALS disease [225]. These mice were created for overexpression of a mutant version of the SOD1 gene, which has the glycine-alanine substitution at amino acid 93 (G93A), implicated in the development of ALS. This mutation is one of the large number of mutations in the SOD1 gene, which accounts for around 20% of fALS cases [22].

The B6SJLTg (SOD1*G93A)1Gur/J line was bought from Jackson Laboratory (Bar Harbor, ME, United States) and six-week-old animals were raised in-house using transgenic male and wild-type female C57BL6/J mice. They were fed ad libitum and had unlimited access to water under a light/dark cycle of 12:12 hours. Genotyping was performed on every mouse by extracting DNA from ear samples and running it through a routine PCR with primers recommended by The Jackson Laboratory. The PCR results were placed onto an agarose gel and visualized using Bio-Rad ChemiDoc (Bio-Rad, Hercules, CA) and Imaging Lab Software under ultraviolet light. Figure 4.1 shows that in all mouse colonies, a single band indicates wild-type mice, while two bands indicate transgenic animals since one of the bands represents the PCR product of the transgene.

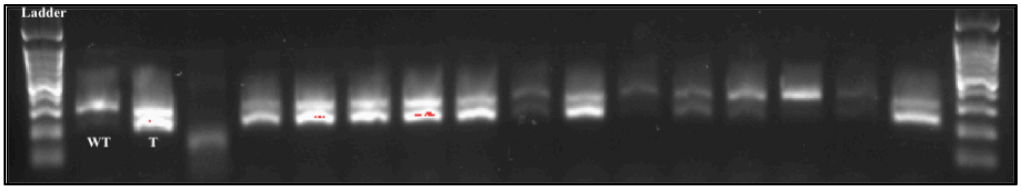

Figure 4.1. Gel electrophoresis image of genotyped transgenic and wild-type mice. (T: transgenic mouse, WT: wild-type mouse)

4.2. NEUROSCORING

Since the SOD1-G93A model mimics some of the pathologic hallmarks of ALS in humans, including motor neuron loss, progressive muscular weakening, atrophy, and subsequently paralysis and death, it has become the most popular mouse model in ALS drug development research. Nonetheless, SOD1-G93A mice occasionally demonstrate variance in the severity and timing of the onset of disease, a condition that has been documented in many transgenic animal models. There was a requirement for a standardized in vivo screening system to evaluate neuromuscular function in SOD1-G93A mice. As a result, Hatzipetros et al. established a technique at the ALS Treatment Development Institute (ALS TDI) for evaluating SOD1-G93A mice's neuromuscular function rapidly and accurately.

Locomotor activity tests, including the tail hang test, gait analysis, and righting reflex measurement, were performed on each mouse, and evaluations were completed using the Neuroscore measurement system described in the same section.

As shown in Figure 4.2, transgenic mice weren't able to completely extend their hind limbs on day 105, whereas wild-type mice did. The NS2 level was determined on day 105; mice were sacrificed on this day and their CNS material was collected. Postnatal day 105 (PND105) was considered a symptomatic group. To avoid age-related parameter changes, CNS tissue of wild-type mice was also collected at this age. In addition, rodents from the pre-symptomatic group were evaluated as NS0 on day 60 and sacrificed at the same age.

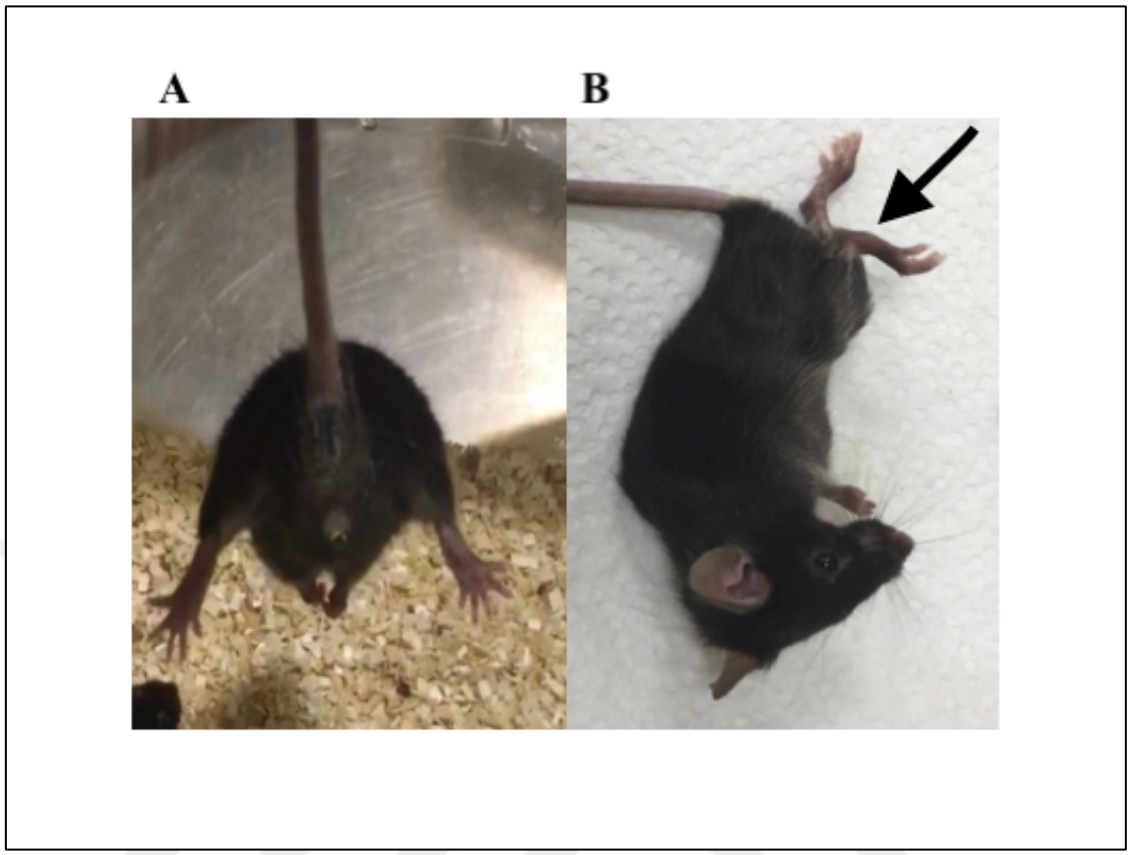

Figure 4.2. Neuroscoring of A) Wild-type and B) transgenic mouse [123]

4.3. PROTEIN EXTRACTION AND DEPLETION

Numerous proteins of therapeutic interest are present in the plasma at low concentrations and are difficult to detect due to the presence of abundant proteins. For identification and quantification of the proteins with lower abundancy in samples by further analysis such as 2D-PAGE, simple WES, and mass spectrometry, the 12 high-abundant proteins are mentioned in Section 3.8. were depleted from all protein samples which are collected from brain and spinal cord tissues.

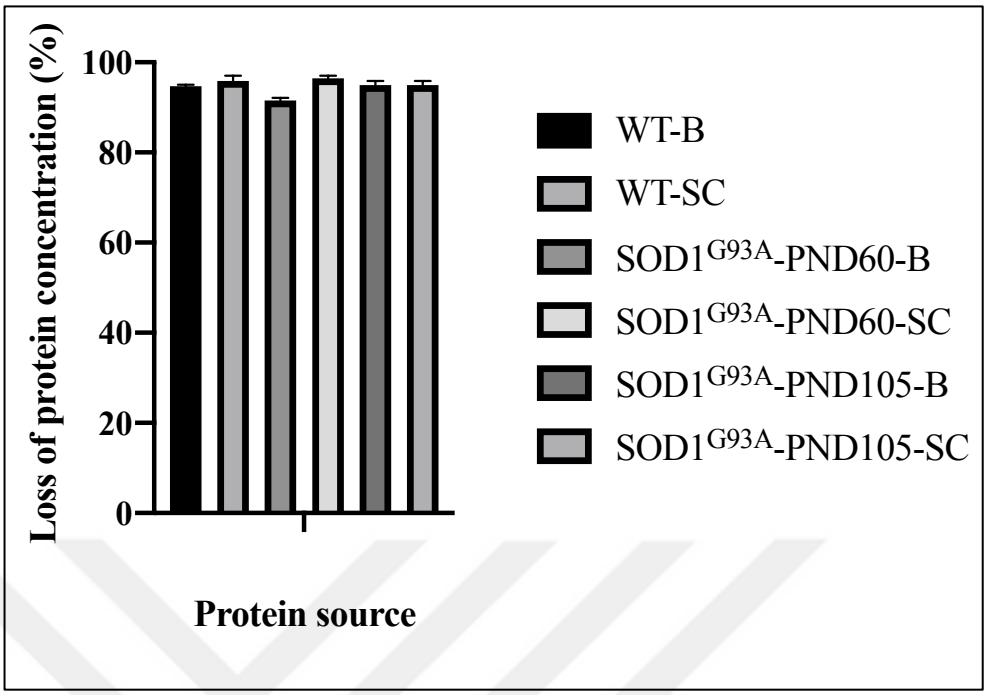

Figure 4.3. Decrease in protein amount of in vivo samples after depletion (B: brain, SC: spinal cord, WT: wild-type, $SOD1^{G93A}$: Transgenic mice, and PND: Postnatal day)

Concentrations of protein samples were measured with a Pierce BCA kit before and after depletion. As stated in Figure 4.2. approximately 95% of proteins in all samples were depleted.

4.4. NSC-34 CELL PROLIFERATION

The neuronal cell line differentiation is essential to assess their morphological and biochemical properties. Since NSC-34 cells exhibit typical motoneuron characteristics, they are used for examining motoneuron-like behavior in the context of ALS. The relationship between cell proliferation and differentiation is remarkably inverse. Precursor cells continue to divide before achieving a fully differentiated state, whereas terminal differentiation typically coincides with a cessation of proliferation and a definitive exit from the cell cycle.

NSC-34 cells were seeded as 4000 cells per centimeter cube for the examination of cell proliferation during the differentiation process. On days 2 (d2), 4 (d4), 6 (d6), and 8 (d8), cells were collected, mixed with a 1:1 ratio of Trypan Blue solution, subsequently 10 µl of

Trypan Blue:cell mixture was placed into Countess cell counting chamber slides and counted via Countess II FL system.

As shown in Figure 4.3., results demonstrate that through the days of differentiation, undifferentiated NSC-34 cells proliferated approximately 1.40, 5.93, 7.23, and 6.25 times more than differentiated ones on d2, d4, d6, and d8 respectively.

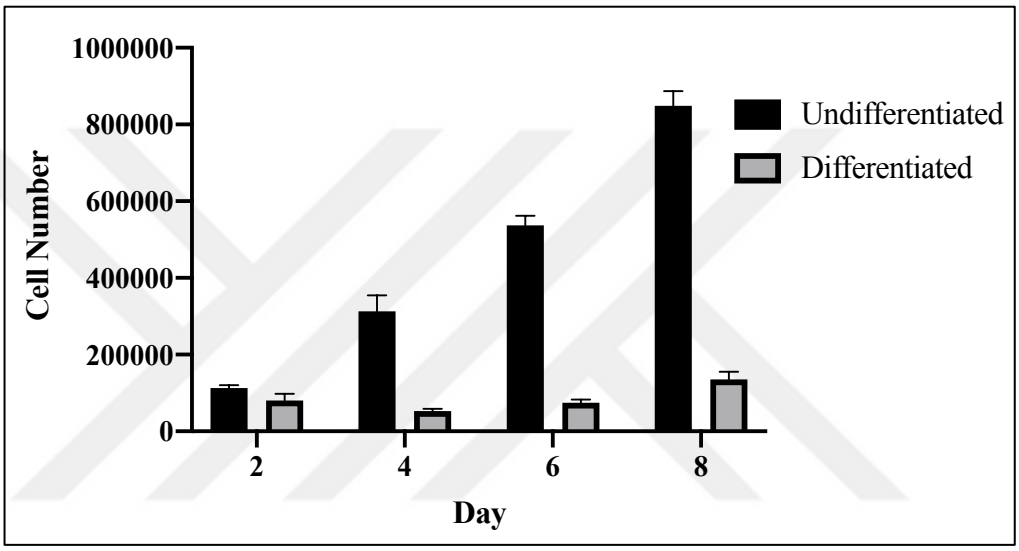

Figure 4.4. The proliferation of differentiated and undifferentiated NSC-34 cells.

4.5. IMMUNOCYTOCHEMISTRY (ICC)

After either the differentiated or undifferentiated cells were cultured for 2, 4, 6, and 8 days, neuron growth was observed under a confocal microscope. To characterize the successful differentiation, cells were stained with β-tubulin III as a neural marker and DAPI as a nuclear counterstain. As seen in Figure 4.4., immunofluorescence staining showed that the neurite lengths of differentiated cells were remarkably greater than those of undifferentiated cells, while the inverse situation was determined in terms of proliferation. It was observed that undifferentiated cells proliferate more than differentiated cells.

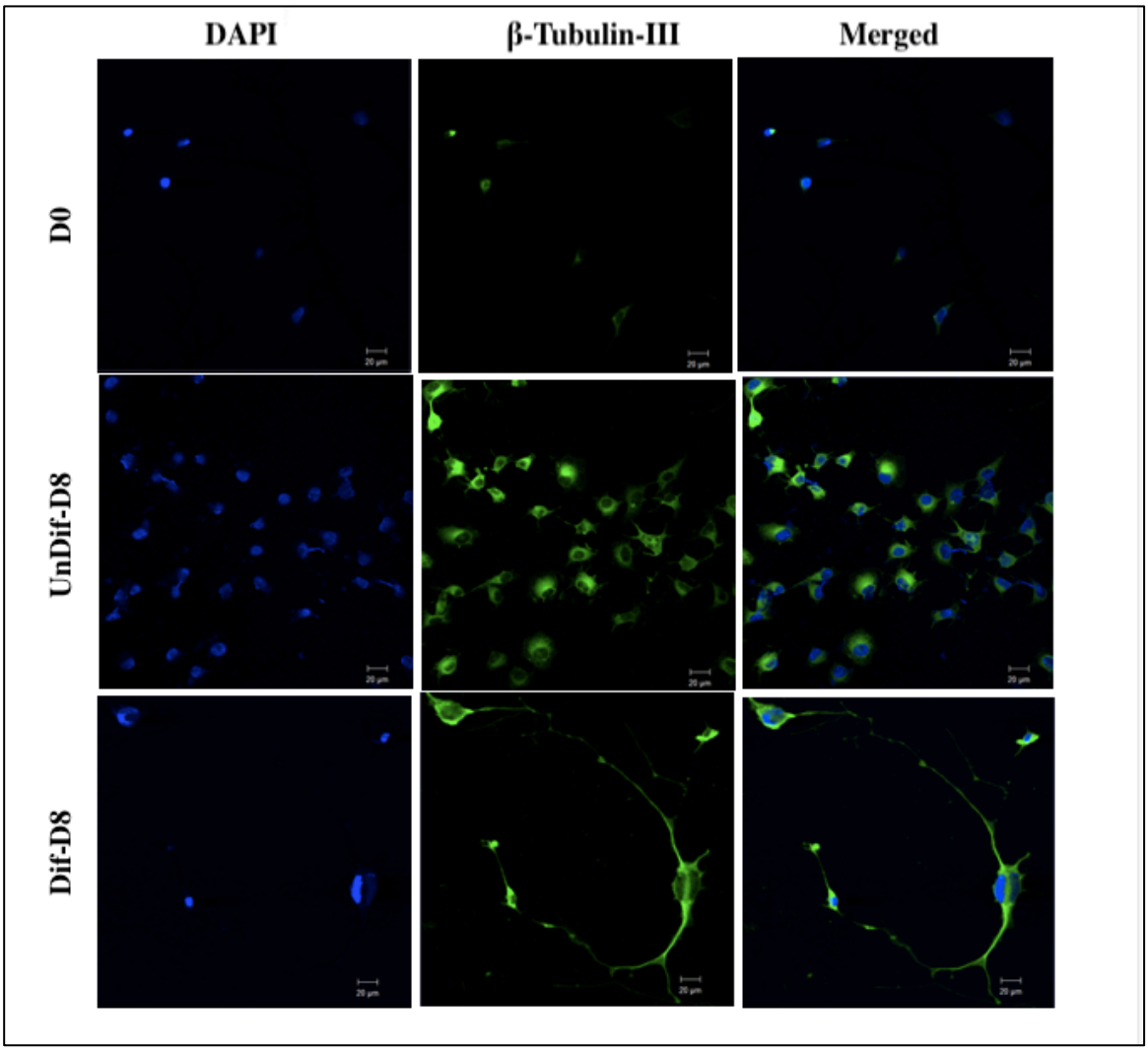

Figure 4.5. Immunocytochemistry assay results of differentiated and undifferentiated NSC-34 cells at the end of 8 days. (Dif-D8: Differentiated NSC-34 cells on day 8, Undif-D8: Differentiated NSC-34 cells on day 8, D0: Day 0)

As a result of the analysis made with ImageJ software, neurite length, which was measured as 8.71 micrometers on day zero, was measured as 174.71 and 20.29 micrometers for differentiated and undifferentiated NSC-34 cells, at the end of the eighth day, respectively. Differentiated cells have neurites 8.61 times longer than undifferentiated cells, which is morphologically characterized by successful differentiation.

4.6. Q-PCR

Target gene expressions, including MAP2, MAPT, and GAP43, were examined by qPCR technique to determine whether NSC-34 cell differentiation was successfully performed. Expression levels of the microtubule-associated proteins MAP2 and MAPT, as well as growth-associated protein 43 (GAP-43), were investigated since morphological and functional differentiation are related to the expression of cytoskeletal markers. Following the differentiation process, the expression levels of mRNA and protein for all three markers increased. 18sRNA gene was chosen as a housekeeping gene and used as a normalization reference.

According to the qPCR results shown in Figure 4.5, the *MAPT* gene was expressed at a higher level in differentiated NSC-34 cells as per other marker genes. Results demonstrated that differentiated NSC-34 cells resulted in around a 5.46-fold increase in MAPT, a 2.68-fold increase in MAP2, and a 2.3-fold increase in GAP43 mRNA expression levels compared to non-differentiated NSC-34 cells.

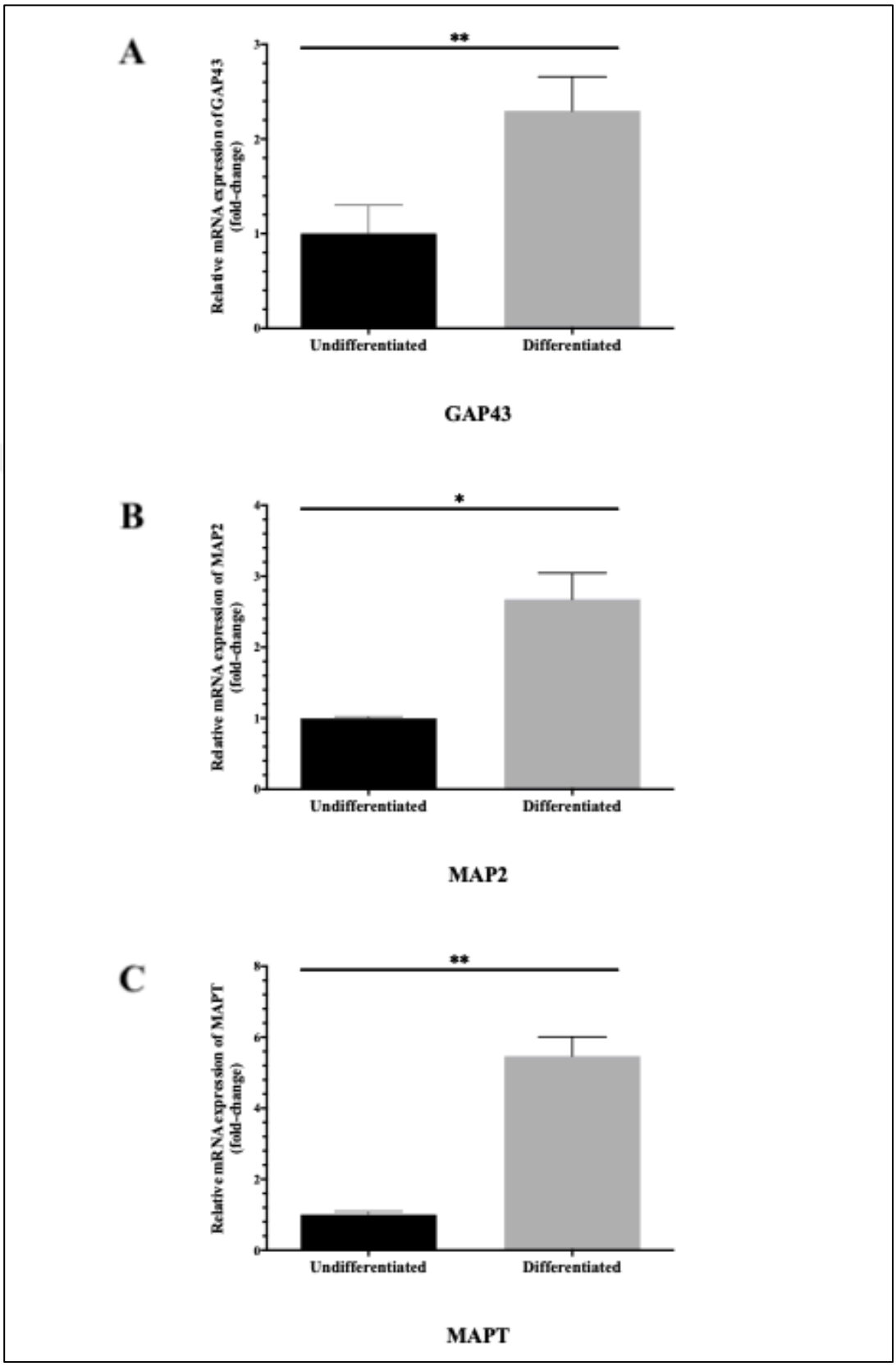

Figure 4.6. Relative mRNA expression of neural marker genes A) GAP43, B) MAP2, C) MAPT

Moreover, after the differentiation process, cholinergic markers, ChAT, and AChE gene expressions have resulted in 6.5, and 7.83-fold increases respectively.

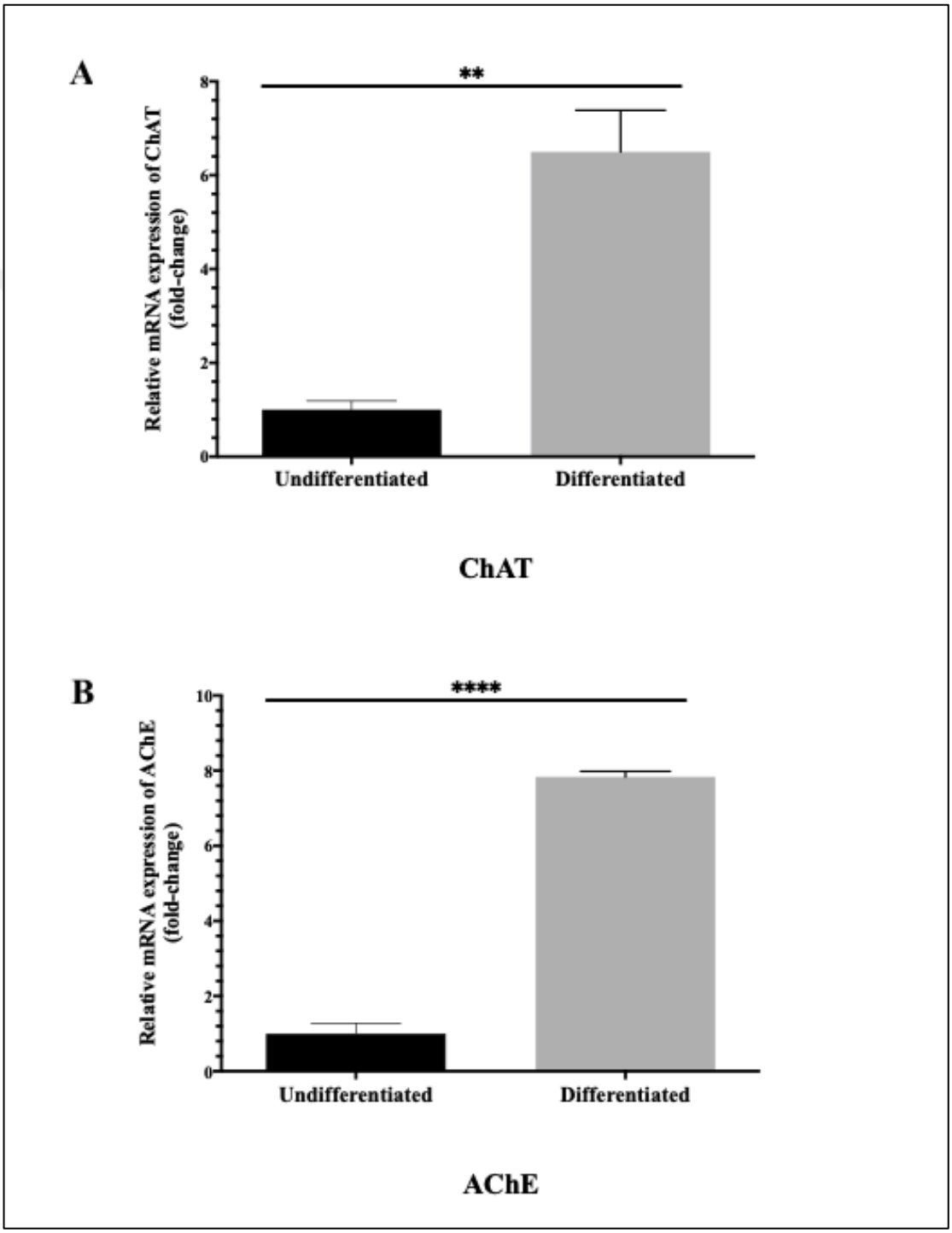

Figure 4.7. Relative mRNA expression of neural marker genes A) ChAT, B) AChE

4.7. TRANSFECTION

In order to examine the transfection of NSC-34 cells with plv-AcGFP-SOD1(G93A) plasmid DNA, plv-AcGFP-SOD1(wt) plasmid DNA via FUGENE, cells were observed under a confocal microscope. Cells were stained with DAPI at the end of 96 hours right before imaging. Figure 4.7. shows that transfection efficiency has been determined as substandard, however, the small presence of GFP indicates that some cells are successfully transfected.

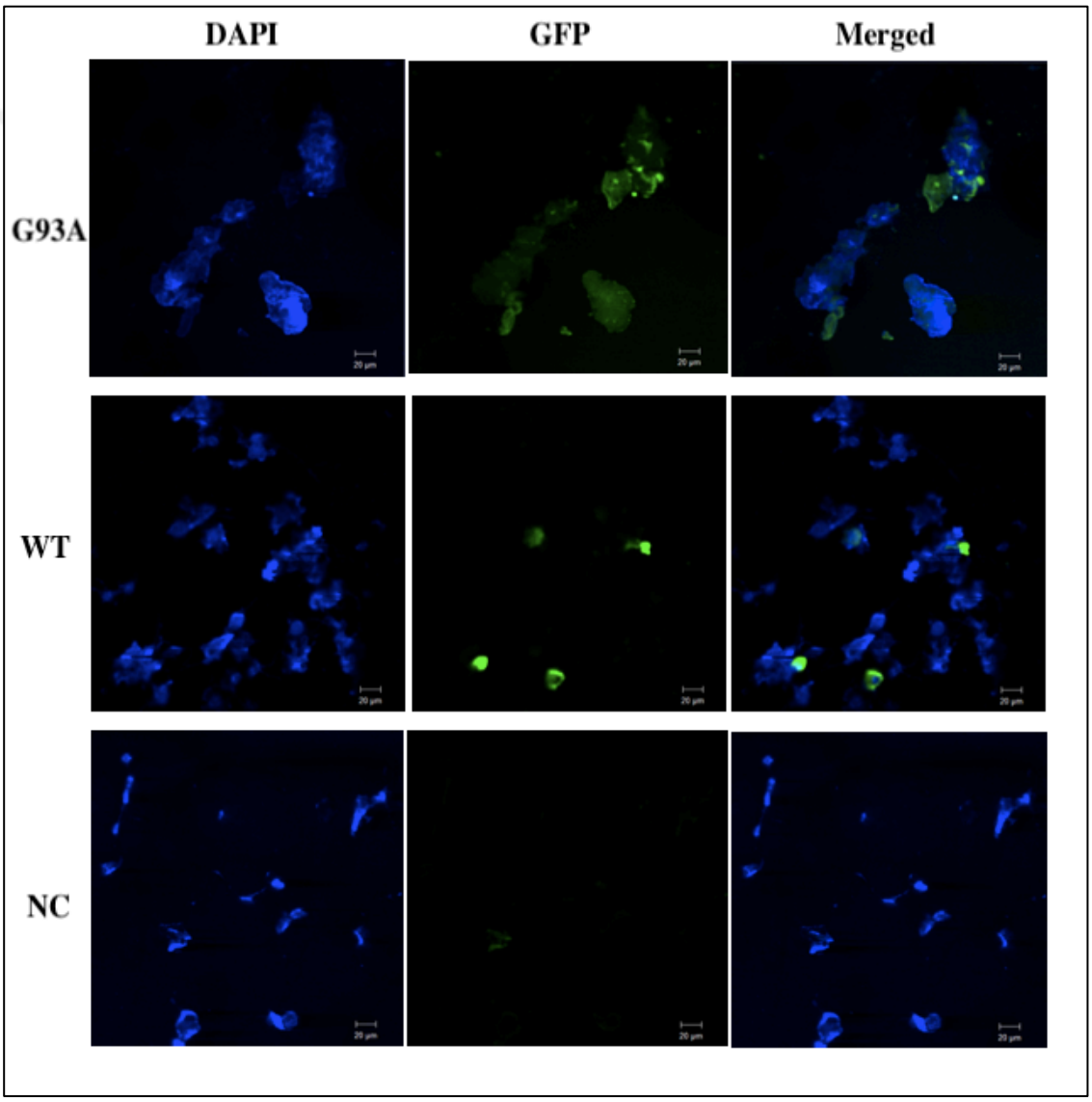

Figure 4.8. Confocal microscope image of transfected NSC-34 cells with GFP and untransfected NSC-34 cells. (NC: untransfected NSC-34 cells, abbreviated as the negative control, WT: NSC-34 cells transfected with plasmid contains wild-type SOD1, G93A: NSC-34 cells transfected with plasmid contains $SOD1^{G93A}$ mutation).

4.8. FLUORESCENCE-ACTIVATED CELL SORTING (FACS)

FACS was performed to enhance the population of transfected NSC-34 cells by sorting them from untransfected ones. The GFP signal was used as the point of reference and cells were collected. As seen in Figure 4.8., the GFP+ cells constituted 47.45 and 26.66% of all living cells transfected by plv-AcGFP-SOD1(wt) plasmid DNA and plv-AcGFP-SOD1(G93A) plasmid DNA respectively. Besides that, 1.94% of non-transfected, but FuGene-treated NSC-34 cells gave false positive results as GFP+.

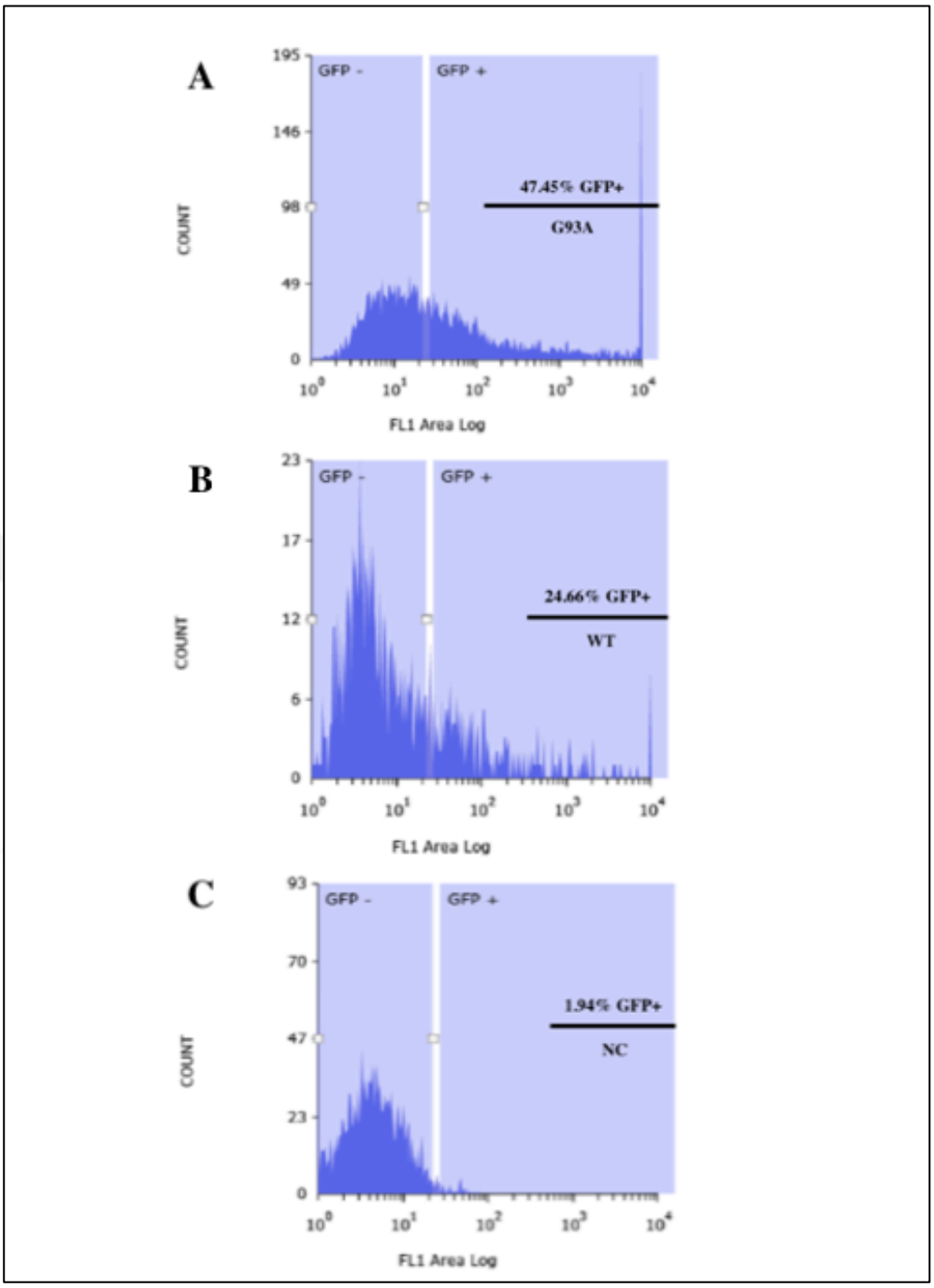

Figure 4.9. Cell sorting analysis of transfected NSC-34 cells with the percentage of GFP+ cells of all living cells. A) SOD1-G93A mutated cells, B) Wild-type SOD1 mutated cells, C) Untransfected cells

4.9. 2D-PAGE ANALYSIS

Proteins derived from brain and spinal cord tissues, depleted of their most abundant proteins, were profiled by 2D PAGE analysis. To accomplish this, 11 cm strips of IPG with a pH range of 4-7 were chosen. Flamingo stain, which is preferred due to its high sensitivity and compatibility with the mass spectrometer, was utilized for painting. After imaging with the ChemiDoc system, 2 distinct protein spots, are shown in the boxes in Figure 4.10. were observed in the profiling of isolated proteins from the brain tissues in four out of six mice, which can be interpreted as an evident distinction between 105 days old transgenic mice and healthy mice. In addition, shifted image of similar protein spots, indicated by the arrow sign, was obtained in two other animals belonging to the same group. Also, these two spots were present at lower concentrations in 2 of all four 60-day-old transgenic animals compared to the 105-day-old animals. As a result of the measurements done with Image J software, it was determined that these two protein spots were between approximately pH 5.2-5.5 and 20 kDa. However, profiling of spinal cord-derived protein samples revealed no remarkable protein spots for either healthy or transgenic mice.

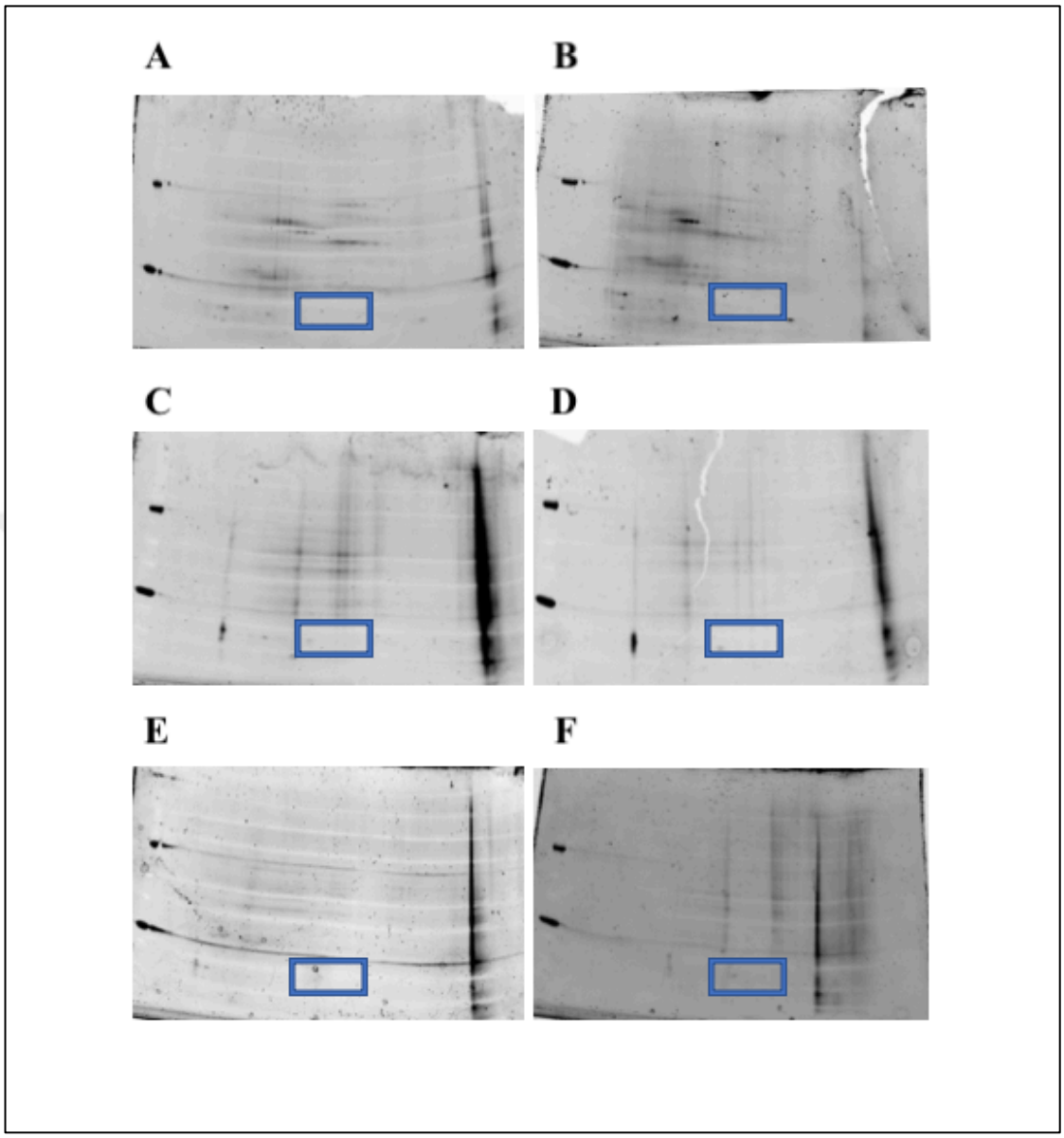

Figure 4.10. 2D-PAGE image of proteins derived from brains of wild-type mice where all images represent different animals of the same group as A) WT-B1, B) WT-B2, C) WT-B3, D) WT-B4, E) WT-B5, F) WT-B6 (WT: Wild-type mouse, B: Brain, PND: Postnatal day)

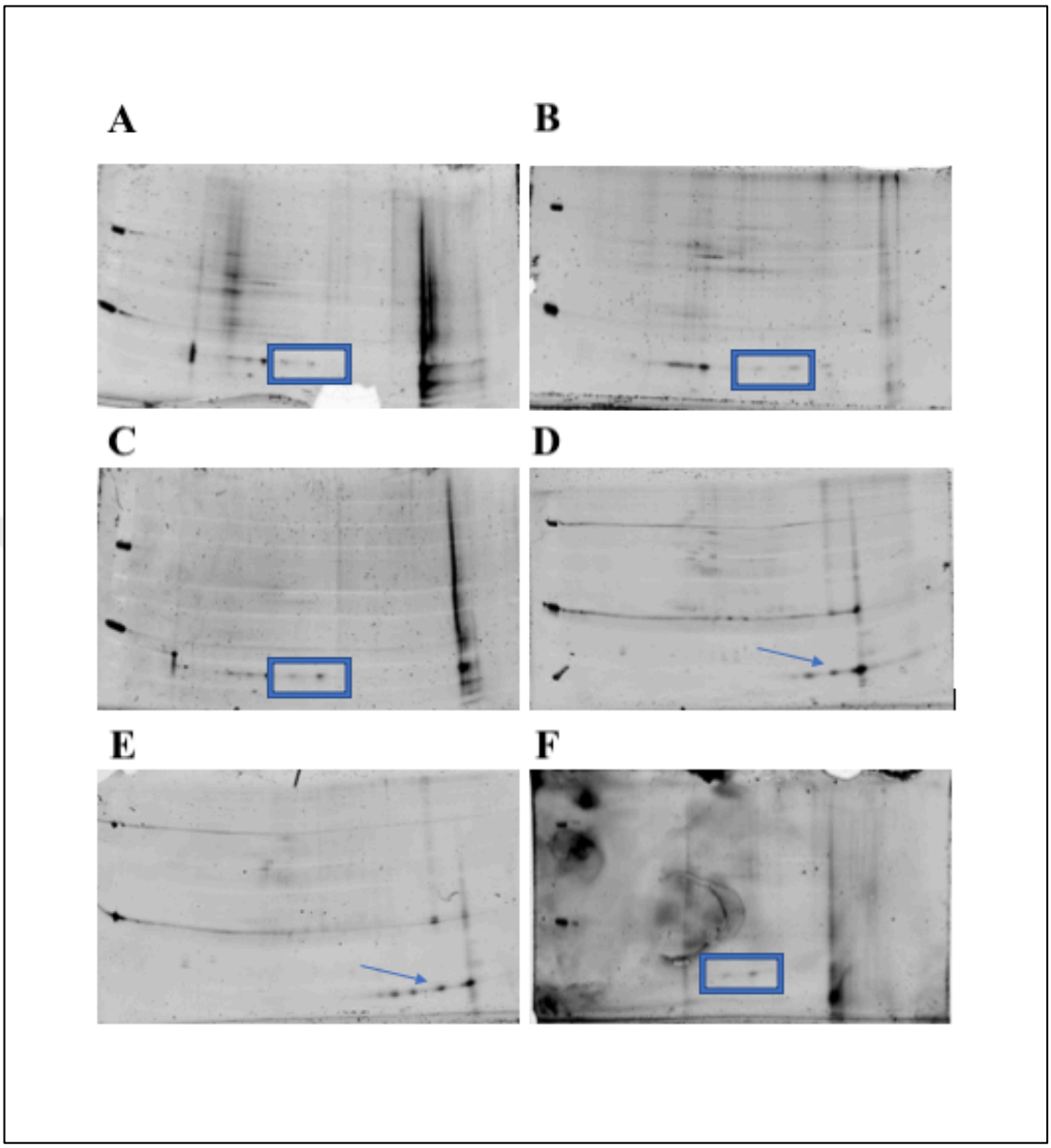

Figure 4.11. 2D-PAGE image of proteins derived from brains of PND105 mice where all images represent different animals of the same group as A) T105-B1 B) T105-B2 C) T105-B3 D) T105-B4 E) T105-B5 F) T105-B6 (T: Transgenic mouse, B: Brain, PND: Postnatal day)

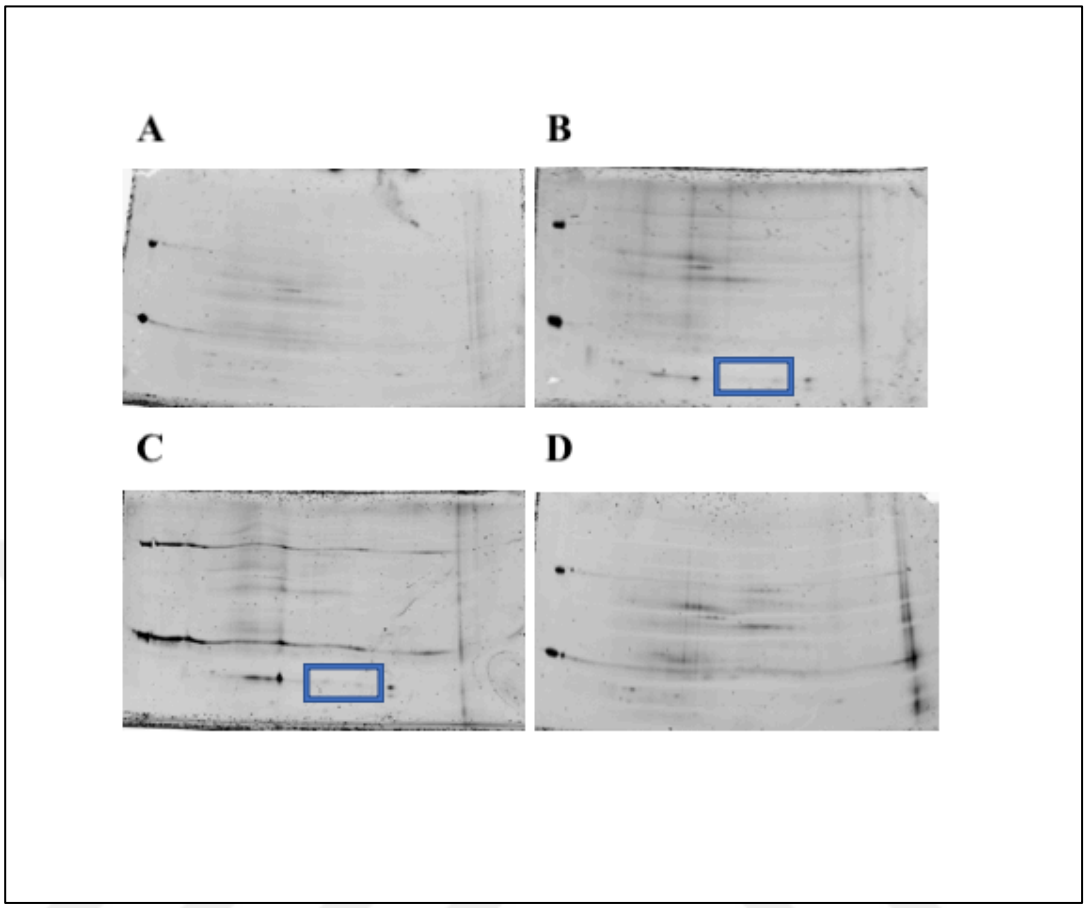

Figure 4.12. 2D-PAGE image of proteins derived from brains of PND60 mice where all images represent different animals of the same group as A) T60-B1 B) T60-B2 C) T60-B3 D) T60-B4 (T: Transgenic mouse, B: Brain, PND: Postnatal day)

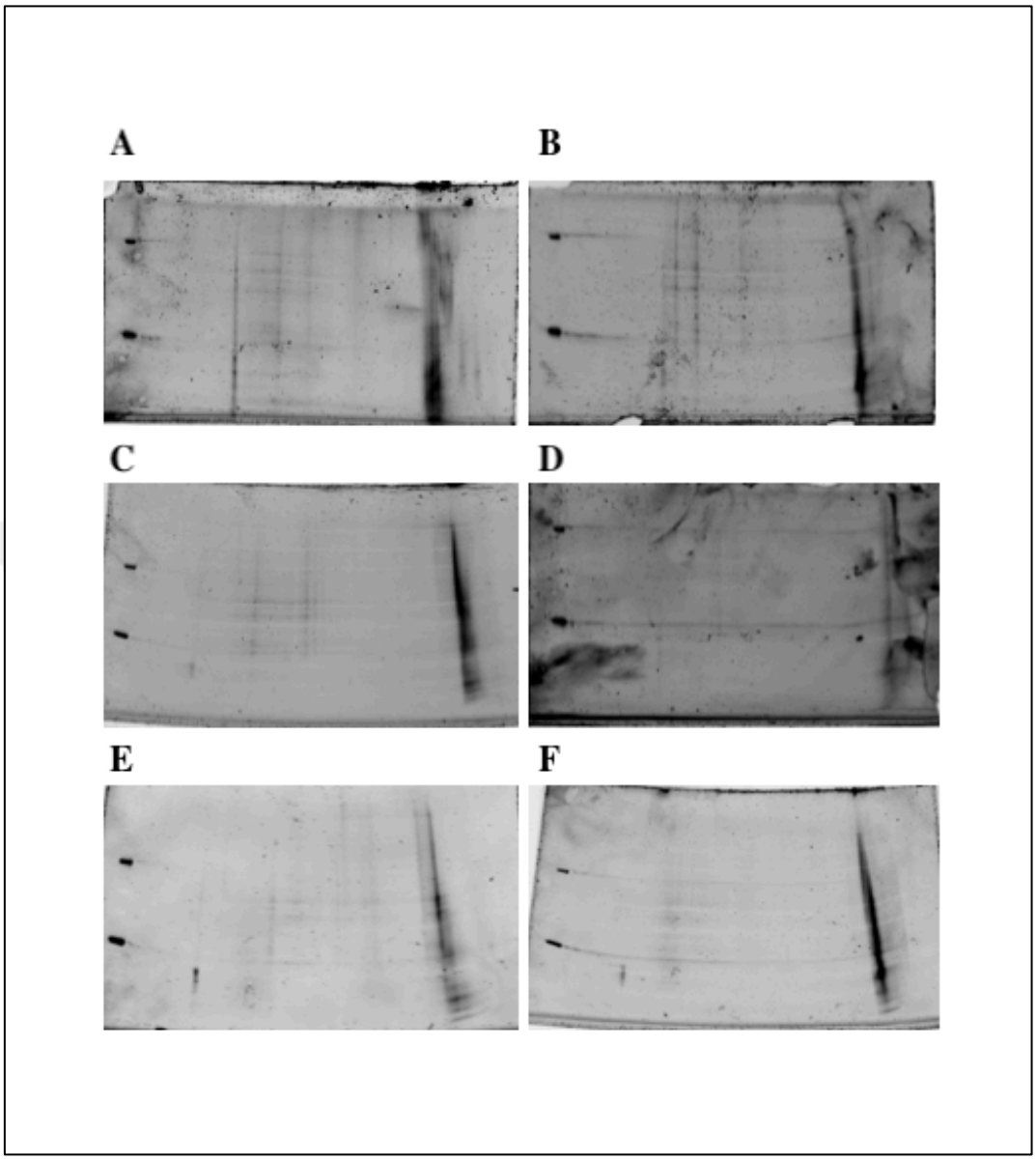

Figure 4.13. 2D-PAGE image of proteins derived from spinal cords of wild-type mice where all images represent different animals of the same group as A) WT-SC1 B) WT-SC2 C) WT-SC3 D) WT-SC4 E) WT-SC5 F)WT-SC6 (T: Transgenic mouse, SC: Spinal cord, PND: Postnatal day)

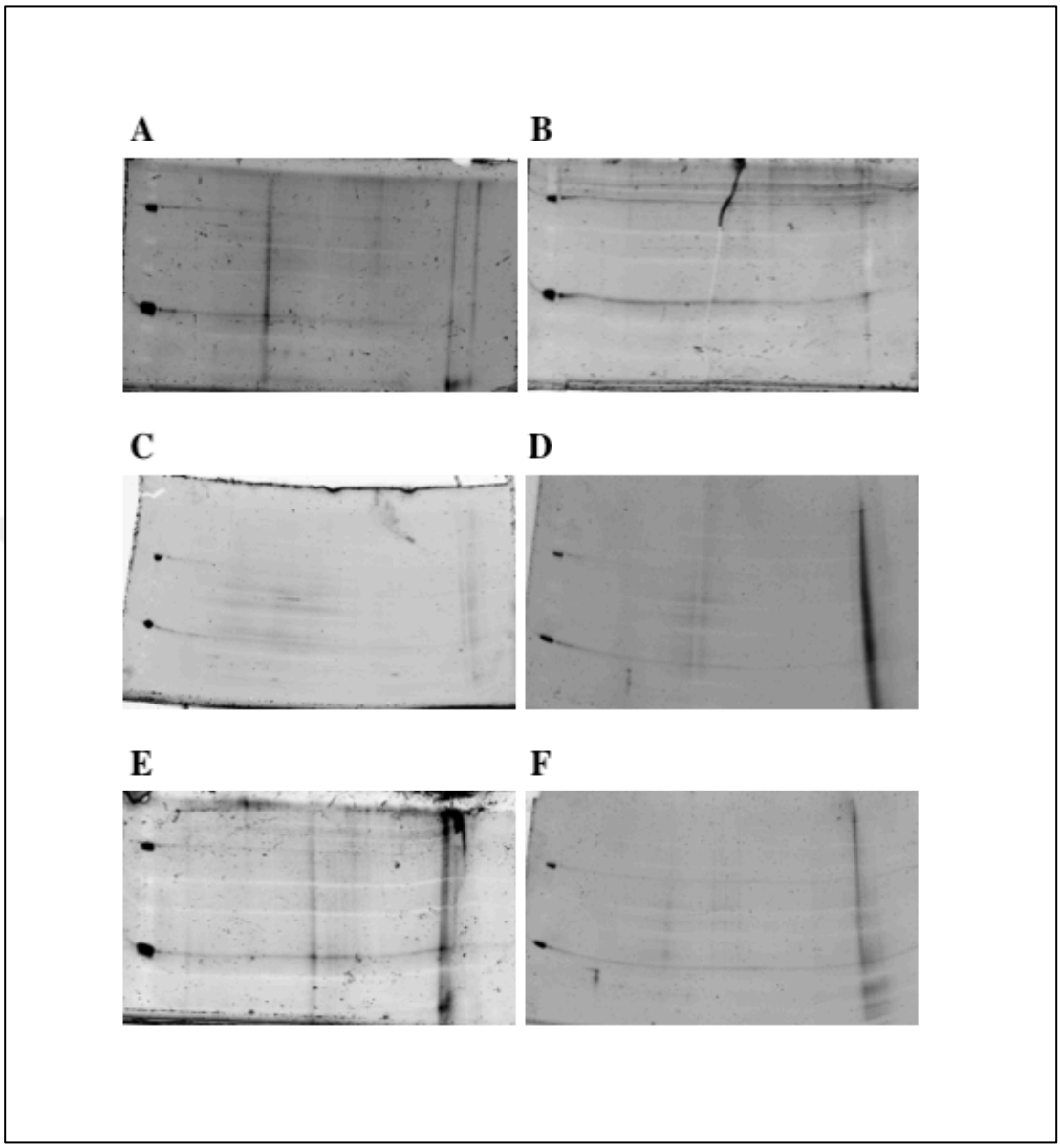

Figure 4.14. 2D-PAGE image of proteins derived from spinal cords of PND105 mice where all images represent different animals of the same group as A) T105-SC1 B) T105-SC2 C) T105-SC3 D)T105-SC4 E)T105-SC5 F)T105-SC6 (T: Transgenic mouse, SC: Spinal cord, PND: Postnatal day)

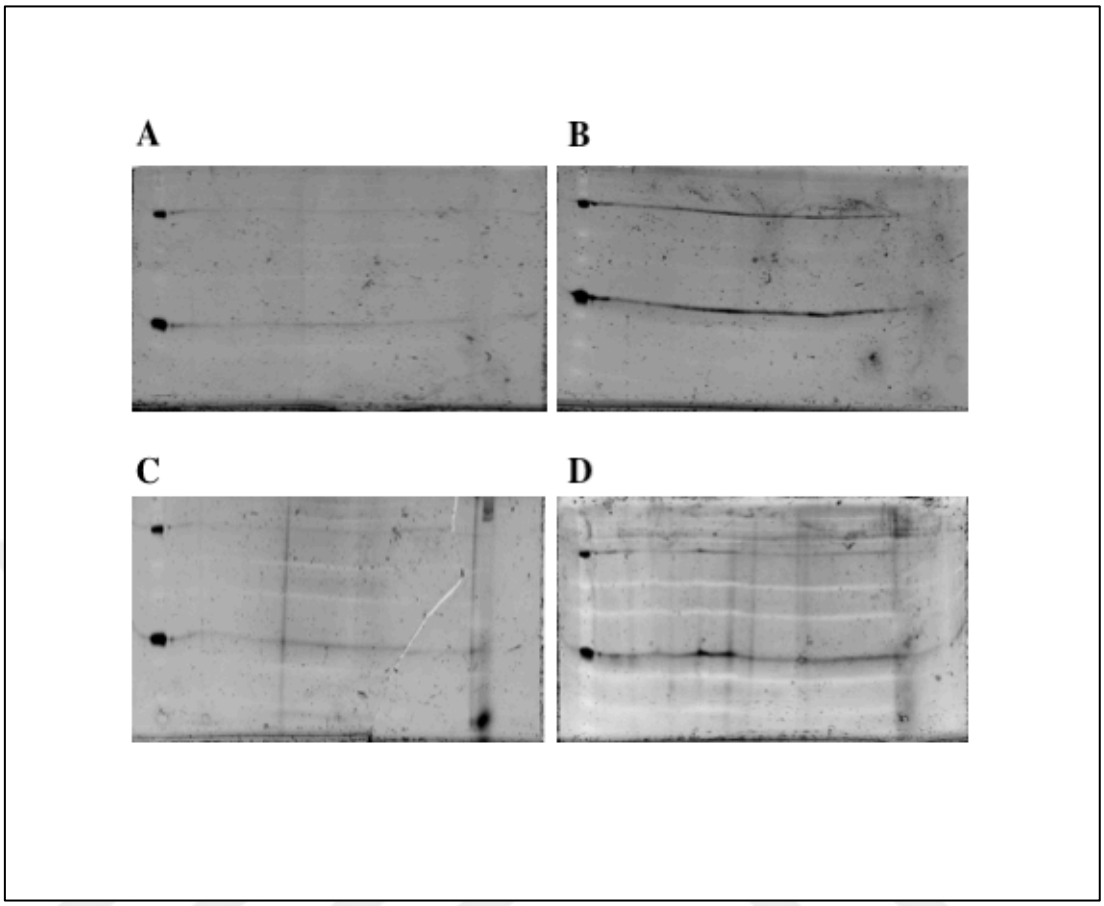

Figure 4.15. 2D-PAGE image of proteins derived from spinal cords of PND60 mice where all images represent different animals of the same group as A) T60-B1 B) T60-B2 C) T60-B3 D) T60-B4 (T: Transgenic mouse, PND: SC: Spinal Cord, Postnatal day)

4.10. SIMPLE WESTERN (WES) ANALYSIS

WES analysis examined whether the target proteins displayed in 2D PAGE analysis, which have the potential to be biomarkers, undergo ubiquitination and sumoylation II-III. In this analysis method based on the cartridge and capillary system, the range of 12-230 kDa was chosen to include the size of the target proteins. Anti-Ubiquitin antibody [Ubi-1] and Sumo-II/III (18H8) rabbit monoclonal antibodies were used as primary antibodies for the detection of ubiquitination and sumoylation II-III respectively, β-actin monoclonal primary antibody was used as the housekeeping gene.

Although protein bands were observed in both post-translational modifications in the control groups, no bands were observed in the determined ranges for proteins obtained from tissues

and NSC-34 cells. However, the housekeeping gene β-actin bands were detected in all protein samples, regardless of in vivo and in vitro origin. This result reveals that the target proteins of this study with the potential to be biomarkers have not undergone ubiquitination and sumoylation modifications.

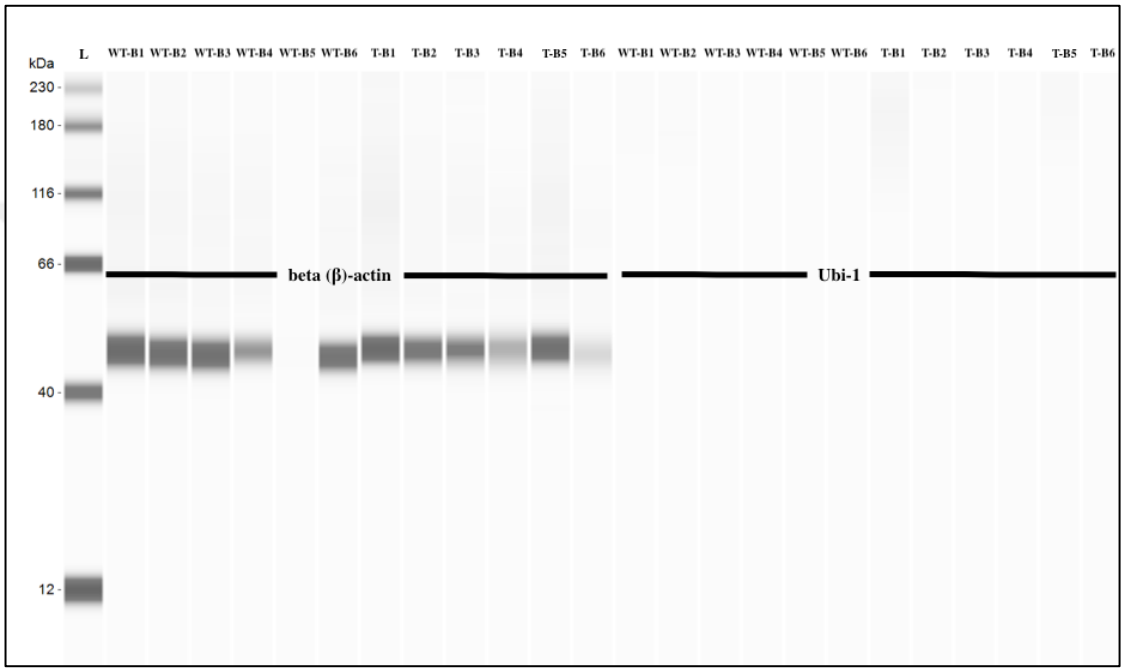

Figure 4.16. Image of Wes analysis with beta (β)-actin and Ubi-1 Antibody (L: Ladder, WT: Wild-type, T: Transgenic PND105 mouse, B: Brain)

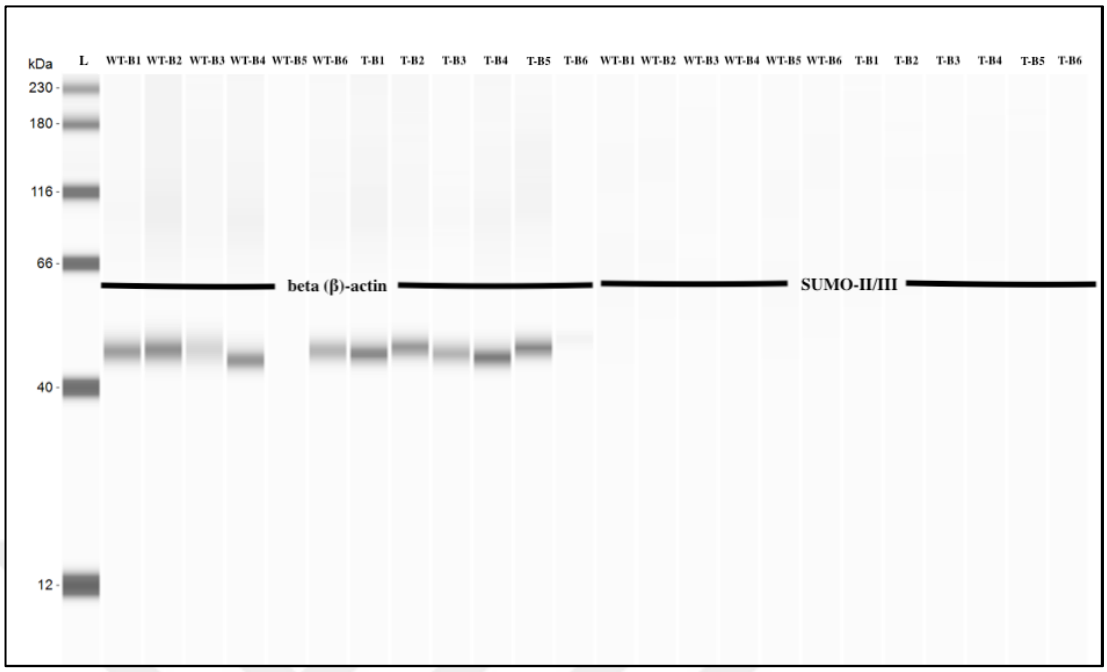

Figure 4.17. Image of Wes analysis with beta (β)-actin and SUMO II/III Antibody (L: Ladder, WT: Wild-type, T: Transgenic PND105 mouse, B: Brain)

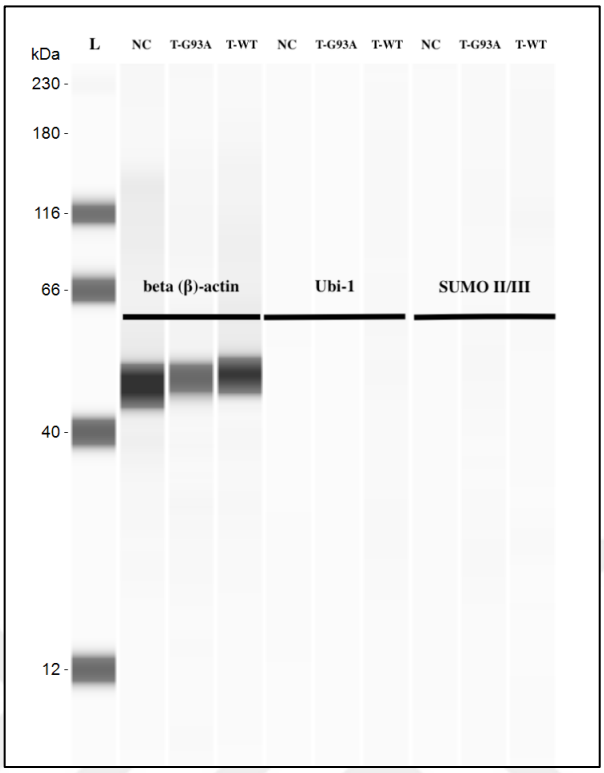

Figure 4.18. Image of Wes analysis with beta (β)-actin, Ubi-1, and SUMO II/III Antibody (L: Ladder, NC: Negative control, untransfected NSC-34 cells, T-G93A: SOD1 G93A mutated transfected NSC-34 cells, T-WT: Wild-type SOD1 mutated NSC-34 cells

4.11. MASS SPECTROSCOPY

As a result of LC-MS/MS analysis, as seen in Figure 4.17, 19 proteins were detected and analyzed via Proteome Discoverer 2.2 software. As a result of the analyzes made and the eliminations set in Section 3.15.3, three proteins listed in Table 4.1 was evaluated. Rho-related GTP binding proteins, whose molecular weight and pI were within the range determined in 2D-PAGE analyses, were targeted as a potential ALS biomarker.

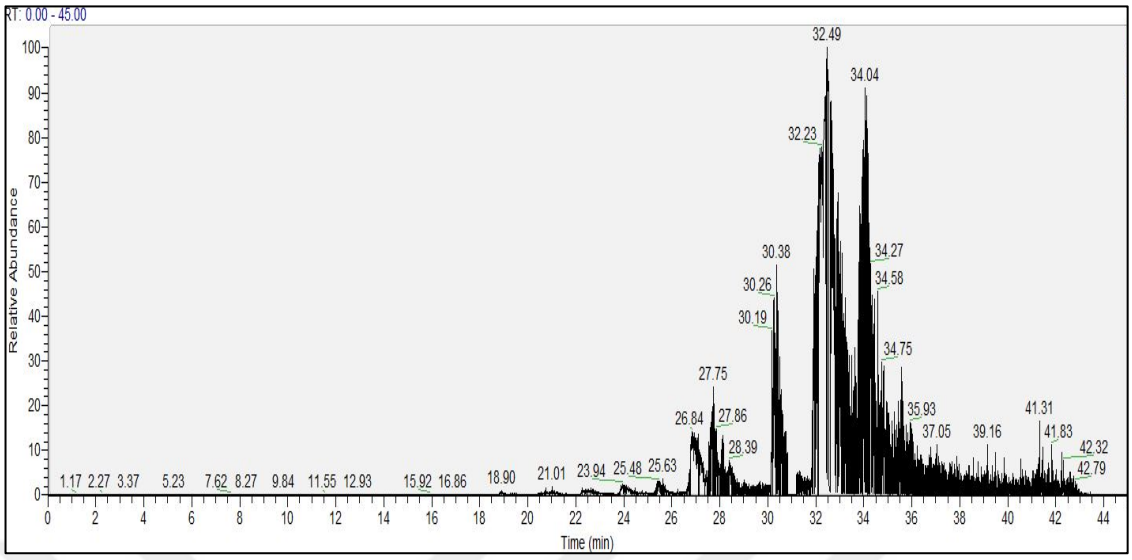

Figure 4.19. Liquid chromatography-mass spectrophotometry (LC-MS/MS) analysis of target protein spot.

Table 4.1 Properties of target proteins

Description	**Coverage (%)**	**Molecular Weight (kDa)**	**Calculated pI**
Zinc finger and BTB domain-containing protein 44, Zbtb44	2	50.1	6.18
Rho-related GTP-binding protein RhoB,	15	22.1	5.24
T-complex protein 1 subunit zeta, Cct6a	7	58.0	7.08

5. DISCUSSION

Amyotrophic lateral sclerosis (ALS) is a neurodegenerative disease characterized by the progressive impairment of muscles resulting from upper and lower motor neuron degeneration. ALS is an adult-onset disease that generally manifests clinical features between the ages of 50-60. From the onset of the disease, the approximate life expectancy is 3-5 years, although uncommonly, some patients have a lifespan of up to 20 years. 5-10% of the cases are hereditary and the etiology is unknown in the remaining cases. There is typically a Mendelian inheritance that follows the autosomal dominant pattern of heredity [12-14].

As similar to other neurodegenerative diseases, the precise molecular mechanism affecting motor neuron degeneration in ALS is still unrevealed, yet it is likely an intricate interaction of multiple pathogenic cellular mechanisms. Pathophysiology of onset and progression is defined by the retraction of motor neuron axons from nerve terminals at the neuromuscular junction, followed by loss of upper and lower motor neuron cell bodies in the motor cortex, brain stem, and spinal cord. As a result, critical connections between the CNS and skeletal muscles are progressively lost, which leads to paralysis and ultimately respiratory failure and death [6-7].

Clinically, LMN findings such as weakness and atrophy are accompanied by UMN findings such as spasticity and hyperreflexia. It causes severe disability in a short time and premature death often associated with respiratory failure. Symptoms such as muscle weakness and cramping, slurred speech, spasticity, fasciculations, and difficulty chewing or swallowing are classified as early symptoms. As the disease progresses, these findings manifest as atrophy, hyperreflexia, dysarthria, and dysphagia [67-68].

Despite the development of medicine for centuries and the technologies it has today, ALS is still one of the neurological diseases that are for diagnosis. In some cases, the diagnosis of ALS can be made using the patient's medical history, clinical findings, and electrophysiological testing; however, a pathological examination is required for a decisive diagnosis. The diagnosis of ALS requires the observation of clinical, electrophysiological, or neuropathological progressive signs of lower and upper motor neuron degeneration.

Various nerve conduction measurements, conventional electromyography, muscle biopsies, and neuroimaging are performed to diagnose patients [78].

SOD1 is a ubiquitously expressed enzyme that has the function to catalyze superoxide detoxification. Mutant SOD1 toxicity is associated with ALS via multiple mechanisms, most notably protein misfolding, and oligomerization, with more than 150 mutations. Mitochondrial dysfunction, axonal degeneration, and axonal transport deficits all contribute to this gain-of-function toxicity. Transgenic mice overexpressing mutant SOD1 exhibit ALS-like phenotype. This transgenic mouse model is important for ALS research. The best mouse models for investigation of motor neuron cell death are those that overexpress a human SOD1 transgene mutated with a guanine to alanine, which mimics the onset, progression, and severity of human disease. This mutation at position 93 is abbreviated as SOD1G93A. As a result of nerve terminals retracting from the neuromuscular junction, 40–50% of motor neurons are lost in the lumbar spinal cord of these rodents. In contrast to human disease, pathology predominantly involves lower motor neurons [60,61].

In this study, B6SJL-Tg (SOD1*G93A)1Gur/J mouse line, was purchased from Jackson Laboratory as a transgenic mouse model. The locomotor behavior of SOD1 transgenic mice was observed to determine disease stages after birth and to harvest their brains and spinal cords at the designated time. Transgenic mice were graded according to a scoring system called NeuroScore (NS), which includes disease progression, motor activity tests, and daily evaluation of hindlimb function, as described in the literature [121]. It was determined that the symptoms of the disease progressed up to the NS2 level on the postnatal day 105 and it was accepted as the symptomatic group. In addition, to investigate a potential biomarker in early diagnosis, postnatal day 60, with NS0 was determined for the pre-symptomatic group. Male mice were chosen to use in experiments to eliminate the physiological variability associated with females' oestrus cycle [124]. Anesthesia is known to impair normal brain function and physiology. The use of anesthesia in this experiment was not a limitation for protein profiling, as tissues were harvested just a few seconds after anesthesia. Since 2 transgenic animals in the PND60 group died during the disease, profiling of the PND60 group was performed on 4 animals.

Ubiquitination is a protein PTM that has crucial functions in homeostasis maintenance at the cellular and physiological levels. The three enzymes involved in this dynamic process are

called E1, ubiquitin-activating enzyme; E2, ubiquitin-conjugating enzyme; and E3, ubiquitin ligase. Deubiquitinating enzymes (DUBs) are responsible for the enzymatic process of ubiquitin removal from certain target proteins, a process known as deubiquitination. DUBs are widely used as inhibitors for ubiquitination [125,126]. Cellular homeostasis and development are only two examples of the many biological processes that benefit from the dynamic posttranslational alteration of proteins known as sumoylation. Two-D08 (2-D08) is a novel protein sumoylation inhibitor that can cross cellular membranes. When combined with camptothecin, this chemical inhibits the sumoylation of topoisomerase I in two distinct cancer cell lines. Moreover, additional analyses revealed that 2-D08 inhibited sumoylation by preventing the transfer of a small ubiquitin-like modifier (SUMO) from the UBC9-SUMO thioester to the substrate, a mechanism of action that had never been observed before. This was achieved without affecting SUMO-activating enzyme E1 (SAE-1/2) or E2 Ubc9-SUMO thioester formation [127]. Using a lysis reagent containing ubiquitination, sumoylation, and protease inhibitors to prevent interactions and cleavage of proteins after collecting tissues, proteins were extracted from tissues and utilized in proteomic studies to identify target proteins that may have potential biomarkers.

The presence of highly abundant proteins, such as albumin, which hinders the efficient identification of less abundant proteins, is a common problem in proteomic studies related to biomarker discovery. These proteins, which dominate 2D-PAGE imaging, can make those with less density difficult to detect. To overcome this situation, the 12 most abundant proteins were separated from the total protein mixture. Concentration determination measurements for each protein sample before and after the depletion process revealed that proteins were removed at a concentration of 90–95%. Thus, visual pollution and discovery limitations that may occur in proteomic analyses such as 2D-PAGE and Wes were prevented.

In 2-dimensional electrophoresis, complex protein mixtures are separated by molecular charge in the first dimension and by mass in the second. The information provided by 2DE analysis consists of molecular weight, pI, and potential post-translational modifications. The ability to simultaneously profile hundreds of proteins extracted from complex protein mixtures is advantageous for identifying biomarker-potential target proteins. Post-translational modifications can alter the molecular weight along with the pI of a protein, resulting in an alteration of the corresponding protein point on the proteomic model. In conjunction with Western blotting, antibodies specific for post-translational modifications

can disclose spots on 2DE patterns containing modified proteins. In this investigation, a pH gradient of 4–7 was determined, and all protein samples were analyzed using 11 cm IPG strips. The compatibility of sensitive protein staining techniques with mass spectrometry is one of the most crucial aspects of protein visualization in 2DE. Thus, a flamingo fluorescence gel stain, was chosen due to its high sensitivity, and being compatible with the mass spectrometer. As shown in Figures 3.9 and Figure 3.10, the two protein spots detected by analysis of proteins from the brains of 105-days-old transgenic mice were not detected in the healthy mouse group, whereas these two protein spots were detected at a lower concentration in the 60-days-old transgenic mouse model. Moreover, the analysis of the proteins extracted from the spinal cord tissue revealed no remarkable differences between healthy and transgenic mice groups. In 2DE models, multiple protein blots comprise multiple proteins with a similar pI. Different proteins of the same molecular weight tend to converge due to the limited range of the pH gradient.

NSC-34 is a hybrid cell line that is created by fusing the mouse embryo spinal cord MNs with mouse neuroblastoma cells N18TG2. These cells have been utilized as an appropriate model for analysis of motor neuron development when differentiated with all-trans-retinoic acid (RA). As a useful model for neural development, cholinergic maturation, and morphological maturation the NSC-34 cell line has garnered increasing attention. An essential molecule involved in embryonic neurogenesis and nervous system homeostasis is retinoic acid. During the development of the central nervous system, RA serves a critical function in neuron differentiation. RA can induce embryonic spinal cord-derived NSCs that differentiate into functional neurons in vitro by promoting the growth of cytodendrites in neuronal cells during the differentiation process [128]. In this study, NSC-34 cells were differentiated for up to 8 days. It is known that there is an inverse relationship between the differentiation and proliferation of cells. Differentiated and undifferentiated NSC-34 cells were counted at the specified times and compared, and it was determined that the proliferation rate of undifferentiated cells was approximately 7 times higher at the end of 8 days of differentiation as expected.

The microtubule network is comprised of two structural components as alpha and beta tubulins. Beta tubulin III (TUJ1) is localized specifically to neurons. Particularly, the expression of TUJ1 is associated with the earliest phases of neuronal differentiation. Therefore, TUJ1 is relevant to the processes of neurogenesis, axon guidance, and axon

maintenance [129]. In this study, beta-tubulin III was used as a marker of positive neuronal identity in immunocytochemistry assays, and the morphological characterization of the differentiation was examined by a confocal microscope. As a result of the measurements, it was observed that the neurite length of the differentiated cells was 8.61 times longer than the undifferentiated ones. When examined in terms of cell proliferation, it was determined that the proliferation of undifferentiated cells was higher, as in the trypan blue assay.

Presynaptic neuronal expansion and plasticity in the nervous system are linked to the growth-associated protein (GAP-43). Current research suggests that GAP-43 might have a function in post-synaptic AMPA receptor trafficking; however, GAP-43 has been demonstrated to be relatively neuron-specific, with a high density in presynaptic terminals in both the PNS and CNS. During development, GAP-43 expression becomes more confined in the central nervous system from its widespread perinatal level. GAP-43 appears to have a role in neurite growth at the cellular level of development by amplifying pathfinding signals from the growth cone [130-132]. Proteins that directly bind microtubules (MTs) and serve to stabilize them are collectively referred to as microtubule-associated proteins (MAPs). MAPs can also serve as scaffolds, directing the localization of other cytoskeleton-modifying proteins or components of signaling pathways. Dendritic MAP2 is widely distributed. It contributes to the definition and maintenance of a dendritic structure. Microtubule-associated protein 2 (MAP 2) is a member of a family of proteins that helps maintain the structure of neurons by stimulating the production of new microtubules and strengthening their connections to other regions of the cytoskeleton. Instructions for producing tau protein are located in the MAPT gene. This protein is widely distributed in neurons and other cell types of the nervous system. Microtubules, stiff hollow fibers that make up the cytoskeleton, are assembled and stabilized with its help. Microtubules have an important function in the structural integrity of cells, the process of cell division, and the intracellular movement of materials [133,134]. The expression of cytoskeletal markers is associated with morphological and functional differentiation. Thus the expression levels of the neural marker genes GAP43, MAPT, and MAP2 were compared with undifferentiated NSC-34 cells by qPCR, and a 5, 6, and 7-fold increase was observed, respectively.

The choline acetyltransferase (ChAT) enzyme catalyzes the biosynthesis of the neurotransmitter acetylcholine (AChE). ACh is produced when ChAT catalyzes the transfer of an acetyl group from the coenzyme acetyl-CoA to choline. Both in the central nervous

system (CNS) and peripheral nervous system (PNS), cholinergic neurons have significant concentrations of ChAT. ChAT is made in the neuron's body and transported to the nerve terminal. A nerve cell is categorized as a "cholinergic" neuron if ChAT is present. ChAT participates in ACh synthesis following the MN maturation stage. AChE is a cholinergic enzyme found primarily at postsynaptic neuromuscular junctions, especially in muscles and nerves. It rapidly hydrolyzes the naturally occurring neurotransmitter acetylcholine (ACh) into acetic acid and choline. The main role of AChE is to terminate transmission between neurons and synaptic signaling, to prevent ACh dispersion and activation of neighboring receptors. The proper operation of cholinergic neurons depends on the co-expression of enzymes involved in the synthesis, storage, and metabolism of ACh [135-137]. Results demonstrated that differentiated NSC-34 cells with significant increases in ChAT and AChE expressions were closer to a mature neuron cell in terms of physiological characteristics, just as in morphological characteristics, compared to undifferentiated ones.

In order to generate the SOD1-G93A mutation and the wild-type SOD1 of the transgenic animal model in the in vitro model, the differentiated NSC-34 cells were transfected with the human SOD1-G93A gene carrying plv-AcGFP-SOD1(G93A) plasmid and also with the wild-type human SOD1 gene carrying plv-AcGFP-SOD1(wt) plasmid., using the FUGENE transfection reagent and incubated for 96 hours. Cells were examined under a confocal microscope to observe the transfection efficiency. The nuclei of cells were stained with DAPI dye. Since the used plasmids carried GFP as the reporter gene, transfected cells were observed in green, while untransfected cells appeared blue. The results revealed that the transfection efficiency was too low to continue. Quantitative results from FACS also revealed that transfection occurred with low efficiency, in agreement with the images obtained from the confocal microscope. GFP+ values were measured as 47.45% and 24.66% for transfections with plasmids carrying G93A-mutated SOD1 and wild-type SOD1, respectively. To eliminate the possibility that multiple cell types in the population might create inconsistencies for further experiments, transfected cells were sorted by FACS and allowed to proliferate.

As a result of LC-MS/MS analyses and screenings, three proteins, Zinc finger and BTB domain-containing protein 44 (Zbtb44), Rho-related GTP-binding protein also known as Ras homolog family member B (RhoB), and T-complex protein 1 subunit zeta (Cct6a) proteins, were determined as targets and evaluated. However, only the RhoB protein

matched the molecular weight and pI value of the region determined by 2D-PAGE imaging, which also shows the highest coverage with 15% of total protein.

Rho-related GTP-binding proteins, also known as Rho GTPases, are members of a family of small GTPases that are essential for cellular signaling and cytoskeletal dynamics. These proteins regulate a wide variety of cellular processes by oscillating between an active GTP-bound state and an inactive GDP-bound state. Rho GTPases have been studied concerning cell migration, cell adhesion, cell division, and actin cytoskeleton organization. They interact with a multitude of downstream effectors, to mediate signaling cascades that regulate diverse cellular functions. Numerous diseases, like cancer, cardiovascular and neurological disorders, and immune system dysfunction, have been linked to Rho GTPase dysregulation. There are numerous members of the Rho GTPase family, such as RhoA, RhoB, RhoC, Rac1, Rac2, and Cdc42. Rho-related GTP-binding protein B plays an essential function in regulating diverse cellular processes, such as cytoskeletal dynamics, cell migration, and vesicle trafficking. RhoB is structurally and functionally analogous to other Rho GTPases, including RhoA and Rac1. RhoB has been implicated in specific cellular events and possesses distinct characteristics [138,139].

RhoB's participation in endocytic trafficking pathways is one of its notable characteristics. RhoB is implicated in the regulation of endosomal trafficking, including endocytosis, and degradation processes, according to studies. RhoB has been implicated in the regulation of the internalization and recycling of numerous cell surface receptors. RhoB has also been linked to other cellular functions and signaling pathways in addition to its role in endocytic trafficking. It has been found related to the regulation of cell survival, apoptosis, and cell cycle progression. RhoB's interaction with downstream effectors and modulation of signaling cascades can influence these processes. Rho GTPases are essential for neuronal development, synaptic plasticity, and axon guidance. Neurodevelopmental disorders such as autism spectrum disorders and intellectual disabilities, along with neurodegenerative diseases like AD and PD, have been related to altered Rho GTPase signaling [140,141].

Although the precise causes of ALS are not completely understood, there have been some studies that investigate the potential relation of Rho-related GTP-binding proteins in the disease. However, the specific association between Rho GTPases and ALS is still the subject

of active research, and the mechanisms underlying their potential role in ALS pathogenesis are not fully understood.

In a study with skeletal muscle tissue obtained from Caucasian ALS patients, Rhob protein was observed to be upregulated by 3.05 times, while in another study with samples obtained from the sciatic nerves of transgenic mice carrying the SOD1-G93A mutation, it was found to be upregulated by 1.35 times [142,143]. On the other hand, in another study, contrary to these findings, RhoB protein was found to be 0.15-fold downregulated in ALS patients [144].

The transcription factor known as Zinc finger and BTB domain-containing protein 44 (ZBTB44) is involved in a multitude of essential molecular processes. This protein possesses both zinc finger domains and a BTB/POZ domain, both of which have established roles in mediating protein-protein interactions and DNA binding. The involvement of ZBTB44 in the control of gene expression has been established, as it has been observed to interact with various transcription factors and co-regulators in order to regulate transcriptional activity. Research has demonstrated its ability to selectively attach to particular DNA sequences and enlist chromatin remodeling complexes in order to modulate the expression of genes. [145]

In recent times, there has been an increasing focus on comprehending the involvement of ZBTB44 in neurodegenerative diseases, specifically ALS. Investigations have indicated a plausible association between ZBTB44 and the etiology of ALS [146]. An investigation revealed a notable decrease in ZBTB44 expression inside the spinal cord of individuals diagnosed with ALS in comparison to a control group of individuals without the condition. Moreover, the researchers demonstrated that the suppression of ZBTB44 in motor neurons resulted in heightened susceptibility to oxidative stress and cellular demise, indicating a potential protective function of ZBTB44 in ALS [147]. In a separate investigation, the molecular pathways responsible for the neuroprotective effects of ZBTB44 in ALS were examined. The researchers discovered that ZBTB44 engages in interaction with the protein TDP-43, which is associated with ALS, and plays a role in governing its distribution inside the nucleus. Additionally, the researchers demonstrated that the overexpression of ZBTB44 mitigated the neurotoxic effects induced by TDP-43 in both cellular and animal models of amyotrophic lateral sclerosis. The aforementioned findings indicate that ZBTB44 potentially assumes a pivotal role in the development of ALS through its influence on gene expression and interaction with proteins associated with ALS. Additional investigation is required in

order to comprehensively comprehend the molecular pathways that underlie the participation of ZBTB44 in ALS and to examine its potential as a therapeutic target for this debilitating neurodegenerative disorder [148].

Chaperonin Containing TCP1 Subunit 6A (CCT6A) represents one of the subunits found inside the TCP1 complex, which is alternatively referred to as the CCT complex (cytosolic chaperonin containing TCP1). The TCP1 complex is an essential molecular chaperone involved in the processes of protein folding and assembly. The process in question pertains to the ATP-dependent facilitation of the folding of a certain group of recently synthesized proteins within the cytosol. This group includes proteins such as actin, tubulin, and tumor suppressor proteins [149]. The TCP1 complex exhibits a toroidal architecture with eight distinct subunits, among which is CCT6A, exhibiting an approximate sequence identity of 30% [150]. CCT6A has been linked in a multitude of cellular functions and pathological conditions. Within the domain of neurodegenerative disorders, such as ALS, the TCP1 complex has demonstrated its involvement in the process of protein folding and stabilization, particularly in relation to the aggregation-prone proteins that amass in these pathological conditions. The TCP1 complex is responsible for facilitating the folding process of huntingtin, a protein that has a tendency to aggregate and is linked to the development of Huntington's disease. Nevertheless, the available information regarding the association between CCT6A and ALS is inadequate [149]. The involvement of CCT6A in facilitating metastasis in non-small-cell lung cancer (NSCLC) has been identified within the domain of cancer research. Researchers have identified it as an inhibitor and direct binding protein of SMAD2, which is a crucial constituent of the TGF-β signaling cascade. The study cdemonstrates that CCT6A acts as a suppressor of SMAD2 activity and facilitates the metastatic potential of NSCLC cells. The research demonstrated that the suppression of TGF-β-mediated metastasis can be effectively achieved through the inhibition of SMAD3 or CCT6A. Outcomes of this study demonstrate that CCT6A potentially has a function in regulating the TGF-β signaling pathway and facilitating the spread of cancer in specific types of tumors [151].

To summarize, CCT6A functions as a constituent of the TCP1 complex, a molecular assembly responsible for protein folding and assembly processes. Although the TCP1 complex has been linked in the pathogenesis of neurological illnesses and CCT6A has been related with increasing metastasis in non-small cell lung cancer (NSCLC), the direct

evidence tying CCT6A to amyotrophic lateral sclerosis (ALS) is still lacking. Additional investigation is required in order to comprehensively comprehend the involvement of CCT6A in neurodegenerative disorders and its prospective utility as a target for therapeutic interventions.

To match the approximate kilodaltons of the targeted protein spots, the WES system examined whether the proteins have ubiquitination and sumoylation modifications using cartilage in the range of 12–230 kDA. The Wes system is a new generation of western blot methods based on gel-free, cartilage, and capillary systems. Protein Simple Wes-based immunoassays are performed on 13 or 25 capillary array disposable cartridges. The proteins derived from the sample plate are independently introduced into a capillary and subsequently segregated based on their size as they migrate through a stacking and separation matrix. The proteins that have been separated are subsequently immobilized on the wall of the capillary through the utilization of photoactivated capture chemistry. Target proteins are identified through the use of a primary antibody in conjunction with an HRP-conjugated secondary antibody and a chemiluminescent substrate. Following that, the chemiluminescent signal is measured and quantified. The Compass software automatically processes assay data based on Western size. Upon completion of the process, the data obtained from the samples is presented in a lane-wise manner, resembling a virtual-blot-like image that closely resembles conventional outcomes. Since 2D-PAGE analyses of proteins obtained from spinal cord tissues could not detect meaningfully different protein patches, Wes analyses were performed only with proteins obtained from brain tissues. Proteins obtained from NSC-34 cells were also analyzed to determine whether there was a correlation between the in vivo and in vitro models. ß-actin was selected as the housekeeping gene, and the b-actin protein band was displayed in all samples as expected, except for WT-5, the fifth animal of the wild-type group. This result indicates that although it was loaded at the same concentration as the other samples, there might not be enough protein left after depletion. The illusion in the concentration calculation also suggests that the protein lysate may have interacted with a chemical during the BCA assay. However, protein bands of neither ubiquitination nor sumoylation modifications could be observed in any of the proteins.

6. CONCLUSION

Amyotrophic lateral sclerosis (ALS) is a neurological disorder defined by the progressive degradation of upper and lower motor neurons, resulting in eventual mortality[1]. The disease is distinguished by the progressive deterioration of motor neurons (MNs) located in the brain stem, motor cortex, and spinal cord, leading to muscle paralysis and, ultimately, death [2].

In this study, the possibility of post-translational modifications of ubiquitylation and sumoylation as a biomarker specific to ALS disease was examined. For this purpose, both in vivo and in vitro derived proteins were profiled and compared by the 2D-PAGE method. As the in vivo model, the transgenic mouse model with the SOD1-G93A mutation, which is the most preferred in ALS studies, was used. Proteins isolated from brain and spinal cord tissues of both transgenic and wild-type mouse models were compared. In doing so, two different disease onsets were identified and the potential to detect a possible biomarker at an early stage was investigated.

NSC-34 cell, which is considered a motor neuron-like cell, was used as an in vitro model. First, differentiated NSC-34 cells were transfected with plasmids with wild-type SOD1 and SOD1-G93A mutations, after successful differentiation characterization, an ALS disease model was established in NSC-34 cells.

Proteins from both in vivo and in vitro sources were profiled by 2D-PAGE, and protein patches were detected in the 105-day-old symptomatic animal group that was not visible in the healthy animal group. As a result of LC-MS/MS analysis, three different proteins were identified as potential biomarkers as, Chaperonin Containing TCP1 Subunit 6A (CCT6A), Zinc finger and BTB domain-containing protein 44 (ZBTB44) and Rho-related GTP-binding protein (RhoB). Among these candidate proteins, ZBTB44 and Rhob are found to have a potential relationship with ALS. However, only RhoB showed matching pI and molecular weight values with the results of the 2D-PAGE analysis.

Ubiquitylation and sumoylation modifications were analyzed with the new generation automated western blot system WES, per the size of the determined target protein spots. However, neither *in vivo* nor *in vitro* analysis of proteins found these modifications.

While this study provides some insight into a potential relationship between RhoB and ALS, further research is necessary to fully understand the extent of their association. ALS is a complex disease involving multiple genetic and environmental factors, and the contribution of RhoB in ALS pathogenesis requires further investigation.

REFERENCES

1. Kumar DR, Aslinia F, Yale SH, Mazza JJ. Jean-Martin Charcot: the father of neurology. Clin Med Res. 2011;9(1):46-49.

2. Walling AD. Amyotrophic lateral sclerosis: Lou Gehrig's disease. Am Fam Physician. 1999;59(6):1489-1496.

3. Tan SY, Shigaki D. Jean-Martin Charcot (1825-1893): pathologist who shaped modern neurology. Singapore Med J. 2007;48(5):383.

4. Goetz CG. Amyotrophic lateral sclerosis: early contributions of Jean-Martin Charcot. Muscle Nerve. 2000;23(3):336-343.

5. Muneer MA, Rajan MS, Shenoy A, Hegde K, Koshy S. A Comprehensive Review on Amyotrophic Lateral Sclerosis.

6. Talbot K. Motor neuron disease: the bare essentials. Pract Neurol. 2009;9(5):303-309.

7. Swash M, Schwartz MS. Motor neuron disease: the clinical syndrome. In: Motor Neuron Disease. London: Springer; 1995. p. 1-17.

8. Ozkan N, Isik A, Fidan U. Design and Acquisition of EOG Based Interactive Communications for ALS Patients. Int J Appl Math Electron Comput. 2017;5:1-4.

9. Wang J, Zhou XF, Wang YJ. Continuous antioxidant drug exposure: a bridge from ideal world to real world of therapy for amyotrophic lateral sclerosis. Life Medicine. 2023;2(1):lnac042.

10. Van Es MA, Hardiman O, Chio A, Al-Chalabi A, Pasterkamp RJ, Veldink JH, Van den Berg LH. Amyotrophic lateral sclerosis. Lancet. 2017;390(10107):2084-2098.

11. Ryan M, Heverin M, McLaughlin RL, Hardiman O. Lifetime risk and heritability of amyotrophic lateral sclerosis. JAMA Neurol. 2019;76(11):1367-1374.

12. Al-Chalabi A, van den Berg LH, Veldink J. Gene discovery in amyotrophic lateral sclerosis: implications for clinical management. Nat Rev Neurol. 2017;13:96-104.

13. Debray S, Race V, Crabbe V, Herdewyn S, Matthijs G, Goris A, Dubois B, Thijs V, Robberecht W, Van Damme P. Frequency of C9orf72 repeat expansions in amyotrophic lateral sclerosis: a Belgian cohort study. Neurobiol Aging. 2013;34:2890.e7-2890.e12.

14. Talbott EO, Malek AM, Lacomis D. The epidemiology of amyotrophic lateral sclerosis. In: Handbook of Clinical Neurology. Vol. 138. Elsevier; 2016. p. 225-238.

15. Hirtz D, Thurman DJ, Gwinn-Hardy K, Mohamed M, Chaudhuri AR, Zalutsky R. How common are the "common" neurologic disorders? Neurology. 2007;68(5):326-337.

16. Mehta P, Antao V, Kaye W, et al. Prevalence of amyotrophic lateral sclerosis—United States, 2010–2011. MMWR Surveill Summ. 2014;63(7):1-13.

17. Martin S, Al Khleifat A, Al-Chalabi A. What causes amyotrophic lateral sclerosis? F1000Res. 2017;6.

18. Ingre C, Roos PM, Piehl F, Kamel F, Fang F. Risk factors for amyotrophic lateral sclerosis. Clin Epidemiol. 2015;7:181-193.

19. Zarei S, Carr K, Reiley L, et al. A comprehensive review of amyotrophic lateral sclerosis. Surg Neurol Int. 2015;6:171.

20. Weisskopf MG, Morozova N, O'Reilly EJ, et al. Prospective study of chemical exposures and amyotrophic lateral sclerosis. J Neurol Neurosurg Psychiatry. 2009;80(5):558-561.

21. Weisskopf MG. Formaldehyde exposure and amyotrophic lateral sclerosis. In: Enironmental and Molecular Mutagensis. Vol. 55. NJ USA: Wiley-Blackwell; 2014. p. S25.

22. Yu Y, Hayashi S, Cai X, et al. Pu-erh tea extract induces the degradation of FET family proteins involved in the pathogenesis of amyotrophic lateral sclerosis. Biomed Res Int. 2014;2014:254680.

23. Beghi E, Logroscino G, Chiò A, et al. Amyotrophic lateral sclerosis, physical exercise, trauma and sports: Results of a population-based pilot case-control study. Amyotroph Lateral Scler. 2010;11(3):289-292.

24. Huisman MH, de Jong SW, van Doormaal PT, et al. Population based epidemiology of amyotrophic lateral sclerosis using capture-recapture methodology. J Neurol Neurosurg Psychiatry. 2011;82(10):1165-1170.

25. Morozova N, Weisskopf MG, McCullough ML, et al. Diet and amyotrophic lateral sclerosis. Epidemiology. 2008;19(2):324-337.

26. Veldink JH, Kalmijn S, Groeneveld GJ, et al. Intake of polyunsaturated fatty acids and Vitamin E reduces the risk of developing amyotrophic lateral sclerosis. J Neurol Neurosurg Psychiatry. 2007;78(4):367-371.

27. Wroe R, Wai-Ling Butler A, Andersen PM, Powell JF, Al-Chalabi A. ALSOD: the Amyotrophic Lateral Sclerosis Online Database. Amyotrophic Lateral Sclerosis. 2008;9(4):249-250.

28. Cleveland DW, Laing N, Hurse PV, Brown RH Jr. Toxic mutants in Charcot's sclerosis. Nature. 1995;378(6555):342-343.

29. Kaur SJ, McKeown SR, Rashid S. Mutant SOD1 mediated pathogenesis of amyotrophic lateral sclerosis. Gene. 2016;577(2):109-118.

30. Rosen DR, Siddique T, Patterson D, et al. Mutations in Cu/Zn superoxide dismutase gene are associated with familial amyotrophic lateral sclerosis. Nature. 1993;362(6415):59.

31. Lee SM, Asress S, Hales CM, et al. TDP-43 cytoplasmic inclusion formation is disrupted in C9orf72-associated amyotrophic lateral sclerosis/frontotemporal lobar degeneration. Brain Commun. 2019;1(1):fcz014.

32. Van Deerlin VM, Leverenz JB, Bekris LM, et al. TARDBP mutations in amyotrophic lateral sclerosis with TDP-43 neuropathology: a genetic and histopathological analysis. Lancet Neurol. 2008;7(5):409-416.

33. Sreedharan J, Blair IP, Tripathi VB, et al. TDP-43 mutations in familial and sporadic amyotrophic lateral sclerosis. Science. 2008;319(5870):1668-1672.

34. Morita M, Al-Chalabi A, Andersen PM, et al. A locus on chromosome 9p confers susceptibility to ALS and frontotemporal dementia. Neurology. 2006;66(6):839–844.

35. Andersen PM, Nilsson P, Forsgren L, Marklund SL. CuZn-Superoxide Dismutase, Extracellular Superoxide Dismutase, and Glutathione Peroxidase in Blood from Individuals Homozygous for Asp90Ala CuZn-Superoxide Dismutase Mutation. J Neurochem. 1998;70(2):715-720.

36. Crapo JD, Oury T, Rabouille C, Slot JW, Chang LY. Copper, zinc superoxide dismutase is primarily a cytosolic protein in human cells. Proc Natl Acad Sci U S A. 1992;89(21):10405-10409.

37. Liu J, Concepcion L, Jonsson PA. Toxicity from copper chaperone and dismutase activity-independent accumulation of familial ALS-causing SOD1 mutants with spinal cord mitochondria. Neuron. 2004;43:5-17.

38. Saccon RA, Bunton-Stasyshyn RK, Fisher EM, Fratta P. Is SOD1 loss of function involved in amyotrophic lateral sclerosis? Brain. 2013;136:2342-2358.

39. Andersen PM. Amyotrophic lateral sclerosis associated with mutations in the CuZn superoxide dismutase gene. Curr Neurol Neurosci Rep. 2006;6:37-46.

40. Valentine JS, Hart PJ. Misfolded CuZnSOD and amyotrophic lateral sclerosis. Proc Natl Acad Sci U S A. 2003;100:3617-3622.

41. Wright G, Antonyuk S, Hasnain S. The biophysics of superoxide dismutase-1 and amyotrophic lateral sclerosis. Q Rev Biophys. 2019;52:E12. doi:10.1017/S003358351900012X

42. Su XW, Broach JR, Connor JR, Gerhard GS, Simmons Z. Genetic heterogeneity of amyotrophic lateral sclerosis: implications for clinical practice and research. Muscle Nerve. 2014;49:786-803.

43. Okado-Matsumoto A, Fridovich I. Amyotrophic lateral sclerosis: a proposed mechanism. Proc Natl Acad Sci U S A. 2002;99:9010-9014.

44. Turner BJ, Ackerley S, Davies KE, Talbot K. Dismutase-competent SOD1 mutant accumulation in myelinating Schwann cells is not detrimental to normal or transgenic ALS model mice. Hum Mol Genet. 2010;19:815-824.

45. Polymenidou M, Cleveland DW. Prion-like spread of protein aggregates in neurodegeneration. J Exp Med. 2012;209:889-893.

46. Araki T, et al. Misfolded SOD1 forms high-density molecular complexes with synaptic molecules in mutant SOD1-linked familial amyotrophic lateral sclerosis cases. J Neurol Sci. 2012;314:92-96.

47. Toivonen JM, et al. MicroRNA-206: a potential circulating biomarker candidate for amyotrophic lateral sclerosis. PLoS ONE. 2014;9:e89065.

48. Honda D, et al. The ALS/FTLD-related RNA-binding proteins TDP-43 and FUS have common downstream RNA targets in cortical neurons. FEBS Open Bio. 2013;4:1-10.

49. Cudkowicz ME, et al. Epidemiology of mutations in superoxide dismutase in amyotrophic lateral sclerosis. Ann Neurol. 1997;41:210-221.

50. Andersen PM, et al. Autosomal recessive adult-onset amyotrophic lateral sclerosis associated with homozygosity for Asp90Ala CuZn-superoxide dismutase mutation. A clinical and genealogical study of 36 patients. Brain. 1996;119:1153-1172.

51. Turner MR, et al. Distinct cerebral lesions in sporadic and 'D90A' SOD1 ALS: studies with [11C]flumazenil PET. Brain. 2005;128:1323-1329.

52. DeJesus-Hernandez M, et al. Expanded GGGGCC hexanucleotide repeat in noncoding region of C9ORF72 causes chromosome 9p-linked FTD and ALS. Neuron. 2011;72(2):245-256.

53. van Blitterswijk M, et al. Association between repeat sizes and clinical and pathological characteristics in carriers of C9ORF72 repeat expansions (Xpansize-72): a cross-sectional cohort study. Lancet Neurol. 2013;12(10):978-988.

54. Gitler AD, Tsuiji H. There has been an awakening: emerging mechanisms of C9orf72 mutations in FTD/ALS. Brain Res. 2016;1647:19-29.

55. Neumann M, et al. Ubiquitinated TDP-43 in frontotemporal lobar degeneration and amyotrophic lateral sclerosis. Science. 2006;314(5796):130-133.

56. Yokoseki A, et al. TDP-43 mutation in familial amyotrophic lateral sclerosis. Ann Neurol. 2008;63(4):538-542.

57. Renton AE, Chiò A, Traynor BJ. State of play in amyotrophic lateral sclerosis genetics. Nat Neurosci. 2014;17(1):17-23.

58. Gurney ME, et al. Motor neuron degeneration in mice that express a human Cu, Zn superoxide dismutase mutation. Science. 1994;264(5166):1772-1775.

59. Wooley CM, et al. Gait analysis detects early changes in transgenic SOD1 (G93A) mice. Muscle Nerve. 2005;32(1):43-50.

60. Ilieva H, Polymenidou M, Cleveland DW. Non-cell autonomous toxicity in neurodegenerative disorders: ALS and beyond. J Cell Biol. 2009;187(6):761-772.

61. Heiman-Patterson TD, Deitch JS, Blankenhorn EP, Erwin KL, Perreault MJ, Alexander BK, et al. Background and gender effects on survival in the TgN (SOD1-G93A) 1Gur mouse model of ALS. J Neurol Sci. 2005;236(1-2):1-7.

62. Zoccolella S, Santamato A, Lamberti P. Current and emerging treatments for amyotrophic lateral sclerosis. Neuropsychiatr Dis Treat. 2009;5:577.

63. N.R. Cashman, H.D. Durham, J.K. Blusztajn, K. Oda, T. Tabira, I.T. Shaw, et al. Neuroblastoma x spinal cord (NSC) hybrid cell lines resemble developing motor neurons. Dev Dyn. 1992;194(3):209-221.

64. H.D. Durham, S. Dahrouge, N.R. Cashman. Evaluation of the spinal cord neuron X neuroblastoma hybrid cell line NSC-34 as a model for neurotoxicity testing. Neurotoxicology. 1993;387-395.

65. Vijayalakshmi K, Alladi PA, Ghosh S, Prasanna VK, Sagar BC, Nalini A, et al. Evidence of endoplasmic reticular stress in the spinal motor neurons exposed to CSF from sporadic amyotrophic lateral sclerosis patients. Neurobiol Dis. 2011;41(3):695-705.

66. O. Maier, J. Böhm, M. Dahm, S. Brück, C. Beyer, S. Johann. Differentiated NSC-34 motoneuron-like cells as experimental model for cholinergic neurodegeneration. Neurochem Int. 2013;62(8):1029-1038.

67. Wolf J, Safer A, Wöhrle JC, Palm F, Nix WA, Maschke M, et al. Variability and prognostic relevance of different phenotypes in amyotrophic lateral sclerosis—Data from a population-based registry. J Neurol Sci. 2014;345(1-2):164-167.

68. Wijesekera LC, Mathers S, Talman P, Galtrey C, Parkinson MH, Ganesalingam J, et al. Natural history and clinical features of the flail arm and flail leg ALS variants. Neurology. 2009;72(12):1087-1094.

69. Politi KA. A Study of the Mechanism of Motor Neuron Death in Amyotrophic Lateral Sclerosis [dissertation]. Columbia University; Year.

70. Turner MR, Barnwell J, Al-Chalabi A, Eisen A. Young-onset amyotrophic lateral sclerosis: historical and other observations. Brain. 2012;135(9):2883-2891.

71. Shoesmith CL, Findlater K, Rowe A, Strong MJ. Prognosis of amyotrophic lateral sclerosis with respiratory onset. J Neurol Neurosurg Psychiatry. 2007;78(6):629-631.

72. Chiò A, Calvo A, Moglia C, Mazzini L, Mora G. Phenotypic heterogeneity of amyotrophic lateral sclerosis: a population-based study. J Neurol Neurosurg Psychiatry. 2011;[page range].

73. Gordon PH, Cheng B, Katz IB, Pinto M, Hays AP, Mitsumoto H, et al. The natural history of primary lateral sclerosis. Neurology. 2006;66(5):647-653.

74. Cedarbaum JM, Stambler N, Malta E, Fuller C, Hilt D, Thurmond B, et al. The ALSFRS-R: a revised ALS functional rating scale that incorporates assessments of respiratory function. J Neurol Sci. 1999;169(1-2):13-21.

75. Crockford C, Newton J, Lonergan K, et al. ALS-specific cognitive and behavior changes associated with advancing disease stage in ALS. Neurology. 2018;91:e1370-e1380.

76. Nicholson K, Murphy A, McDonnell E, et al. Improving symptom management for people with amyotrophic lateral sclerosis. Muscle Nerve. 2018;57:20-24.

77. Elamin M, Bede P, Byrne S, et al. Cognitive changes predict functional decline in ALS: a population-based longitudinal study. Neurology. 2013;80:1590-1597.

78. Zarei S, Carr K, Reiley L, et al. A comprehensive review of amyotrophic lateral sclerosis. Surg Neurol Int. 2015;6.

79. Hardiman O, Van Den Berg LH, Kiernan MC. Clinical diagnosis and management of amyotrophic lateral sclerosis. Nat Rev Neurol. 2011;7(11):639.

80. Davenport RJ, Swingler RJ, Chancellor AM, Warlow CP. Avoiding false positive diagnoses of motor neuron disease: lessons from the Scottish Motor Neuron Disease Register. J Neurol Neurosurg Psychiatry. 1996;60(2):147-151.

81. Van den Berg J, Kalmijn S, Lindeman E, et al. Multidisciplinary ALS care improves quality of life in patients with ALS. Neurology. 2005;65(8):1264-1267.

82. de Carvalho M, Dengler R, Eisen A, et al. Electrodiagnostic criteria for diagnosis of ALS. Clin Neurophysiol. 2008;119(3):497-503.

83. Joyce NC, Carter GT. Electrodiagnosis in persons with amyotrophic lateral sclerosis. PM&R. 2013;5(5):S89-S95.

84. Kollewe K, Körner S, Dengler R, Petri S, Mohammadi B. Magnetic resonance imaging in amyotrophic lateral sclerosis. Neurol Res Int. 2012;2012.

85. Matsuoka M. Human T-cell leukemia virus type I (HTLV-I) infection and the onset of adult T-cell leukemia (ATL). Retrovirology. 2005;2:27.

86. Alfahad T, Nath A. Retroviruses and amyotrophic lateral sclerosis. Antiviral Res. 2013;99(2):180-187.

87. Tai H, Cui L, Guan Y, et al. Correlation of creatine kinase levels with clinical features and survival in amyotrophic lateral sclerosis. Front Neurol. 2017;8:322.

88. Zoccolella S, Beghi E, Palagano G, et al. Predictors of delay in the diagnosis and clinical trial entry of amyotrophic lateral sclerosis patients: a population-based study. J Neurol Sci. 2006;250(1-2):45-49.

89. Tao QQ, Wu ZY. Amyotrophic lateral sclerosis: Precise diagnosis and individualized treatment. Chin Med J (Engl). 2017;130(19):2269-2272.

90. Ryberg H, Bowser R. Protein biomarkers for amyotrophic lateral sclerosis. Expert Rev Proteomics. 2008;5(2):249-262.

91. Hu S, Loo JA, Wong DT. Human body fluid proteome analysis. Proteomics. 2006;6(23):6326-6353.

92. Kawamata T, Akiyama H, Yamada T, McGeer PL. Immunologic reactions in amyotrophic lateral sclerosis brain and spinal cord tissue. Am J Pathol. 1992;140(3):691.

93. Tarasiuk J, Kułakowska A, Drozdowski W, Kornhuber J, Lewczuk P. CSF markers in amyotrophic lateral sclerosis. J Neural Transm. 2012;119(7):747-757.

94. Yiangou Y, Facer P, Durrenberger P, et al. COX-2, CB2 and P2X7-immunoreactivities are increased in activated microglial cells/macrophages of multiple sclerosis and amyotrophic lateral sclerosis spinal cord. BMC Neurol. 2006;6(1):12.

95. Shaw PJ, Ince PG, Falkous G, Mantle D. Oxidative damage to protein in sporadic motor neuron disease spinal cord. Ann Neurol. 1995;38(4):691-695.

96. Tohgi H, Abe T, Yamazaki K, Murata T, Ishizaki E, Isobe C. Increase in oxidized NO products and reduction in oxidized glutathione in cerebrospinal fluid from patients with sporadic form of amyotrophic lateral sclerosis. Neurosci Lett. 1999;260(3):204-206.

97. Ihara Y, Nobukuni K, Takata H, Hayabara T. Oxidative stress and metal content in blood and cerebrospinal fluid of amyotrophic lateral sclerosis patients with and without a Cu, Zn-superoxide dismutase mutation. Neurol Res. 2005;27(1):105-108.

98. Carriedo SG, Sensi SL, Yin HZ, Weiss JH. AMPA exposures induce mitochondrial Ca2+ overload and ROS generation in spinal motor neurons in vitro. J Neurosci. 2000;20(1):240-250.

99. Beuche W, Yushchenko M, Mäder M, Maliszewska M, Felgenhauer K, Weber F. Matrix metalloproteinase-9 is elevated in serum of patients with amyotrophic lateral sclerosis. Neuroreport. 2000;11(16):3419-3422.

100. Jokic N, Gonzalez de Aguilar JL, Pradat PF, et al. Nogo expression in muscle correlates with amyotrophic lateral sclerosis severity. Ann Neurol. 2005;57(4):553-556.

101. Rattan SI, Derventzi A, Clark BF. Protein synthesis, posttranslational modifications, and aginga. Ann N Y Acad Sci. 1992;663(1):48-62.

102. Blom N, Sicheritz-Pontén T, Gupta R, Gammeltoft S, Brunak S. Prediction of post-translational glycosylation and phosphorylation of proteins from the amino acid sequence. Proteomics. 2004;4(6):1633-1649.

103. Walsh CT, Garneau-Tsodikova S, Gatto GJ Jr. Protein posttranslational modifications: the chemistry of proteome diversifications. Angew Chem Int Ed. 2005;44(45):7342-7372.

104. Reinders J, Sickmann A. Modificomics: posttranslational modifications beyond protein phosphorylation and glycosylation. Biomol Eng. 2007;24(2):169-177.

105. Ribet D, Cossart P. Pathogen-mediated posttranslational modifications: a re-emerging field. Cell. 2010;143(5):694-702.

106. Meek DW, Anderson CW. Posttranslational modification of p53: cooperative integrators of function. Cold Spring Harb Perspect Biol. 2009;1(6):a000950.

107. Wang YC, Peterson SE, Loring JF. Protein post-translational modifications and regulation of pluripotency in human stem cells. Cell Res. 2014;24(2):143.

108. Stringer DK, Piper RC. Terminating protein ubiquitination: Hasta la vista, ubiquitin. Cell Cycle. 2011;10(18):3067-3071.

109. Bachiller S, Alonso-Bellido IM, Real LM, et al. The ubiquitin proteasome system in neuromuscular disorders: moving beyond movement. Int J Mol Sci. 2020;21(17):6429.

110. Mao Y. Structure, dynamics and function of the 26S proteasome. In: Macromolecular Protein Complexes III: Structure and Function. 2021:1-51.

111. Anderson DB, Zanella CA, Henley JM, Cimarosti H. Sumoylation: implications for neurodegenerative diseases. In: SUMO Regulation of Cellular Processes. Springer, Cham; 2017:261-281.

112. Wilkinson KA, Henley JM. Mechanisms, regulation and consequences of protein SUMOylation. Biochem J. 2010;428(2):133-145.

113. Song J, Durrin LK, Wilkinson TA, Krontiris TG, Chen Y. Identification of a SUMO-binding motif that recognizes SUMO-modified proteins. Proc Natl Acad Sci USA. 2004;101(40):14373-14378.

114. UniProt Consortium. UniProt: a hub for protein information. Nucleic Acids Res. 2014;43(D1):D204-D212.

115. Powers AD, Palecek SP. Protein analytical assays for diagnosing, monitoring, and choosing treatment for cancer patients. J Healthc Eng. 2012;3(4):503-534.

116. Zhang J., Guy M., Norman H., Chen Y., Xu Q., Dong X.et al.. Top-down quantitative proteomics identified phosphorylation of cardiac troponin i as a candidate biomarker for chronic heart failure. Journal of Proteome Research 2011;10(9):4054-4065. https://doi.org/10.1021/pr200258m

117. Schwarz UR, Geiger J, Walter U, Eigenthaler M. Flow cytometry analysis of intracellular VASP phosphorylation for the assessment of activating and inhibitory signal transfection pathways in human platelets. Thromb Haemost. 1999;81(03):1145-1152.

118. Heist RS, Christiani D. EGFR-targeted therapies in lung cancer: predictors of response and toxicity.

119. Hayashi S., Nagaoka K., & Tanaka Y.. Blood-based biomarkers in hepatitis b virus-related hepatocellular carcinoma, including the viral genome and glycosylated proteins. International Journal of Molecular Sciences 2021;22(20):11051. https://doi.org/10.3390/ijms222011051

120. Rezaei-Ghaleh N. , Amininasab M. , Kumar S. , Walter J. , & Zweckstetter M.. Phosphorylation modifies the molecular stability of β-amyloid deposits. Nature Communications 2016;7(1). https://doi.org/10.1038/ncomms11359

121. Hatzipetros T, Kidd JD, Moreno AJ, Thompson K, Gill A, Vieira FG. A quick phenotypic neurological scoring system for evaluating disease progression in the SOD1-G93A mouse model of ALS. J Vis Exp. 2015;104:e53257.

122. Simard JR, Lee L, Vieux E, Improgo R, Tieu T, Phillips AJ, Fisher SL, Pollock RM, Park E. High-throughput quantitative assay technologies for accelerating the discovery and optimization of targeted protein degradation therapeutics. SLAS Discov. 2021;26(4):503-517.

123. Senturk NB. Contribution of cell type specific changes of monocarboxylate transporters to Amyotrophic Lateral Sclerosis (ALS) Disease and application of boron derivatives as an alternative treatment [dissertation]. Yeditepe University; date unknown.

124. Lindhardt TB, Gutiérrez-Jiménez E, Liang Z, Hansen B. Male and female C57BL/6 mice respond differently to awake magnetic resonance imaging habituation. Front Neurosci. 2022 Jun 10;16:853527.

125. Zhang Y, Yu H, Zhang J, Gao H, Wang S, Li S, Wei P, Liang J, Yu G, Wang X, et al. Cul4A-DDB1-mediated monoubiquitination of phosphoglycerate dehydrogenase promotes colorectal cancer metastasis via increased S-adenosylmethionine. J Clin Invest. 2021;131:e146187.

126. Xiao Z, Zhang P, Ma L. The role of deubiquitinases in breast cancer. Cancer Metastasis Rev. 2016;35:589-600.

127. Kim YS, Keyser SG, Schneekloth JS Jr. Synthesis of 2',3',4'-trihydroxyflavone (2-D08), an inhibitor of protein sumoylation. Bioorg Med Chem Lett. 2014 Feb 15;24(4):1094-1097.

128. Tan BT, Wang L, Li S, Long ZY, Wu YM, Liu Y. Retinoic acid induced the differentiation of neural stem cells from embryonic spinal cord into functional neurons in vitro. Int J Clin Exp Pathol. 2015;8(7):8129.

129. Katsetos C, Legido A, Perentes E, Mörk S. Class III beta-tubulin isotype: a key cytoskeletal protein at the crossroads of developmental neurobiology and tumor neuropathology. J Child Neurol. 2003;18:851-866.

130. Vitkovic L, Steisslinger HW, Aloyo VJ, Mersel M. The 43-kDa neuronal growth-associated protein (GAP-43) is present in plasma membranes of rat astrocytes. Proc Natl Acad Sci U S A. 1988;85(21):8296-8300.

131. Han MH, Jiao S, Jia JM, et al. The novel caspase-3 substrate Gap43 is involved in AMPA receptor endocytosis and long-term depression. Mol Cell Proteomics. 2013;12(12):3719-3731.

132. Strittmatter SM, Fankhauser C, Huang PL, Mashimo H, Fishman MC. Neuronal pathfinding is abnormal in mice lacking the neuronal growth cone protein GAP-43. Cell. 1995;80(3):445-452.

133. Bodakuntla S, Jijumon AS, Villablanca C, Gonzalez-Billault C, Janke C. Microtubule-associated proteins: structuring the cytoskeleton. Trends Cell Biol. 2019;29(10):804-819.

134. Baker M, Litvan I, Houlden H, Adamson J, Dickson D, Perez-Tur J, Hardy J, Lynch T, Bigio E, Hutton M. Association of an extended haplotype in the tau gene with progressive supranuclear palsy. Hum Mol Genet. 1999 Apr;8(4):711-715.

135. McHardy SF, Wang HL, McCowen SV, Valdez MC. Recent advances in acetylcholinesterase inhibitors and reactivators: an update on the patent literature (2012-2015). Expert Opin Ther Pat. 2017 Apr;27(4):455-476.

136. Oda Y. Choline acetyltransferase: the structure, distribution and pathologic changes in the central nervous system. Pathol Int. 1999 Nov;49(11):921-937.

137. Oda Y. Choline acetyltransferase: the structure, distribution and pathologic changes in the central nervous system. Pathol Int. 2000;49(11):921-937.

138. Bustelo XR, Sauzeau V, Berenjeno IM. GTP-binding proteins of the Rho/Rac family: regulation, effectors and functions in vivo. Bioessays. 2007 Apr;29(4):356-370.

139. Ridley AJ. RhoA, RhoB and RhoC have different roles in cancer cell migration. J Microsc. 2013 Sep;251(3):242-249.

140. Vega FM, Ridley AJ. The RhoB small GTPase in physiology and disease. Small GTPases. 2018 Sep 3;9(5):384-393.

141. DeGeer J, Lamarche-Vane N. Rho GTPases in neurodegeneration diseases. Exp Cell Res. 2013 Sep 10;319(15):2384-2394.

142. Bernardini C, Censi F, Lattanzi W, Barba M, Calcagnini G, Giuliani A, Tasca G, Sabatelli M, Ricci E, Michetti F. Mitochondrial network genes in the skeletal muscle of amyotrophic lateral sclerosis patients. PLoS One. 2013 Feb 28;8(2):e57739.

143. Alves CJ, Maximino JR, Chadi G. Dysregulated expression of death, stress and mitochondrion related genes in the sciatic nerve of presymptomatic SOD1G93A mouse model of Amyotrophic Lateral Sclerosis. Front Cell Neurosci. 2015 Sep 1;9:332.

144. Jiang YM, Yamamoto M, Kobayashi Y, Yoshihara T, Liang Y, Terao S, Takeuchi H, Ishigaki S, Katsuno M, Adachi H, Niwa JI. Gene expression profile of spinal motor neurons in sporadic amyotrophic lateral sclerosis. Ann Neurol. 2005 Feb;57(2):236-251.

145. Gamsjaeger R, Liew CK, Mackay JP. Way out of the BTB domain fold. Protein Science. 2007;16(11):2470-2478.

146. Li H, Zhang Z. The BTB/POZ domain-containing protein ZBTB44 regulates the transcription of genes involved in the development of the human nervous system. Experimental Cell Research. 2016;349(2):324-332.

147. Chen Y, Wang J, Cui W, Zhang Y, Shen Y. ZBTB44 protects motor neurons from inflammation-induced cell death by modulating A20 expression. Cell Death & Disease. 2018;9(2):1-14.

148. Zhang Y, Chen Y, Gu J, Zhao J, Yuan Z, Shen Y. ZBTB44 protects against motor neuron degeneration by promoting nuclear import of FUS and FUS/TLS-related chimeric proteins. Cell Death & Disease. 2019;10(1):1-14.

149. Knowlton J, Gestaut D, Ma B, Taylor G, Seven A, Leitner A, Dermody T, et al. Structural and functional dissection of reovirus capsid folding and assembly by the prefoldin-tric/cct chaperone network. Proceedings of the National Academy of Sciences. 2021;118(11). doi: 10.1073/pnas.2018127118.

150. Liang X, Shen W, Sun H, Prakash T, Crooke S. Tcp1 complex proteins interact with phosphorothioate oligonucleotides and can co-localize in oligonucleotide-induced nuclear bodies in mammalian cells. Nucleic Acids Research. 2014;42(12):7819-7832. doi: 10.1093/nar/gku484.

151. Ying Z, Tian H, Li Y, Lian R, Li W, Wu S, Li M, et al. Cct6a suppresses smad2 and promotes prometastatic tgf-β signaling. Journal of Clinical Investigation. 2017;127(5):1725-1740. doi: 10.1172/jci90439.

APPENDIX A: ETHICS STATEMENTS

YEDİTEPE ÜNİVERSİTESİ

T.C. YEDİTEPE ÜNİVERSİTESİ, DENEY HAYVANLARI ETİK KURULU

(YÜDHEK)

ETİK KURUL KARARI

Toplantı Tarihi	Karar No	İlgi	Proje Yürütücüsü
27.07.2018	678	19.06.2018	Prof. Dr. Fikrettin ŞAHİN

"ALS hayvan modelinde post translasyonal modifikasyonların incelenmesi" adlı bilimsel çalışma etik kurulumuzda görüşülmüş olup, çalışmanın etik kurallara uygun olduğuna oy birliğiyle karar verilmiştir.

Etik Onay Geçerlilik Süresi: 3 Yıl	**Hayvan Türü ve cinsiyeti:** Fare ♂	**Hayvan Sayısı:** 30

GÖREVİ	ADI SOYADI	
Başkan	Prof. Dr. Bayram YILMAZ	
Başkan Yardımcısı	Prof. Dr. Erdem YEŞİLADA	
Raportör	Vet. Hekim Engin SÜMER	
Üye	Prof. Dr. M. Ece GENÇ	**KATILMADI**
Üye	Prof. Dr. Rukset ATTAR	
Üye	Doç. Dr. Soner DOĞAN	
Üye	Doç. Dr. Ediz DENİZ	**KATILMADI**
Üye	Prof. Dr. Gamze TORUN KÖSE	**KATILMADI**
Üye	Doç. Dr. Aylin YABA UÇAR	**KATILMADI**
Üye	Hakan GÖKSEL	
Üye	Ahmet ŞENKARDEŞLER	